
Electronic Thesis and Dissertation Repository

12-12-2016 12:00 AM

Insights into the role of connexin26 and connexin30 in skin health, syndromic disease, and cutaneous wound healing

Eric R. Press, *The University of Western Ontario*

Supervisor: Dr. Dale W. Laird, *The University of Western Ontario*

A thesis submitted in partial fulfillment of the requirements for the Master of Science degree in Physiology and Pharmacology

© Eric R. Press 2016

Follow this and additional works at: <https://ir.lib.uwo.ca/etd>



Part of the [Cell Biology Commons](#)

Recommended Citation

Press, Eric R., "Insights into the role of connexin26 and connexin30 in skin health, syndromic disease, and cutaneous wound healing" (2016). *Electronic Thesis and Dissertation Repository*. 4286.
<https://ir.lib.uwo.ca/etd/4286>

This Dissertation/Thesis is brought to you for free and open access by Scholarship@Western. It has been accepted for inclusion in Electronic Thesis and Dissertation Repository by an authorized administrator of Scholarship@Western. For more information, please contact wlsadmin@uwo.ca.

Abstract

Connexin26 (Cx26) and Cx30 facilitate gap junctional intercellular communication (GJIC) in the epidermis and are linked to several syndromic skin diseases. We investigated 5 disease-linked Cx26 mutants and demonstrated that the severity and extent of disease can be predicted from the gain- or loss-of function properties of each mutant, as well as the ability to induce cell death. We also used transgenic mice expressing S17F Cx26 (linked to keratitis-ichthyosis-deafness syndrome) or A88V Cx30 (linked to Clouston Syndrome) to investigate the pathophysiology these skin diseases. We demonstrated that S17F Cx26, but not A88V Cx30, promotes palmoplantar keratoderma by disrupting keratinocyte differentiation. Primary keratinocyte cultures from these mice demonstrated the mutants can also affect gap junction intercellular communication and cell migration. Lastly, we showed that mutant mice retain most wound healing properties. Together, we suggest that syndromic mutants often display gain-of-function properties and can disrupt keratinocyte differentiation in the epidermis.

Keywords

Gap junction, Hemichannel, Connexin, Cx26, Cx30, Cx43, Skin Disease, Syndromic Hearing Loss, Epidermis, Keratinocyte, Keratitis-Ichthyosis-Deafness Syndrome, Clouston Syndrome, N14K, S17F, D50N, N54K, A88V, M163V, S183F, Mutant Mouse Model, Wound Healing, Palmoplantar Keratoderma, Differentiation, Confocal Laser Microscopy

Co-Authorship Statement

Chapter 1

Dr. Jared Churko originally created the epidermal connexin expression diagram (Figure 1.1)

Charles Walewski generated the Cx26 and Cx30 polypeptide diagrams (Figures 1.2 and 1.3)

Chapter 2

Dr. John J. Kelly designed and assisted with the hemichannel assay.

Katrina Chin performed the microinjection experiments on HeLa cells expressing GFP-tagged Cx26 mutants alone.

Anton Alaga performed the microinjection experiments on HeLa cells co-expressing GFP-tagged Cx26 mutants and RFP-tagged Cx26.

Dr. Qing Shao generated the Cx26-GFP cDNA construct and verified all other cDNA constructs by sequencing.

Chapter 3

Katanya C. Alaga equally contributed the maintenance and characterization of the Cx26^{K14-S17F/+} mouse line.

Kevin Barr originally established the Cx26^{K14-S17F/+} mouse line, bred the Cx30^{A88V/+} mouse line, and was the expert consultant for all mouse related work within this project.

Dr. Qing Shao was instrumental in my technical training for cell culture, western blotting, and immunolabelling work.

Dr. Felicitas Bosen originally generated the Cx30^{A88V/+} mouse line.

Dr. Klaus Willecke provided the Cx26^{flloxS17F/+} mouse line.

Acknowledgements

My time in the Laird Lab will undoubtedly have a lasting effect on me, much thanks to the wonderful people who have supported me through the past 2 years. I would like to extend my sincerest gratitude to the following people:

To my family for their unyielding love and support for all my aspirations. Thank you for your positivity in the good and difficult times, and for proudly shaping me into the person I am today.

To Jessica Goncalves for her constant love and inspiring dedication to improve the lives of others. Your joyful, virtuous nature and passion for life continue to make me a better person.

To Dale Laird for fostering within all his trainees, a strong dedication to scientific rigor, teamwork, and professionalism. In just 2 years, your mentorship has significantly influenced my academic and personal growth and you have instilled in me values that I will carry throughout my career.

To Cindy Shao and Kevin Barr for their relentless devotion to assisting us budding scientists, and for making our time in the lab as productive as possible. Your guidance, support, and expertise have contributed enormously to my learning experience.

To all the trainees in the Laird Lab for sharing 2 years of struggles, learning experiences, and laughs. Your kind support and friendship have given me many fond memories to cherish moving forward.

To Dr. Cheryle Séguin, Dr. Robert Gros, and Dr. Andy Babwah for providing much appreciated insight and support on my advisory committee.

To Tom Stavraky, Jamie Simek, Chris Webb, and Boun Thai for creating an excellent TA experience in Physiology 3130Z.

To the Canadian Institutes of Health Research for funding this research.

Table of Contents

Abstract	ii
Keywords	iii
Co-Authorship Statement.....	iv
Acknowledgements.....	v
Table of Contents.....	vi
List of Figures	xi
List of Appendices	xiii
List of Abbreviations	xiv
Chapter 1	1
1 Introduction	1
1.1.1 Structure, Function, and Life-Cycle of Connexins and Gap Junctions.....	1
1.1.2 Connexin Gene Mutations and Human Disease.....	2
1.1.3 Physiology of Human Epidermis	3
1.1.4 Cutaneous Wound Healing	7
1.1.5 Connexins Involved in Cutaneous Wound Healing.....	8
1.1.6 <i>GJB2</i> Mutations Involved in Skin Disease	8
1.1.7 <i>GJB6</i> Mutations Involved in Skin Disease	11
1.1.8 Modeling Connexin-Linked Skin Disease	14

1.1.9 Hypothesis.....	15
1.1.10 Objectives.....	16
1.2 References.....	17
Chapter 2.....	25
2 Induction of cell death and gain-of-function properties of Cx26 mutants predict the severity of diseases linked to <i>GJB2</i> mutations	25
2.1 Introduction.....	26
2.2 Materials and Methods.....	27
2.2.1 Cell Culture	27
2.2.2 cDNA Constructs and Transfections.....	28
2.2.3 Immunofluorescent Labeling	28
2.2.4 Dye Transfer Studies.....	29
2.2.5 Hemichannel Assay.....	29
2.2.6 Statistical Analysis.....	30
2.3 Results.....	30
2.3.1 N14K and D50N mutants induce cell death <i>in vitro</i>	30
2.3.2 N54K and S183F mutants have trafficking defects and impaired dye transfer ability	33
2.3.3 Cx26 mutants exhibit a dominant negative reduction of Cx26 function to varying degrees	33
2.3.4 N54K and S183F mutants display trans-dominant effects on Cx30	38

2.3.5 N54K displays a mild trans-dominant effect on endogenous Cx43.....	38
2.3.6 N54K and S183F mutants display reduced hemichannel function.....	43
2.4 Discussion	43
2.5 Acknowledgements and Funding.....	51
2.6 References	52
Chapter 3	57
3 Disease-linked Cx26 and Cx30 mutants promote volar skin abnormalities and wound healing defects in mice.....	57
3.1 Introduction.....	58
3.2 Materials and Methods.....	60
3.2.1 Genetically Modified Mice	60
3.2.2 Mouse Genotyping.....	61
3.2.3 Skeletal Staining	61
3.2.4 Micro-Computed Tomography	61
3.2.5 Tissue Lysates and Immunoblotting	62
3.2.6 Immunohistochemistry and Immunofluorescence Imaging.....	62
3.2.7 Wound Healing assays	63
3.2.8 Cell Lines	63
3.2.9 Primary Murine Keratinocyte Culture	63
3.2.10 Calcein-AM Dye Recovery.....	64

3.2.11 Scratch Wound Assay	64
3.2.12 Scrape-Load Assay	65
3.2.13 Statistical Analysis.....	65
3.3 Results.....	65
3.3.1 Epidermal expression of S17F Cx26 but not A88V Cx30 generates severe skin features and additional Cx26-linked phenotypes	65
3.3.2 S17F Cx26 but not A88V Cx30 disrupts keratinocyte differentiation in foot pad epidermis	68
3.3.3 Primary keratinocytes harvested from S17F/+ mice exhibit reduce GJIC and collective cell migration.....	68
3.3.4 S17F/+ mice display irregular dorsal skin remodeling and tail skin wound healing	77
3.4 Discussion	86
3.5 Acknowledgements and Funding.....	89
3.6 References.....	90
Chapter 4.....	90
4 General Discussion.....	95
4.1 Learning outcomes from transgenic mice	95
4.2 Therapeutic strategies for connexin-linked skin diseases and wound healing.....	99
4.3 References	101
Appendix 1 Cx26 ^{K14-S17F/+} neonates display an intact epidermal barrier	105

Appendix 2	Permission for Artwork Reproduction	108
Appendix 3	Animal Use Protocol Approval	109
Curriculum Vitae		110

List of Figures

Figure 1.1 Connexin expression in unwounded and wounded epidermis	4
Figure 1.2 Schematic diagram of disease causing Cx26 mutants.....	9
Figure 1.3 Schematic diagram of disease causing Cx30 mutants.....	12
Figure 2.1 N14K and D50N Cx26 mutants linked to KIDS induce cell death.....	31
Figure 2.2 Cx26 mutants linked to skin disease are frequently localized to intracellular compartments and have limited dye transfer capability	34
Figure 2.3 Cx26 mutants exhibit dominant-negative properties on Cx26 in HeLa cells....	36
Figure 2.4 Cx26 mutants linked to syndromic disease exhibit trans-dominant properties on Cx30 in HeLa cells.....	39
Figure 2.5 N54K Cx26 displays trans-dominant inhibition of endogenous Cx43 in REKs	41
Figure 2.6 Cx26 mutants linked to syndromic disease display reduced hemichannel function in HeLa cells	44
Figure 2.7 Modeling the cellular characteristics autosomal dominant <i>GJB2</i> mutations	47
Figure 3.1 S17F/+ mice mimic KIDS skin characteristics and have several additional phenotypes	66
Figure 3.2 S17F/+ mice display thicker foot pad and tail epidermis and deregulated epidermal connexin expression.....	69
Figure 3.3 A88V/+ and A88V/A88V mice display normal foot pad epidermis and connexin expression	71

Figure 3.4 S17F/+ mice display abnormal keratinocyte differentiation in foot pad epidermis	73
Figure 3.5 A88V/+ and A88V/A88V mice display normal keratinocyte differentiation and proliferation in foot pad epidermis	75
Figure 3.6 Isolated keratinocyte cultures are highly pure.....	78
Figure 3.7 Keratinocytes isolated from S17F/+ neonates have reduced GJIC and collective cell migration.....	80
Figure 3.8 Keratinocytes isolated from A88V/A88V neonates display normal GJIC but increased collective cell migration.....	82
Figure 3.9 Mutant mice display normal wound closure, but S17F/+ mice exhibit abnormal epidermis remodeling.....	84

List of Appendices

Appendix 1	Cx26 ^{K14-S17F/+} neonates display an intact epidermal barrier	105
Appendix 2	Permissions for Artwork Reproduction	108
Appendix 3	Animal Use Protocol Approval.....	110

List of Abbreviations

3D – Three-dimensional

ANOVA – Analysis of variance

ATP – Adenosine triphosphate

AUC – Area under the curve

BSA – Bovine serum albumin

Ca²⁺ – Calcium

CaCl₂ – Calcium chloride

CC3 – Cleaved caspase 3

CT – Carboxy terminus

Cx26 – Connexin26

Cx26-RFP – red fluorescent protein tagged connexin26

Cx30 – Connexin30

Cx30-RFP – red fluorescent protein tagged connexin30

Cx43 – Connexin43

DCF-ECS – Divalent cation free extracellular solution

ddH₂O – double distilled water

DMEM – Dulbecco's modified Eagle's medium

dNTP – deoxynucleoside triphosphate

D50 – Aspartic acid at amino acid position 50

D50N – Aspartic acid to asparagine substitution at amino acid position 50

ECS – Extracellular solution

EDTA – Ethylenediaminetetraacetic acid

EL1 – Extracellular loop 1

EL2 – Extracellular loop 2

ER – Endoplasmic reticulum

GAPDH – Glyceraldehyde 3-phosphate dehydrogenase

GFP- Green fluorescent protein

GJB2 – Human gene for connexin26

Gjb2 – Mouse gene for connexin26

GJB6 – Human gene for connexin30

IL – Intracellular loop

IP₃ – Inositol trisphosphate

(k)Da – (kilo) Dalton

KIDS – Keratitis-ichthyosis-deafness syndrome

KOH – Potassium hydroxide

K-SFM – Keratinocyte serum-free medium

K14 – Keratin 14

L56 – Leucine at amino acid position 56

Mg²⁺ – Magnesium

mRNA – messenger ribonucleic acid

μCT – Micro-computed tomography

M163V – Methionine to valine substitution at amino acid position 163

NT – Amino terminus

N14 – Asparagine at amino acid position 14

N14K – Asparagine to lysine substitution at amino acid position 14

N54 – Asparagine at amino acid position 54

N54K – Asparagine to lysine substitution at amino acid position 54

Opti-MEM – Optimal minimal essential medium

PBS – Phosphate buffered saline

PBST – Phosphate buffered saline + Tween 20

PCNA – Proliferating cell nuclear antigen

PCR – Polymerase chain reaction

PDI – Protein disulfide isomerase

PGN – Peptidoglycan

PI – Propidium iodide

PPK – Palmoplantar keratoderma

REK – Rat epidermal keratinocyte

RFP – Red fluorescent protein

SDS-PAGE – Sodium dodecyl sulfate – polyacrylamide gel electrophoresis

SEM – Standard error of the mean

S17F – Serine to phenylalanine substitution at amino acid position 17

S183 – Serine at amino acid position 183

S183F – Serine to phenylalanine substitution at amino acid position 183

WT – Wild-type

Chapter 1

1.1 Introduction

1.1.1 Structure, Function and Life-Cycle of Connexins and Gap Junctions

Gap junctions are multimeric transmembrane channels that allow adjacent cells to communicate via the exchange of ions and small molecular messengers less than 1 kDa (Alexander and Goldberg, 2003). Gap junctions and their individual connexin monomers have been studied extensively since their discovery and characterization in the 1960's (Revel and Karnovsky, 1967). Cellular communication through gap junction channels plays an important role in cell physiology and these molecules have proven indispensable to human health (Garcia et al., 2016b). Connexins are 4-pass transmembrane proteins that can be found in nearly all cell types in humans (Laird, 2006). Every connexin molecule contains cytosolic amino (NT) and carboxy termini (CT), 2 extracellular loops (E1, E2), and one intracellular loop (IL) which serve specific roles to make a functional gap junction channel with various properties of molecular selectivity, channel gating, docking compatibility, and trafficking (Yeager and Harris, 2007). For example, the crystal structure of the Cx26 channel demonstrates that the NT can be located inside the pore suggesting it acts like a plug controlling channel gating and molecular selectivity (Maeda et al., 2009). Furthermore, Cx26 has a smaller pore size compared to other connexins (e.g. Cx43) which restricts molecular permeability (Weber et al., 2004).

Connexins are named according to their molecular weight in kDa: for example, connexin26 (Cx26) is approximately 26 kDa. They are organized into compatibility subgroups in which members can oligomerize to form mixed channels that have distinct channel properties from channels composed of the individual connexin types; for example Cx26 and Cx30 can intermix in connexons and gap junctions (Richard, 2000). Homomeric and heteromeric channels differ because they are composed of one or multiple connexin types, respectively (Richard, 2000). This variability dramatically increases the number of channel possibilities and intercellular communication characteristics in cells expressing multiple connexins – further reinforcing their complexity in cellular communication.

Connexins are co-translationally inserted into the endoplasmic reticulum and travel to the Golgi apparatus where many oligomerize to form connexons (Musil and Goodenough, 1993). Small vesicles containing connexons traffic and fuse with the plasma membrane where they may function as un-docked hemichannels to couple the cell to the extracellular milieu (Goodenough and Paul, 2003). When a connexon docks with another from an adjacent cell, a gap junction channel is formed, which allows for signaling molecules to pass between the cytosol of both cells in a process called gap junctional intercellular communication (GJIC) (Goodenough and Paul, 2009). Gap junction channels often tightly cluster in the plasma membrane to form highly organized structures called gap junction plaques which create an appositional region with a high degree of cytosolic coupling. Some connexins can be phosphorylated to influence channel function (Lampe and Lau, 2004) or bind with any number of intracellular proteins suggesting they may have additional non-channel functions (Laird, 2006). For example, the C-terminus of Cx43 is known to bind to several intracellular proteins including a specific domain of the zona-occludens-1 protein which is best known to be involved in the formation of tight junctions (Giepmans and Moolenaar, 1998; Toyofuku et al., 1998). These findings suggest gap junctions at the membrane may also support intercellular adhesion in addition to communication (Prochnow and Dermietzel, 2008). Gap junction plaques can vary greatly in size (Zampighi et al., 1989) and composition wherein different channel types are known to mix, or form separate clusters within a larger combined plaque (Kelly et al., 2015). Gap junctions generally have a half-life of 2 to 5 hours (Beardslee et al., 1998; Fallon and Goodenough, 1981) and it is thought that their rapid turnover and reassembly allows the cell to respond quickly to disruptions in tissue homeostasis by making necessary changes in the level of GJIC: for example, following tissue injury (Churko and Laird, 2013).

1.1.2 Connexin Gene Mutations and Human Disease

Twenty-one members exist in the connexin family and all have distinct, yet often overlapping tissue expression profiles, suggesting they are critical to human physiology (Avshalumova et al., 2014; van Steensel, 2004). Furthermore, connexin gene mutations have been linked to many human pathologies including skin disorders, hearing loss, cardiopathies, neurodegenerative diseases, bone and cartilage abnormalities, and cataracts (Garcia et al., 2016b). Due to the complexity of the connexin life cycle, connexin mutations can affect their

intracellular trafficking, hemichannel function, gap junction function, stability at the cell membrane, or even compatibility with other connexins (Garcia et al., 2016a; Kelly et al., 2014; Scott et al., 2012). Not surprisingly, connexin gene mutations often result in disease affecting multiple tissues that express the specific connexin (Garcia et al., 2016b). This is exemplified in patients harbouring *GJB2* mutations that have hearing loss with the comorbidity of skin disease due to the expression of Cx26 in both the inner ear and epidermis (Arita et al., 2006; de Zwart-Storm et al., 2008b; Martin and van Steensel, 2015; Richard et al., 2004). In addition, some connexin mutants produce no disease at all, likely because connexins have the ability to compensate for others within the same subgroup (Zheng-Fischhofer et al., 2007). This phenomenon is evident in the case of the Bart-Pumphrey Syndrome-causing N54K Cx26 mutant in the skin, which lowers Cx26 expression, but is compensated by an increased expression of Cx30 (Richard et al., 2004). Human epidermis expresses 7 connexin proteins in overlapping stages of keratinocyte differentiation including Cx26, Cx30, and Cx43, making the skin an extremely complex tissue in terms of intercellular communication. (Di et al., 2001; Martin et al., 2014). Due to the dynamic nature of this outward-facing stratified epithelium, a high level of intercellular communication is likely required to coordinate the correct balance of keratinocyte proliferation and differentiation.

1.1.3 Epidermal Physiology

Human and mouse epidermis (**Fig. 1.1**) consist of four principle strata of keratinocytes; the stratum basale, stratum spinosum, stratum granulosum, and stratum corneum which faces the external environment (Menon et al., 2012). Highly proliferative basal keratinocytes detach from the underlying basement membrane and undergo a ~14-day terminal differentiation program as they transition through the epidermal layers (Candi et al., 2005; Segre, 2006). Keratinocytes of the stratum spinosum synthesize keratin filaments that form an extensive cytoskeleton to provide mechanical strength to cells (Segre, 2006). Keratinocytes of the stratum granulosum produce intracellular keratohyaline granules and lamellar bodies that release structural proteins and ceramides which further provide cells with mechanical strength and hydrophobicity. An important keratin filament aggregating protein, filaggrin, is released from keratohyaline granules and condenses the keratin cytoskeleton of differentiating keratinocytes to form flat sheet-like cells (Sandilands et al., 2009). Additionally, filaggrin is

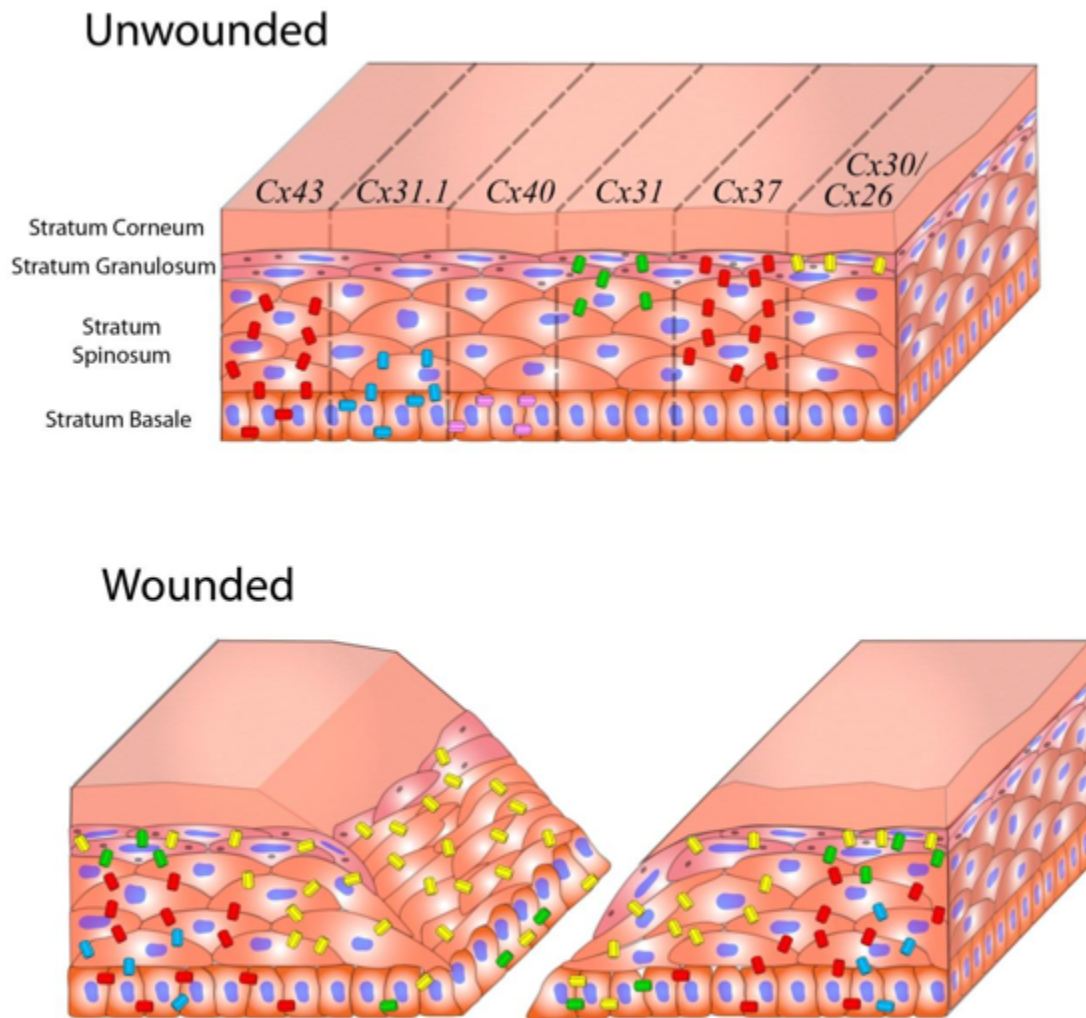


Figure 1.1

Figure 1.1. Connexin protein expression in unwounded and wounded mouse epidermis.

Adult epidermis is composed of 4 layers of keratinocytes (stratum basale, stratum spinosum, stratum granulosum, stratum corneum) which express up to 7 distinct connexin proteins in overlapping distribution patterns. Notably, Cx43 is expressed mostly in the stratum spinosum and in some cells of the stratum basale, while Cx26 and Cx30 are weakly expressed in the stratum granulosum. Twenty-four hours after an epidermal wound, Cx26 and Cx30 are expressed in keratinocytes at the wound margins, whereas Cx31.1, Cx40, and notably, Cx43 are markedly downregulated in keratinocytes at the wound margin. Figure used with permission from Dr. Jared Churko.

degraded by proteases in the stratum corneum into free amino acids and derivatives which constitute the skin's natural moisturizing factor (Sandilands et al., 2009). Terminal differentiation involves a specialized form of apoptosis, called cornification (Eckhart et al., 2013), whereby keratinocytes transition into enucleate flattened cells, which amongst many layers, weave together to form a protective external covering (Menon et al., 2012). Between interlocked corneocytes is a mortar of hydrophobic ceramides that generates an effective outward-in waterproof barrier (Menon et al., 2012). Together these layers give the epidermis its structural integrity, resiliency to damage, and impermeability to water and microbes (Segre, 2006). It is important to note that the epidermis (especially the stratum corneum) varies greatly in thickness between volar skin where it is thickest, and dorsal skin where it is considerably thinner (Segre, 2006). Epidermal thickness may correlate with the amount of mechanical stress endured by each anatomical region of skin.

A key factor thought to be involved in keratinocyte differentiation is an increasing calcium (Ca^{2+}) gradient found between cells of the stratum basale and granulosum (Bikle et al., 2012). Approximately $2\mu\text{M}$ of Ca^{2+} are found in the basal layer which triple by the granular layer, and fall to very low levels in the stratum corneum (Behne et al., 2011). Hemichannels have been shown to release adenosine triphosphate (ATP) that can influence purinergic signaling and intracellular Ca^{2+} handling in an autocrine/paracrine fashion (Baroja-Mazo et al., 2013), which may affect the natural calcium gradient. Furthermore, GJs regularly permit the passage of inositol-trisphosphate (IP_3) (Alexander and Goldberg, 2003) which is known to affect Ca^{2+} mobilization, and is likely important in the establishment and maintenance of this gradient, and therefore keratinocyte differentiation.

Cx43 has been highly characterized in many tissues including the skin due to its nearly ubiquitous expression and implication in human diseases (Laird, 2008). Cx43 is expressed in dermal fibroblasts as well as the keratinocytes of the stratum basale, spinosum, and granulosum (Churko and Laird, 2013). However, approximately 10% of basal cells do not express Cx43 and these are thought to resemble stem cells (Matic et al., 2002). Both Cx26 and Cx30 are expressed at low levels in the stratum granulosum and minimally in the stratum spinosum (Scott et al., 2012; Wiszniewski et al., 2000). Currently, the roles of Cx26 and Cx30 are not well understood in the skin but some studies have revealed Cx26 may influence

keratinocyte differentiation and/or proliferation (Djalilian et al., 2006; Lucke et al., 1999; Maher et al., 2005). However, researchers are uncovering the importance of connexins in skin health and wound healing as 11 inheritable skin diseases are correlated with mutations in 5 distinct connexin genes (Lilly et al., 2016).

1.1.4 Cutaneous Wound Healing

In the case of injury, the skin repairs itself through a highly dynamic process in which key events spatially and temporally overlap (Martin, 1997; Reinke and Sorg, 2012). Immediately following an injurious breach of the skin barrier, damaged blood vessels vasoconstrict to prevent excessive blood loss while thrombogenesis initiates the generation of a protective clot that plugs the exposed wound (Reinke and Sorg, 2012). Along with the release of cytokines from platelets, local blood vessels dilate to recruit immune cells to clean up debris and opportunistic pathogens (Martin, 1997). Damaged keratinocytes, endothelial cells, and invading immune cells secrete growth factors to initiate fibroblast proliferation and angiogenesis which infiltrates the thrombus to generate a dense granulation tissue composed of fibroblasts, thick collagen bundles, immune cells, and a dense capillary network (Martin, 1997). Growth factors also stimulate wound edge keratinocytes to adopt migratory behaviour wherein they crawl along the underside of the granulation tissue, while keratinocytes behind wound margins become highly proliferative to aid in re-epithelialization (Martin, 1997). Upon re-epithelialization, keratinocytes differentiate to re-establish the functional epidermal layers as cells in the granulation tissue undergo apoptosis until the entire tissue and clot are lost (Reinke and Sorg, 2012). The time required for complete epidermal re-establishment following wounding can vary greatly depending on the severity and type of wound, the age of the individual, and the presence of infection (Martin, 1997). Notably, diabetics display poor wound healing capabilities and often develop chronic non-healing wounds (Lim et al., 2015). While this context is undoubtedly multi-factorial, some suggest that a deregulation of epidermal connexins contributes to impaired healing in diabetics (Wang et al., 2007a). In addition, chronic venous leg ulcers have repeatedly demonstrated chronically upregulated Cx26, Cx30, and Cx43, suggesting that dynamic connexin regulation is necessary for proper wound healing (Brandner et al., 2004; Ghatnekar et al., 2015; Mendoza-Naranjo et al., 2012; Sutcliffe et al., 2015).

1.1.5 Connexins Involved in Cutaneous Wound Healing

It has been found that during normal wound healing, extensive gap junction remodeling occurs (Becker et al., 2012; Churko and Laird, 2013). Several studies have shown a dramatic decrease in the expression of Cx43 in keratinocytes surrounding the wound site at the onset of healing (Brandner et al., 2004; Goliger and Paul, 1995; Kretz et al., 2003; Lampe et al., 1998). Furthermore, reducing Cx43 expression has been shown to improve keratinocyte proliferation and migration, limit inflammation and scarring, and promote overall beneficial wound healing outcomes (Churko et al., 2012; Ghatnekar et al., 2015; Mori et al., 2006; Qiu et al., 2003). On the other hand, both Cx26 and Cx30, which are normally located in the stratum granulosum, are expressed at high levels throughout all layers of the epidermis surrounding the wound site early in healing (Coutinho et al., 2003; Davis et al., 2013; Djalilian et al., 2006; Goliger and Paul, 1995; Kretz et al., 2003; Lemaitre et al., 2006). Down-regulation of these connexins later in the healing process is normal and may be necessary for later stages of healing (Brandner et al., 2004; Djalilian et al., 2006). Shortly after wounding, keratinocyte hyperproliferation results in epidermal thickening (Martin, 1997), and since numerous gain of function Cx26 and Cx30 mutants lead to hyperproliferative skin diseases (Xu and Nicholson, 2013), it is possible these connexins may promote a proliferative burst to jump start wound healing. However, little is known as to what roles Cx26 and Cx30 play in maintaining healthy epidermis. Furthermore, although their remodeling has been demonstrated during wound healing, it is unknown whether Cx26 and Cx30 gene mutations alter wound healing properties.

1.1.6 *GJB2* Mutations Involved in Skin Disease

Cx26 is encoded by the *GJB2* gene and is becoming a highly characterized member of the connexin family. To date, well over 100 distinct *GJB2* mutations have been reported in patients with skin disease and/or hearing loss (Connexin-deafness [homepage](#)) (Laird, 2006; Lilly et al., 2016; Xu and Nicholson, 2013). Refer to **Fig. 1.2** for an extensive depiction of these mutants on the Cx26 polypeptide. Six distinct skin diseases are specifically linked to *GJB2* mutations that present with focal, or generalized skin abnormalities and often feature keratoderma (thickening of the epidermis) (Lilly et al., 2016). For example, Keratitis-Ichthyosis-Deafness Syndrome (KIDS), Bart-Pumphrey Syndrome and Vohwinkel

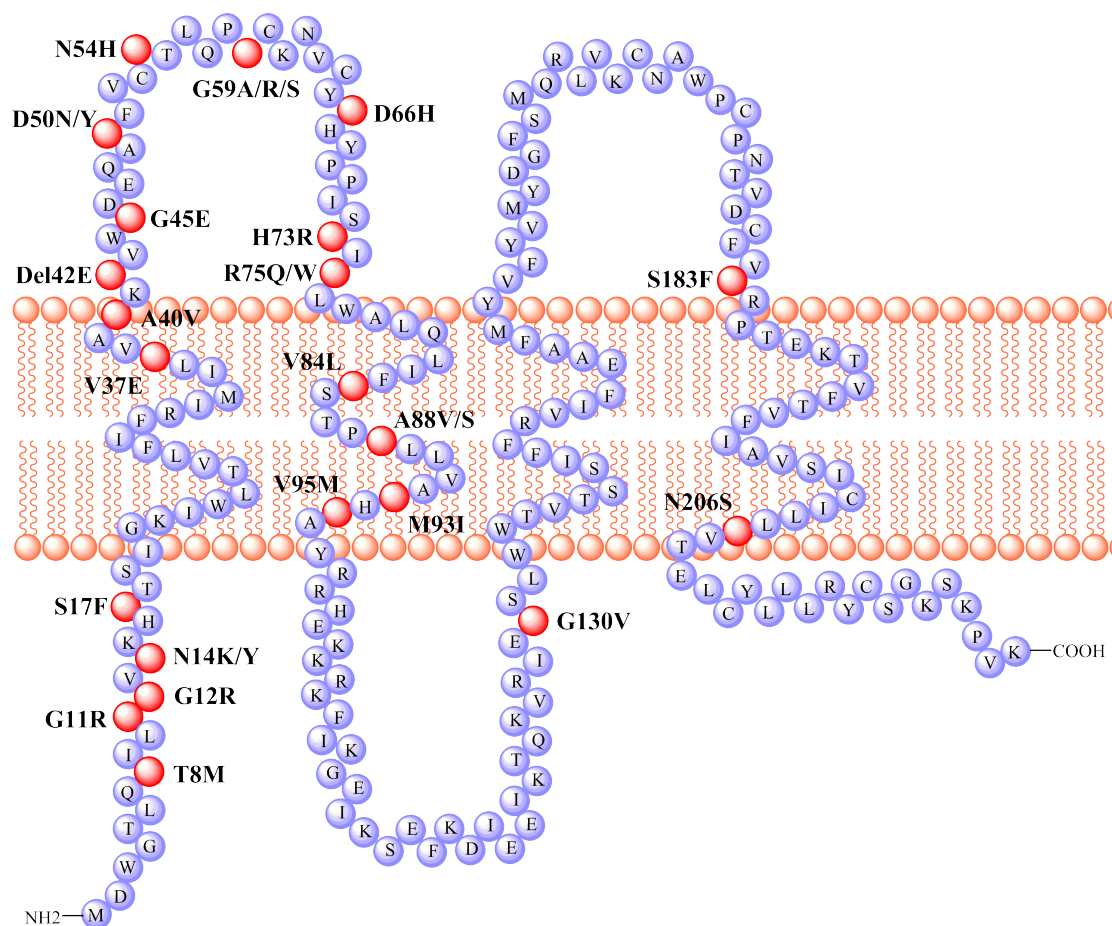


Figure 1.2

Figure 1.2. Composite diagram of reported disease-linked Cx26 mutants.

The Cx26 polypeptide sequence highlighting the location of numerous disease-linked mutants. Spanning every domain of the Cx26 protein, over 100 distinct Cx26 mutants (not all shown) are linked to non-syndromic hearing loss (green circles) and syndromic skin disease (red circles).

Syndrome, stem from *GJB2* mutations and are characterized as diffuse, hyperproliferative skin diseases, whereas palmoplantar keratoderma with deafness can present with focal keratoderma on volar skin (Avshalumova et al., 2014). A *GJB2* gene mutation however, may lead to skin disease, hearing impairments, or both, and some mutations lead to more profound disease than others (Lee and White, 2009). For example, in KIDS alone, the G45E Cx26 mutant leads to an infant-lethal form (Koppelhus et al., 2011), while a milder form is caused by the N14K mutant (Lazic et al., 2008). Numerous mutants affecting the NT (amino acids, 1-20) and EL1 (amino acids 41-75) domains are known to form leaky hemichannels (G11R, G12R, N14K, N14Y, S17F, A40V, G45E, D50A, D50N) and are linked to syndromic pathologies displaying severe skin disease and hearing impairments (Garcia et al., 2016a). Interestingly, the S17F Cx26 mutant has been reported to bind with Cx43, a non-traditional binding partner, and form leaky heteromeric hemichannels (Garcia et al., 2015). The connection between leaky hemichannels and syndromic disease suggests they may contribute to both skin disease and hearing loss in patients. Studies have also shown that some *GJB2* mutations render non-functional Cx26 gap junctions but do not confer any form of skin disease, likely due to compensation from other connexins in the epidermis (Scott et al., 2012). A possible reason for these differences among disease potential could be due to certain mutations acting in a trans-dominant manner by affecting other connexins. While many mutations have been identified, it is not fully understood how and which mutant connexins interact with other connexins, modify channel properties, and finally disrupt tissue homeostasis.

1.1.7 *GJB6* Mutations Involved in Skin Disease

Cx30 is encoded by the *GJB6* gene and has received less investigative attention than Cx26 and Cx43. Currently, five mutations are linked to syndromic skin diseases (Clouston Syndrome, KIDS, and Vohwinkel Syndrome) and two are linked to non-syndromic hearing loss (**Fig.1.3**). Clouston Syndrome is a rare condition characterized by varying severities of palmoplantar keratoderma, alopecia, and nail dystrophy (Lamartine et al., 2000) and is prevalent among the French-Canadian population due to a founder effect (Kibar et al., 2000). Some mutations leading to skin disease have been shown to induce cell death pathways *in vitro* (V37E and A88V) (Berger et al., 2014), while others display trafficking defects (G11R and G59R) (Essenfelder et al., 2004; Nemoto-Hasebe et al., 2009). Furthermore, G11R and

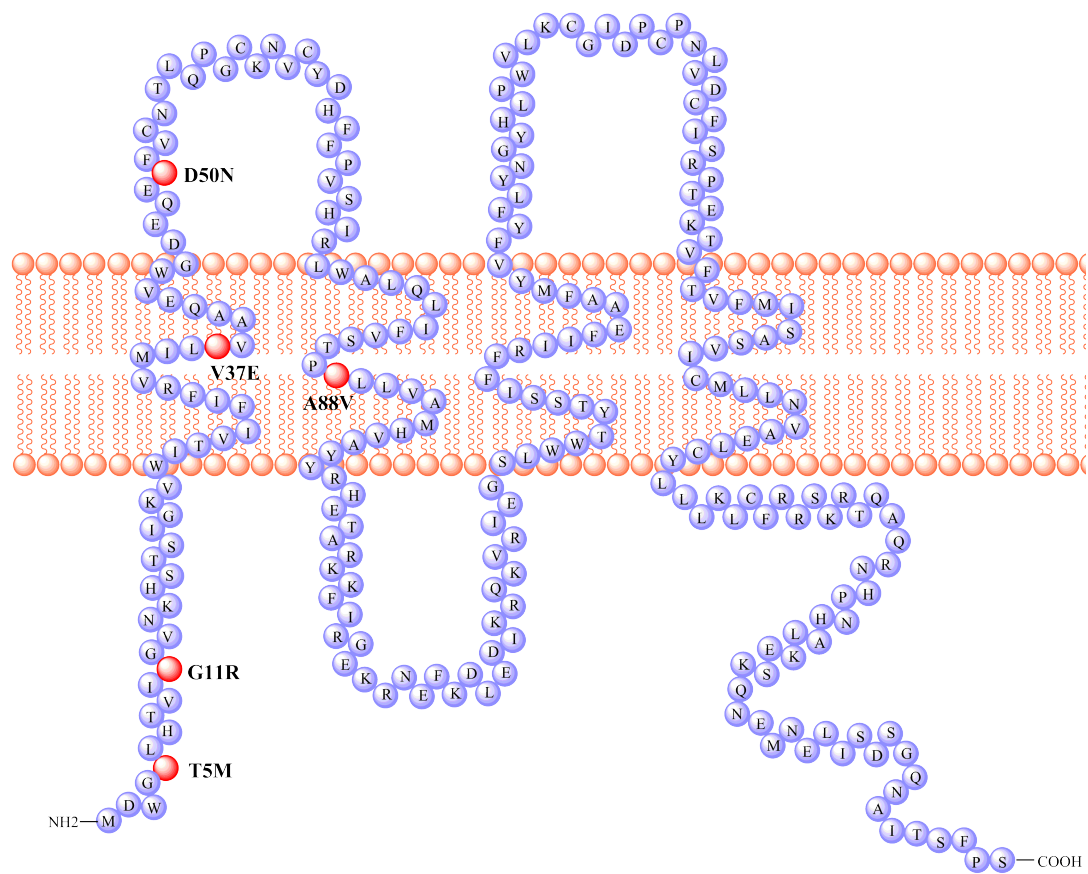


Figure 1.3

Figure 1.3. Composite diagram of reported disease-linked Cx30 mutants.

The Cx30 polypeptide sequence highlighting the location of disease-linked mutants. T5M and A40V are the only mutants linked to non-syndromic hearing loss (green circles), whereas the 5 other mutants are associated with syndromic skin diseases (red circles).

A88V Cx30 may form leaky hemichannels that increase purinergic signaling and deregulate keratinocyte proliferation/differentiation (Berger et al., 2014; Essensfelder et al., 2004). Despite these observations, it is still poorly understood how Cx30 contributes to overall skin integrity. However, relative to Cx26, the lack of Cx30 mutations linked to hearing loss and skin disease predicts that Cx30 may have a smaller contribution to auditory and epidermal physiology.

1.1.8 Modeling Connexin-Linked Skin Disease

While cellular based experiments are useful for understanding certain aspects of gap junction function or malfunction, animal based models are superior for understanding the role of connexins in the skin as a complete tissue. Numerous researchers have employed rodent models to study connexins in the skin and also to investigate their effects on wound healing (Bakirtzis et al., 2003; Bosen et al., 2014; Churko et al., 2011a; Djalilian et al., 2006; Schutz et al., 2011; Wang et al., 2007a). Several of these models express connexin mutants to genetically mirror human connexin-linked skin diseases. For example, the G60S Cx43 mouse represents human oculodentodigital dysplasia (Churko et al., 2011a), the conditional D66H Cx26 mouse represents true Vohwinkel Syndrome (Bakirtzis et al., 2003), the F137L Cx31 mouse represents erythrokeratoderma variabilis (Schnichels et al., 2007), and as I will discuss, the S17F Cx26 and A88V Cx30 mice represent human KIDS, and Clouston Syndrome, respectively (Bosen et al., 2014; Schutz et al., 2011). Additionally, numerous studies, including previous work from our lab (Churko et al., 2012; Churko et al., 2010; Churko et al., 2011b; Langlois et al., 2007; Maher et al., 2005), have generated a greater understanding of the role of Cx43 in the epidermis, its effects on wound healing, and how certain mutations impact skin health. Some researchers have repeatedly demonstrated the benefits of Cx43 inhibition during healing (Coutinho et al., 2005; Ghatnekar et al., 2015; Grek et al., 2015; Grupcheva et al., 2012; Qiu et al., 2003) and even started companies to develop and commercialize Cx43-targeted wound therapies (Colin Green and David Becker – CoDa Therapeutics; Gautnam Ghatnekar – FirstString Research). There is, however, only one Cx26 mouse model that has been used to assess the influence of Cx26 on wound healing, which has proposed a role for Cx26 during wound inflammation and epidermal remodeling (Djalilian et al., 2006). Despite this, and the evidence suggesting Cx26 and Cx30 are dynamically regulated

during proper wound healing, there remains insufficient animal models to investigate their impact and potential therapeutic value towards wound healing.

Recently, a group from Germany lead by Klaus Willecke has generated two disease-linked mutant mouse strains that are suitable models of human KIDS and Clouston Syndrome: the Cx26^{S17F/+} mouse and Cx30^{A88V/+} mouse, respectively (Bosen et al., 2014; Schutz et al., 2011). As described in this thesis, our laboratory has generated a tissue specific S17F Cx26 mouse (Cx26^{K14-S17F/+}) in which the mutant connexin was expressed solely in tissues expressing keratin 14 (K14). Cre-recombinase insertion of the mutant gene only occurred in tissues expressing K14 and resulted in selective expression of S17F Cx26 in basal cells of the epidermis and a few other stratified epithelial tissues, while under the expression of the endogenous Cx26 promoter. This allowed us to study the effect of the S17F Cx26 mutant on the epidermis with presumably far less complications from its expression in other tissues such as the liver, kidney, intestine, placenta, mammary gland, and brain (Filippov et al., 2003; McLachlan et al., 2007). In addition, we have obtained the A88V Cx30 mutant mice (Cx30^{A88V/+} and Cx30^{A88V/A88V}) from the Willecke laboratory. Together, we will use these mice to gain insight into the physiological and pathological mechanisms in which connexins and connexin mutants affect epidermal homeostasis and wound healing. The importance of using disease-relevant mouse models lies in the genetic consistency that reference cell experiments cannot recapitulate. These mice have the correct ratio of mutant to wild-type alleles; something that is very difficult to reliably attain in cellular transfection-based experiments. This gives us the advantage of being able to use mutant mice to culture primary keratinocytes for *in vitro* experiments, while the genetic dosage of the mutant alleles mirrors that of the human disease. Lastly, these mice allowed us to examine the temporal and spatial localization of mutant connexins within intact murine epidermis while establishing a platform to perform wound healing experiments.

1.1.9 Hypothesis

We hypothesized that disease-linked Cx26 and Cx30 mutants disrupt epidermal homeostasis and wound healing through modification of keratinocyte proliferation, differentiation, and migration. To test this hypothesis, we expressed five Cx26 mutants (N14K, D50N, N54K,

M163V, S183F) in reference cells and keratinocytes to evaluate their cellular characteristics. For each mutant, we investigated their ability to traffic, form gap junction channels, plasma membrane hemichannels, and to exhibit trans-dominant effects on Cx30 and Cx43, as well as the ability to induce cell death. We further modeled connexin-linked skin diseases using a tissue-specific S17F Cx26 mutant mouse, and a global A88V Cx30 mutant mouse. The foot pad skin of these mice were assessed to investigate the effect of the mutants on keratinocyte differentiation, proliferation, and skin morphology. Primary keratinocytes were isolated from these mice to assess connexin localization, overall GJIC competency, and collective cell migration. Finally, wound healing was assessed in these mice using a standard dorsal skin punch biopsy. The goal of these investigations was to determine the effect of Cx26 and Cx30 mutants on the epidermis and wound healing, and to shed light on the role of Cx26 and Cx30 in normal healthy skin.

1.1.10 Objectives

The specific objectives for this study were to:

1. Characterize the skin phenotype in mice harbouring Cx26 and Cx30 mutants.
2. Examine the consequences of keratinocytes harbouring connexin mutants in primary mouse cultures and cells engineered to express Cx26 mutants.
3. Assess epidermal wound closure and remodeling in response to wounding in mutant mice and littermate controls.

1.2 References

- Alexander, D.B., and G.S. Goldberg. 2003. Transfer of biologically important molecules between cells through gap junction channels. *Curr Med Chem.* 10:2045-2058.
- Arita, K., M. Akiyama, T. Aizawa, Y. Umetsu, I. Segawa, M. Goto, D. Sawamura, M. Demura, K. Kawano, and H. Shimizu. 2006. A novel N14Y mutation in Connexin26 in keratitis-ichthyosis-deafness syndrome: analyses of altered gap junctional communication and molecular structure of N terminus of mutated Connexin26. *Am J Pathol.* 169:416-423.
- Avshalumova, L., J. Fabrikant, and A. Koriakos. 2014. Overview of skin diseases linked to connexin gene mutations. *Int J Dermatol.* 53:192-205.
- Bakirtzis, G., R. Choudhry, T. Aasen, L. Shore, K. Brown, S. Bryson, S. Forrow, L. Tetley, M. Finbow, D. Greenhalgh, and M. Hodgins. 2003. Targeted epidermal expression of mutant Connexin 26(D66H) mimics true Vohwinkel syndrome and provides a model for the pathogenesis of dominant connexin disorders. *Hum Mol Genet.* 12:1737-1744.
- Baroja-Mazo, A., M. Barbera-Cremades, and P. Pelegrin. 2013. The participation of plasma membrane hemichannels to purinergic signaling. *Biochim Biophys Acta.* 1828:79-93.
- Beardslee, M.A., J.G. Laing, E.C. Beyer, and J.E. Saffitz. 1998. Rapid turnover of connexin43 in the adult rat heart. *Circ Res.* 83:629-635.
- Becker, D.L., C. Thrasivoulou, and A.R. Phillips. 2012. Connexins in wound healing; perspectives in diabetic patients. *Biochim Biophys Acta.* 1818:2068-2075.
- Behne, M.J., S. Sanchez, N.P. Barry, N. Kirschner, W. Meyer, T.M. Mauro, I. Moll, and E. Gratton. 2011. Major translocation of calcium upon epidermal barrier insult: imaging and quantification via FLIM/Fourier vector analysis. *Arch Dermatol Res.* 303:103-115.
- Berger, A.C., J.J. Kelly, P. Lajoie, Q. Shao, and D.W. Laird. 2014. Mutations in Cx30 that are linked to skin disease and non-syndromic hearing loss exhibit several distinct cellular pathologies. *J Cell Sci.* 127:1751-1764.
- Bikle, D.D., Z. Xie, and C.L. Tu. 2012. Calcium regulation of keratinocyte differentiation. *Expert Rev Endocrinol Metab.* 7:461-472.
- Bosen, F., M. Schutz, A. Beinhauer, N. Strenzke, T. Franz, and K. Willecke. 2014. The Clouston syndrome mutation connexin30 A88V leads to hyperproliferation of sebaceous glands and hearing impairments in mice. *FEBS Lett.* 588:1795-1801.
- Brandner, J.M., P. Houdek, B. Husing, C. Kaiser, and I. Moll. 2004. Connexins 26, 30, and 43: differences among spontaneous, chronic, and accelerated human wound healing. *J Invest Dermatol.* 122:1310-1320.

- Candi, E., R. Schmidt, and G. Melino. 2005. The cornified envelope: a model of cell death in the skin. *Nat Rev Mol Cell Biol.* 6:328-340.
- Churko, J.M., J. Chan, Q. Shao, and D.W. Laird. 2011a. The G60S connexin43 mutant regulates hair growth and hair fiber morphology in a mouse model of human oculodentodigital dysplasia. *J Invest Dermatol.* 131:2197-2204.
- Churko, J.M., J.J. Kelly, A. Macdonald, J. Lee, J. Sampson, D. Bai, and D.W. Laird. 2012. The G60S Cx43 mutant enhances keratinocyte proliferation and differentiation. *Exp Dermatol.* 21:612-618.
- Churko, J.M., and D.W. Laird. 2013. Gap junction remodeling in skin repair following wounding and disease. *Physiology (Bethesda).* 28:190-198.
- Churko, J.M., S. Langlois, X. Pan, Q. Shao, and D.W. Laird. 2010. The potency of the fs260 connexin43 mutant to impair keratinocyte differentiation is distinct from other disease-linked connexin43 mutants. *Biochem J.* 429:473-483.
- Churko, J.M., Q. Shao, X.Q. Gong, K.J. Swoboda, D. Bai, J. Sampson, and D.W. Laird. 2011b. Human dermal fibroblasts derived from oculodentodigital dysplasia patients suggest that patients may have wound-healing defects. *Hum Mutat.* 32:456-466.
- Coutinho, P., C. Qiu, S. Frank, K. Tamber, and D. Becker. 2003. Dynamic changes in connexin expression correlate with key events in the wound healing process. *Cell Biol Int.* 27:525-541.
- Coutinho, P., C. Qiu, S. Frank, C.M. Wang, T. Brown, C.R. Green, and D.L. Becker. 2005. Limiting burn extension by transient inhibition of Connexin43 expression at the site of injury. *Br J Plast Surg.* 58:658-667.
- Davis, N.G., A. Phillips, and D.L. Becker. 2013. Connexin dynamics in the privileged wound healing of the buccal mucosa. *Wound Repair Regen.* 21:571-578.
- de Zwart-Storm, E.A., M. van Geel, P.A. van Neer, P.M. Steijlen, P.E. Martin, and M.A. van Steensel. 2008. A novel missense mutation in the second extracellular domain of GJB2, p.Ser183Phe, causes a syndrome of focal palmoplantar keratoderma with deafness. *Am J Pathol.* 173:1113-1119.
- Di, W.L., E.L. Rugg, I.M. Leigh, and D.P. Kelsell. 2001. Multiple epidermal connexins are expressed in different keratinocyte subpopulations including connexin 31. *J Invest Dermatol.* 117:958-964.
- Djalilian, A.R., D. McGaughey, S. Patel, E.Y. Seo, C. Yang, J. Cheng, M. Tomic, S. Sinha, A. Ishida-Yamamoto, and J.A. Segre. 2006. Connexin 26 regulates epidermal barrier and wound remodeling and promotes psoriasiform response. *J Clin Invest.* 116:1243-1253.

- Eckhart, L., S. Lippens, E. Tschachler, and W. Declercq. 2013. Cell death by cornification. *Biochim Biophys Acta*. 1833:3471-3480.
- Essenfelder, G.M., R. Bruzzone, J. Lamartine, A. Charollais, C. Blanchet-Bardon, M.T. Barbe, P. Meda, and G. Waksman. 2004. Connexin30 mutations responsible for hidrotic ectodermal dysplasia cause abnormal hemichannel activity. *Hum Mol Genet*. 13:1703-1714.
- Fallon, R.F., and D.A. Goodenough. 1981. Five-hour half-life of mouse liver gap-junction protein. *J Cell Biol*. 90:521-526.
- Filippov, M.A., S.G. Hormuzdi, E.C. Fuchs, and H. Monyer. 2003. A reporter allele for investigating connexin 26 gene expression in the mouse brain. *Eur J Neurosci*. 18:3183-3192.
- Garcia, I.E., F. Bosen, P. Mujica, A. Pupo, C. Flores-Munoz, O. Jara, C. Gonzalez, K. Willecke, and A.D. Martinez. 2016a. From Hyperactive Connexin26 Hemichannels to Impairments in Epidermal Calcium Gradient and Permeability Barrier in the Keratitis-Ichthyosis-Deafness Syndrome. *J Invest Dermatol*. 136:574-583.
- Garcia, I.E., J. Maripillan, O. Jara, R. Ceriani, A. Palacios-Munoz, J. Ramachandran, P. Olivero, T. Perez-Acle, C. Gonzalez, J.C. Saez, J.E. Contreras, and A.D. Martinez. 2015. Keratitis-ichthyosis-deafness syndrome-associated Cx26 mutants produce nonfunctional gap junctions but hyperactive hemichannels when co-expressed with wild type Cx43. *J Invest Dermatol*. 135:1338-1347.
- Garcia, I.E., P. Prado, A. Pupo, O. Jara, D. Rojas-Gomez, P. Mujica, C. Flores-Munoz, J. Gonzalez-Casanova, C. Soto-Riveros, B.I. Pinto, M.A. Retamal, C. Gonzalez, and A.D. Martinez. 2016b. Connexinopathies: a structural and functional glimpse. *BMC Cell Biol*. 17 Suppl 1:17.
- Ghatnekar, G.S., C.L. Grek, D.G. Armstrong, S.C. Desai, and R.G. Gourdie. 2015. The effect of a connexin43-based Peptide on the healing of chronic venous leg ulcers: a multicenter, randomized trial. *J Invest Dermatol*. 135:289-298.
- Giepman, B.N., and W.H. Moolenaar. 1998. The gap junction protein connexin43 interacts with the second PDZ domain of the zona occludens-1 protein. *Curr Biol*. 8:931-934.
- Goliger, J.A., and D.L. Paul. 1995. Wounding alters epidermal connexin expression and gap junction-mediated intercellular communication. *Mol Biol Cell*. 6:1491-1501.
- Goodenough, D.A., and D.L. Paul. 2003. Beyond the gap: functions of unpaired connexon channels. *Nat Rev Mol Cell Biol*. 4:285-294.
- Goodenough, D.A., and D.L. Paul. 2009. Gap junctions. *Cold Spring Harb Perspect Biol*. 1:a002576.

- Grek, C.L., G.M. Prasad, V. Viswanathan, D.G. Armstrong, R.G. Gourdie, and G.S. Ghatnekar. 2015. Topical administration of a connexin43-based peptide augments healing of chronic neuropathic diabetic foot ulcers: A multicenter, randomized trial. *Wound Repair Regen.* 23:203-212.
- Grupcheva, C.N., W.T. Laux, I.D. Rupenthal, J. McGhee, C.N. McGhee, and C.R. Green. 2012. Improved corneal wound healing through modulation of gap junction communication using connexin43-specific antisense oligodeoxynucleotides. *Invest Ophthalmol Vis Sci.* 53:1130-1138.
- Kelly, J.J., Q. Shao, D.J. Jagger, and D.W. Laird. 2015. Cx30 exhibits unique characteristics including a long half-life when assembled into gap junctions. *J Cell Sci.* 128:3947-3960.
- Kibar, Z., M.P. Dube, J. Powell, C. McCuaig, S.J. Hayflick, J. Zonana, A. Hovnanian, U. Radhakrishna, S.E. Antonarakis, A. Benohanian, A.D. Sheeran, M.L. Stephan, R. Gosselin, D.P. Kelsell, A.L. Christianson, F.C. Fraser, V.M. Der Kaloustian, and G.A. Rouleau. 2000. Clouston hidrotic ectodermal dysplasia (HED): genetic homogeneity, presence of a founder effect in the French Canadian population and fine genetic mapping. *Eur J Hum Genet.* 8:372-380.
- Koppelhus, U., L. Tranebjaerg, G. Esberg, M. Ramsing, M. Lodahl, N.D. Rendtorff, H.V. Olesen, and M. Sommerlund. 2011. A novel mutation in the connexin 26 gene (GJB2) in a child with clinical and histological features of keratitis-ichthyosis-deafness (KID) syndrome. *Clin Exp Dermatol.* 36:142-148.
- Kretz, M., C. Euwens, S. Hombach, D. Eckardt, B. Teubner, O. Traub, K. Willecke, and T. Ott. 2003. Altered connexin expression and wound healing in the epidermis of connexin-deficient mice. *J Cell Sci.* 116:3443-3452.
- Laird, D.W. 2006. Life cycle of connexins in health and disease. *Biochem J.* 394:527-543.
- Laird, D.W. 2008. Closing the gap on autosomal dominant connexin-26 and connexin-43 mutants linked to human disease. *J Biol Chem.* 283:2997-3001.
- Lamartine, J., G. Munhoz Essenfelder, Z. Kibar, I. Lanneluc, E. Callouet, D. Laoudj, G. Lemaitre, C. Hand, S.J. Hayflick, J. Zonana, S. Antonarakis, U. Radhakrishna, D.P. Kelsell, A.L. Christianson, A. Pitaval, V. Der Kaloustian, C. Fraser, C. Blanchet-Bardon, G.A. Rouleau, and G. Waksman. 2000. Mutations in GJB6 cause hidrotic ectodermal dysplasia. *Nat Genet.* 26:142-144.
- Lampe, P.D., and A.F. Lau. 2004. The effects of connexin phosphorylation on gap junctional communication. *Int J Biochem Cell Biol.* 36:1171-1186.

- Lampe, P.D., B.P. Nguyen, S. Gil, M. Usui, J. Olerud, Y. Takada, and W.G. Carter. 1998. Cellular interaction of integrin $\alpha 3 \beta 1$ with laminin 5 promotes gap junctional communication. *J Cell Biol.* 143:1735-1747.
- Langlois, S., A.C. Maher, J.L. Manias, Q. Shao, G.M. Kidder, and D.W. Laird. 2007. Connexin levels regulate keratinocyte differentiation in the epidermis. *J Biol Chem.* 282:30171-30180.
- Lazic, T., K.A. Horii, G. Richard, D.I. Wasserman, and R.J. Antaya. 2008. A report of GJB2 (N14K) Connexin 26 mutation in two patients--a new subtype of KID syndrome? *Pediatr Dermatol.* 25:535-540.
- Lee, J.R., and T.W. White. 2009. Connexin-26 mutations in deafness and skin disease. *Expert Rev Mol Med.* 11:e35.
- Lemaitre, G., V. Sivan, J. Lamartine, J.M. Cosset, B. Cavelier-Balloy, D. Salomon, G. Waksman, and M.T. Martin. 2006. Connexin 30, a new marker of hyperproliferative epidermis. *Br J Dermatol.* 155:844-846.
- Lilly, E., C. Sellitto, L.M. Milstone, and T.W. White. 2016. Connexin channels in congenital skin disorders. *Semin Cell Dev Biol.* 50:4-12.
- Lim, Y.C., M.P. Bhatt, M.H. Kwon, D. Park, S. Na, Y.M. Kim, and K.S. Ha. 2015. Proinsulin C-peptide prevents impaired wound healing by activating angiogenesis in diabetes. *J Invest Dermatol.* 135:269-278.
- Lucke, T., R. Choudhry, R. Thom, I.S. Selmer, A.D. Burden, and M.B. Hodgins. 1999. Upregulation of connexin 26 is a feature of keratinocyte differentiation in hyperproliferative epidermis, vaginal epithelium, and buccal epithelium. *J Invest Dermatol.* 112:354-361.
- Maeda, S., S. Nakagawa, M. Suga, E. Yamashita, A. Oshima, Y. Fujiyoshi, and T. Tsukihara. 2009. Structure of the connexin 26 gap junction channel at 3.5 Å resolution. *Nature.* 458:597-602.
- Maher, A.C., T. Thomas, J.L. Riley, G. Veitch, Q. Shao, and D.W. Laird. 2005. Rat epidermal keratinocytes as an organotypic model for examining the role of Cx43 and Cx26 in skin differentiation. *Cell Commun Adhes.* 12:219-230.
- Martin, P. 1997. Wound healing--aiming for perfect skin regeneration. *Science.* 276:75-81.
- Martin, P.E., J.A. Easton, M.B. Hodgins, and C.S. Wright. 2014. Connexins: sensors of epidermal integrity that are therapeutic targets. *FEBS Lett.* 588:1304-1314.
- Martin, P.E., and M. van Steensel. 2015. Connexins and skin disease: insights into the role of beta connexins in skin homeostasis. *Cell Tissue Res.* 360:645-658.

- Matic, M., W.H. Evans, P.R. Brink, and M. Simon. 2002. Epidermal stem cells do not communicate through gap junctions. *J Invest Dermatol.* 118:110-116.
- McLachlan, E., Q. Shao, and D.W. Laird. 2007. Connexins and gap junctions in mammary gland development and breast cancer progression. *J Membr Biol.* 218:107-121.
- Mendoza-Naranjo, A., P. Cormie, A.E. Serrano, R. Hu, S. O'Neill, C.M. Wang, C. Thrasivoulou, K.T. Power, A. White, T. Serena, A.R. Phillips, and D.L. Becker. 2012. Targeting Cx43 and N-cadherin, which are abnormally upregulated in venous leg ulcers, influences migration, adhesion and activation of Rho GTPases. *PLoS One.* 7:e37374.
- Menon, G.K., G.W. Cleary, and M.E. Lane. 2012. The structure and function of the stratum corneum. *Int J Pharm.* 435:3-9.
- Mori, R., K.T. Power, C.M. Wang, P. Martin, and D.L. Becker. 2006. Acute downregulation of connexin43 at wound sites leads to a reduced inflammatory response, enhanced keratinocyte proliferation and wound fibroblast migration. *J Cell Sci.* 119:5193-5203.
- Musil, L.S., and D.A. Goodenough. 1993. Multisubunit assembly of an integral plasma membrane channel protein, gap junction connexin43, occurs after exit from the ER. *Cell.* 74:1065-1077.
- Nemoto-Hasebe, I., M. Akiyama, S. Kudo, A. Ishiko, A. Tanaka, K. Arita, and H. Shimizu. 2009. Novel mutation p.Gly59Arg in GJB6 encoding connexin 30 underlies palmoplantar keratoderma with pseudoainhum, knuckle pads and hearing loss. *Br J Dermatol.* 161:452-455.
- Prochnow, N., and R. Dermietzel. 2008. Connexons and cell adhesion: a romantic phase. *Histochem Cell Biol.* 130:71-77.
- Qiu, C., P. Coutinho, S. Frank, S. Franke, L.Y. Law, P. Martin, C.R. Green, and D.L. Becker. 2003. Targeting connexin43 expression accelerates the rate of wound repair. *Current Biology.* 13:1697-1703.
- Reinke, J.M., and H. Sorg. 2012. Wound repair and regeneration. *Eur Surg Res.* 49:35-43.
- Revel, J.P., and M.J. Karnovsky. 1967. Hexagonal array of subunits in intercellular junctions of the mouse heart and liver. *J Cell Biol.* 33:C7-C12.
- Richard, G. 2000. Connexins: a connection with the skin. *Exp Dermatol.* 9:77-96.
- Richard, G., N. Brown, A. Ishida-Yamamoto, and A. Krol. 2004. Expanding the phenotypic spectrum of Cx26 disorders: Bart-Pumphrey syndrome is caused by a novel missense mutation in GJB2. *J Invest Dermatol.* 123:856-863.

- Sandilands, A., C. Sutherland, A.D. Irvine, and W.H. McLean. 2009. Filaggrin in the frontline: role in skin barrier function and disease. *J Cell Sci.* 122:1285-1294.
- Schnichels, M., P. Worsdorfer, R. Dobrowolski, C. Markopoulos, M. Kretz, G. Schwarz, E. Winterhager, and K. Willecke. 2007. The connexin31 F137L mutant mouse as a model for the human skin disease erythrokeratoderma variabilis (EKV). *Hum Mol Genet.* 16:1216-1224.
- Schutz, M., T. Auth, A. Gehrt, F. Bosen, I. Korber, N. Strenzke, T. Moser, and K. Willecke. 2011. The connexin26 S17F mouse mutant represents a model for the human hereditary keratitis-ichthyosis-deafness syndrome. *Hum Mol Genet.* 20:28-39.
- Scott, C.A., D. Tattersall, E.A. O'Toole, and D.P. Kelsell. 2012. Connexins in epidermal homeostasis and skin disease. *Biochim Biophys Acta.* 1818:1952-1961.
- Segre, J.A. 2006. Epidermal barrier formation and recovery in skin disorders. *J Clin Invest.* 116:1150-1158.
- Sutcliffe, J.E., K.Y. Chin, C. Thrasivoulou, T.E. Serena, S. O'Neil, R. Hu, A.M. White, L. Madden, T. Richards, A.R. Phillips, and D.L. Becker. 2015. Abnormal connexin expression in human chronic wounds. *Br J Dermatol.* 173:1205-1215.
- Toyofuku, T., M. Yabuki, K. Otsu, T. Kuzuya, M. Hori, and M. Tada. 1998. Direct association of the gap junction protein connexin-43 with ZO-1 in cardiac myocytes. *J Biol Chem.* 273:12725-12731.
- van Steensel, M.A. 2004. Gap junction diseases of the skin. *Am J Med Genet C Semin Med Genet.* 131C:12-19.
- Wang, C.M., J. Lincoln, J.E. Cook, and D.L. Becker. 2007. Abnormal connexin expression underlies delayed wound healing in diabetic skin. *Diabetes.* 56:2809-2817.
- Weber, P.A., H.C. Chang, K.E. Spaeth, J.M. Nitsche, and B.J. Nicholson. 2004. The permeability of gap junction channels to probes of different size is dependent on connexin composition and permeant-pore affinities. *Biophys J.* 87:958-973.
- Wiszniewski, L., A. Limat, J.H. Saurat, P. Meda, and D. Salomon. 2000. Differential expression of connexins during stratification of human keratinocytes. *J Invest Dermatol.* 115:278-285.
- Xu, J., and B.J. Nicholson. 2013. The role of connexins in ear and skin physiology - functional insights from disease-associated mutations. *Biochim Biophys Acta.* 1828:167-178.
- Yeager, M., and A.L. Harris. 2007. Gap junction channel structure in the early 21st century: facts and fantasies. *Curr Opin Cell Biol.* 19:521-528.

- Zampighi, G.A., J.E. Hall, G.R. Ehrling, and S.A. Simon. 1989. The structural organization and protein composition of lens fiber junctions. *J Cell Biol.* 108:2255-2275.
- Zheng-Fischhofer, Q., M. Kibschull, M. Schnichels, M. Kretz, E. Petrasch-Parwez, J. Strotmann, H. Reucher, B.D. Lynn, J.I. Nagy, S.J. Lye, E. Winterhager, and K. Willecke. 2007. Characterization of connexin31.1-deficient mice reveals impaired placental development. *Dev Biol.* 312:258-271.

Chapter 2

Induction of cell death and gain-of-function properties of Cx26 mutants predict the severity of diseases linked to *GJB2* mutations

Here we investigated five autosomal dominant Cx26 mutants (N14K, D50N, N54K, M163V, S183F) that are linked to various syndromic or non-syndromic diseases to uncover the molecular mechanisms underpinning their link to disease. We demonstrated that when the N14K and D50N mutants were expressed in gap junction-deficient HeLa cells, cells were triggered into a cell death pathway. The N54K mutant was retained primarily within intracellular compartments and displayed trans-dominant properties on coexpressed Cx30 and Cx43. The S183F mutant formed some gap junction plaques but was largely retained within the cell and exhibited only a mild trans-dominant reduction in gap junctional intercellular communication when co-expressed with Cx30. The M163V mutant which causes hearing loss alone exhibited impaired gap junction function and showed no trans-dominant interactions. Taken together, we suggest that Cx26 mutants that promote cell death or cause reductions in the functions of connexins co-expressed in keratinocytes will lead to skin diseases and hearing loss while mutants that have reduced channel function but exhibit no aberrant effects on co-expressed connexins cause only hearing loss. Moreover, *GJB2* mutations that cause cell death lead to more severe syndromic disease.

A version of this chapter will be submitted for publication by the end of the month.

Authors: Eric R. Press, John J. Kelly, Katrina Chin, Anton Alaga, Qing Shao, and Dale W. Laird

2.1 Introduction

The *GJB2* gene encoding connexin26 (Cx26) has an estimated mutation prevalence of 3% in the general population (Chan and Chang, 2014). Globally, an estimated 17.3% of hearing loss cases are linked to bi-allelic *GJB2* mutations highlighting the importance of Cx26 in hearing (Chan and Chang, 2014). In addition, numerous syndromic diseases exhibiting hearing deficits and a variety of skin abnormalities are linked to *GJB2* missense mutations with autosomal dominant inheritance (Avshalumova et al., 2014). Interestingly, some speculate the pervasiveness of *GJB2* mutations may result from a selective heterozygote advantage (Chan and Chang, 2014) conferred by sub-clinical epidermal thickening and a stronger cutaneous barrier (D'Adamo et al., 2009). In humans, Cx26 is expressed in a variety of tissues and not surprisingly, in several cell types within the cochlea (Jagger and Forge, 2015) and in keratinocytes of the epidermis (Scott et al., 2012). Within these tissues, several other members of the connexin family are expressed, most notably Cx30 and Cx43, wherein mutations in their genes have also been implicated in syndromic diseases sharing some similar features (Avshalumova et al., 2014; Martin et al., 2014; Scott et al., 2012).

Cx26 is a gap junction protein that oligomerizes in the cell to form hexameric transmembrane channels called connexons (Laird, 2006). Connexons that span the plasma membrane are called hemichannels and may allow a cell to pass small signalling molecules between the cytosol and the extracellular environment (Laird, 2006). However, when hemichannels from adjacent cells dock together, they form a single conduit called a gap junction channel which connects the cytosol of these cells and facilitates gap junctional intercellular communication (GJIC) (Laird, 2006). ATP, IP₃, and cations frequently pass through Cx26 gap junction channels and have been shown to play important roles in regulating cell proliferation and differentiation as well as maintaining ionic homeostasis within tissues. (Alexander and Goldberg, 2003; Djalilian et al., 2006).

The Cx26 polypeptide chain has four transmembrane domains, two extracellular loops, an intracellular loop, and cytosolic N- and C- termini. The N-terminal domain (amino acid residues 1-20) is suggested to play a major role in voltage sensing and channel gating (Maeda et al., 2009). The extracellular loops (E1 and E2) (amino acid residues 41-75 and 155-192, respectively) are thought to be key domains for oligomerization and inter-channel docking

(Maeda et al., 2009). Disease-causing point mutations have been documented to affect every domain of the Cx26 polypeptide, and depending on the mutation and the motif that harbors the altered residue, variations can occur in connexin folding and trafficking, channel assembly, channel gating, half-life, degradation, and/or interactions between other co-expressed connexins (Laird, 2006). Some mutants have been shown to disrupt several connexin life-cycle characteristics (Garcia et al., 2015) increasing the complexity of delineating how *GJB2* gene mutations can cause diseases that affect one or more organs and vary in severity.

In this study we selected 5 autosomal dominant *GJB2* missense mutations that result in single amino acid substitutions in various domains of the Cx26 polypeptide and are linked to an array of auditory and skin pathologies. The N14K mutant causes a disease that shares symptoms with Clouston Syndrome and KIDS (Lazic et al., 2008), the D50N mutant leads to KIDS (Mazereeuw-Hautier et al., 2007), the N54K mutant results in Bart-Pumphrey syndrome (Richard et al., 2004), and the S183F mutant causes palmoplantar keratoderma and hearing loss (de Zwart-Storm et al., 2008b). Finally, the M163V mutant is linked to moderate hearing loss only (Marlin et al., 2001). Considering the pleiotropic nature of the Cx26 mutants, we proposed that mutants which give rise to similar clinical presentations would share common mechanisms of action.

Here we found that the N14K and D50N mutants leading to wide spread erythrokeratoderma and severe hearing loss caused cell death, the N54K and S183F mutants leading to palmoplantar keratoderma and hearing loss had trafficking defects and reduced channel function, and the M183V mutant leading to hearing loss alone had reduced channel function. Lastly, all mutants linked to syndromic disease had trans-dominant effects on co-expressed connexins.

2.2 Materials and Methods

2.2.1 Cell Culture

Connexin-deficient cervical cancer cells (HeLa) as described in (Elfgang et al., 1995) were purchased from ATCC and Rat Epidermal Keratinocytes (REKs) originally characterized in (Baden and Kubitius, 1983) were generously provided by Dr. Vincent Hascall. All cells were

grown in DMEM (Life Technologies Cat# 11965-092) supplemented with fetal bovine serum, 2 mM L-glutamine (Life Technologies Cat# 25030-081), penicillin and streptomycin according to (Penuela et al., 2007).

2.2.2 cDNA Constructs and Transfections

cDNA encoding human Cx26 was provided by Dr. C. G. Naus (University of British Columbia, Vancouver, BC, Canada). PCR was used to add XhoI and EcoRI restriction sites to the 5' and 3' ends of Cx26 and the resulting cDNAs were cloned into the pEGFP-N1 vector (BD Biosciences Clontech) and sequenced for verification with a 17-amino-acid linker sequence separating the Cx26 and GFP moieties. Constructs encoding human N14K, D50N, N54K, M163V, and S183F Cx26-GFP were further obtained from NorClone by using a QuikChange site-directed mutagenesis kit (Stratagene, La Jolla, CA) in accordance with the manufacturer's instructions. RFP-tagged Cx30 and Cx26 constructs were previously described (Berger et al., 2014). All constructs were validated by sequencing. GFP and RFP tags were shown not to dramatically affect connexin trafficking or protein function as previously shown (Thomas et al., 2005). Cells at ~60% confluency in 35 mm dishes were transiently transfected using Lipofectamine 2000. Transfection mixtures contained 200 μ l of Opti-MEM Reduced Serum Medium (Life Technologies Cat# 31985-070), 1 μ l of LF2000 transfection reagent (Invitrogen Cat# 11668019), and 1 μ g of GFP-tagged Cx26, N14K, D50N, N54K, M163V, or S183F cDNA constructs. For co-expression experiments, transfection mixtures differed in that 0.5 μ g of GFP-tagged constructs plus 0.5 μ g of RFP-tagged Cx26 or Cx30 were added to produce roughly equal expression of mutant to WT connexins. The mixture was gently swirled, incubated at room temperature for 10 minutes, and added drop-wise to cells growing in DMEM. All cells were used for experiments between 24-48 hours following transfection.

2.2.3 Immunofluorescent labeling

HeLa cells or REKs grown to ~80% confluency on sterile glass coverslips, were washed with phosphate-buffered saline (PBS), and fixed in an ice-cold solution of 80% methanol and 20% acetone for 10 minutes. Coverslips were then washed in PBS, blocked in a 2% bovine serum albumin (BSA) solution (diluted in PBS) for 30 minutes then incubated at room temperature for 1 hour with the following primary antibodies diluted in BSA solution: 1/500 mouse anti-protein disulfide isomerase (PDI) (Assay Designs Cat# SPA-891) or 1/500 rabbit anti-Cx43

(Sigma-Aldrich Cat# C6219) or 1/200 rabbit anti-cleaved caspase 3 (Sigma-Aldrich Cat# C8487). Secondary antibodies 1/500 Alexa-488-conjugated anti-mouse (Invitrogen: Cat# A11017) and 1/500 Alexa-555-conjugated anti-rabbit (Invitrogen Cat#A21429) were used to detect primary antibodies. Cells were then incubated for 10 minutes at room temperature with Hoechst 33342 (1/1000 diluted in ddH₂O) (Molecular Probes Cat# H3570), mounted with Airvol (containing 15% polyvinyl alcohol, 33% glycerin, and 0.1% sodium azide), and imaged with a Zeiss LSM 800 confocal Airyscan microscope equipped with ZenWorks software. Images were captured with a 63x oil immersion objective. Gap junction plaques between REKs were quantified in a blinded fashion by counting the number of green and red punctae at individual cell-cell interfaces. A minimum of 24 separate images were captured for each mutant and a one-way ANOVA was performed on the means of 3 biological replicates.

2.2.4 Dye Transfer Studies

HeLa cells or REKs grown to ~60% confluency and engineered to express GFP-tagged Cx26 or Cx26 mutants (and RFP-tagged connexins for co-expression experiments) as described above were microinjected with Alexa-Fluor-350 (410 Da, Molecular Probes Cat# A10439) to assess gap junction dye transfer previously described (Huang et al., 2013). Briefly, cells were microinjected using a fine glass needle attached to an Eppendorf FemtoJet automated microinjector. Cells were imaged using a Leica DM IRE2 epifluorescent microscope to visualize GFP and RFP, then one minute following microinjection, they were imaged again to visualize the spread of Alexa-Fluor-350. All images were captured with a 20x objective. The incidence of dye transfer within each trial was quantified as the percent of microinjected cells that passed dye to neighbouring cells and a one-way ANOVA was performed on the means of at least 3 replicates. Tukey's post-hoc test compared the means of each condition to the condition in which cells expressed GFP-tagged WT Cx26. Untransfected HeLa cells were used as negative controls and HeLa cells expressing Cx26-GFP only, or in addition to Cx26-RFP or Cx30-RFP served as positive controls for all dye transfer experiments in HeLa cells. Lastly, for dye transfer experiments in REKs, untransfected REKs, or REKs expressing Cx26-GFP were used as positive controls.

2.2.5 Hemichannel Assay

HeLa cells were seeded at low density to isolate cells from one another and then were

engineered to express Cx26 or Cx26 mutants as described above. Propidium iodide (PI) dye uptake assays to assess hemichannel activity were performed as noted in (Berger et al., 2014). Briefly, cells were washed in extracellular solution (ECS) (142 mM NaCl, 5.4 mM KCl, 1.4 mM MgCl₂, 2 mM CaCl₂, 10 mM HEPES, 25 mM D-glucose, osmolarity 298 mOsm, pH adjusted to 7.35 using NaOH) and then twice in either ECS or divalent cation free solution (DCF-ECS) (same as ECS but with Ca²⁺ and Mg²⁺ substituted for 2 mM EGTA). ECS or DCF-ECS containing 1 mg/ml PI (668.4 Da, Invitrogen) was added to the cells and incubated at 37°C for 15 minutes. Cells were washed 3 times with ECS, then ~40 isolated cells per replicate were imaged to visualize GFP and PI using the Leica microscope and OpenLab software. For each replicate, the number of cells containing PI was recorded as a percentage of the total number of GFP-positive cells and a two-way ANOVA was performed on the means of at least 3 replicates. Sidak's post-hoc test compared the means of ECS and DCF-ECF conditions.

2.2.6 Statistical Analysis

Graph Pad Prism version 6 was used for all statistical analysis and statistical significance was noted when $p < 0.05$. All histogram values represent the mean + SEM.

2.3 Results

2.3.1 N14K and D50N mutants induce cell death *in vitro*

In order to assess the impact of Cx26 mutants on cellular health, specific Cx26 mutants were expressed in GJIC-deficient HeLa cells. HeLa cells expressing the N14K and D50N mutants displayed pyknotic nuclei and blebbing as early as 24 hours post transfection, therefore we immunolabelled cleaved caspase 3 (CC3) to determine if cells expressing these mutants were undergoing apoptosis (**Fig 2.1A**). HeLa cells expressing the GFP-tagged N14K and D50N mutants displayed a high degree of CC3 immunolabeling (**Fig. 2.1B**), similar to cells treated with staurosporine, suggesting that the expression of these mutants in HeLa cells triggers apoptosis *in vitro*. Consequently, cell expressing the N14K or D50N mutants were deemed not suitable for further mutant localization or functional studies.

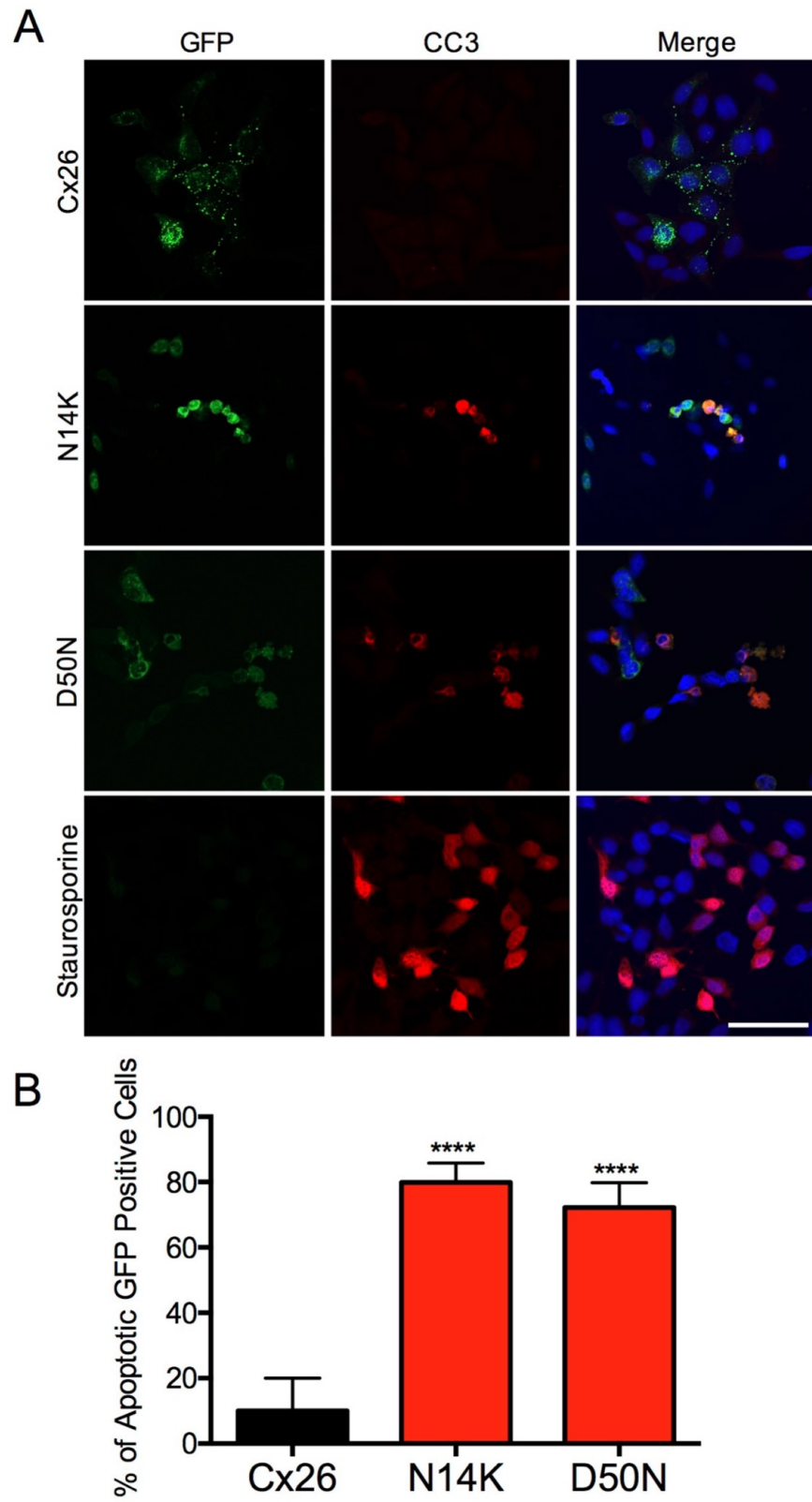


Figure 2.1

Fig. 2.1. N14K and D50N Cx26 mutants linked to KIDS induce cell death. (A) HeLa cells expressing GFP-tagged Cx26, N14K, and D50N mutants (green) were immunolabelled to highlight cleaved-caspase-3 (red) indicating cells undergoing apoptosis and nuclei were stained with Hoechst (blue). Cells treated for 2 hours with 1 μ M staurosporine were used as a positive control for apoptotic cells. (B) Cells expressing N14K and D50N mutants were often apoptotic compared to Cx26 expressing cells ****p<0.0001, N=3 separate experiments. Scale bar = 40 μ m.

2.3.2 N54K and S183F mutants have trafficking defects and impaired dye-transfer ability

Cx26 mutants associated with hearing loss and various skin diseases were expressed in HeLa cells to examine how a substituted amino acid in Cx26 may affect its trafficking, cellular localization, or gap junction function. Cx26 and the M163V mutant formed abundant gap junction plaques at cell-cell interfaces (**Fig. 2.2A**). The S183F mutant was retained primarily in intracellular compartments but formed a small number of gap junction plaques while the N54K mutant colocalized extensively with PDI labelling of the endoplasmic reticulum (ER) (**Fig. 2.2A**). The ability of the disease-linked mutants to form functional gap junction channels was assessed by quantifying intercellular transfer of microinjected Alexa-Fluor-350 in HeLa cells expressing Cx26 or the various mutants. Paired cells expressing Cx26 had nearly 100% incidence of dye transfer (**Fig. 2.2B**) while cells expressing the M163V mutant passed dye approximately 40% of the time. Cells expressing either the N54K or S183F mutants were essentially unable to establishing gap junction channels capable of dye transfer similar to controls (**Fig. 2.2B**).

2.3.3 Cx26 mutants exhibit dominant-negative effects on Cx26 function.

To assess the distribution and function of Cx26 mutants under physiological conditions where both wild type and mutant Cx26 are expressed in the same cell, we engineered HeLa cells to express RFP-tagged Cx26 and GFP-tagged Cx26 mutants at approximately a 1:1 ratio. Cx26 and the M163V mutant formed numerous gap junction plaques at the cell surface and were highly colocalized (**Fig. 2.3A**). Surprisingly, the N54K mutant was able to traffic to the cell surface and form intermixed gap junction plaques when co-expressed with Cx26 (**Fig. 2.3A**). The S183F mutant remained distributed in intracellular compartments, however was also found in several plaques when co-expressed with Cx26 (**Fig. 2.3A**). These findings suggest that all mutants were more readily assembled into a gap junction plaque when co-expressed with Cx26. To further examine the interaction between the Cx26 mutants and wild-type Cx26, we quantified Alexa-Fluor-350 dye-transfer between HeLa cells that coexpressed the mutants and Cx26 (**Fig. 2.3B**). Cells expressing M163V and S183F mutants reduced the overall functional gap junctional status of Cx26. However, the N54K mutant abolished the functional gap junctional status of co-expressed Cx26 as assessed by the ability to pass a fluorescent dye. (**Fig 2.3B**).

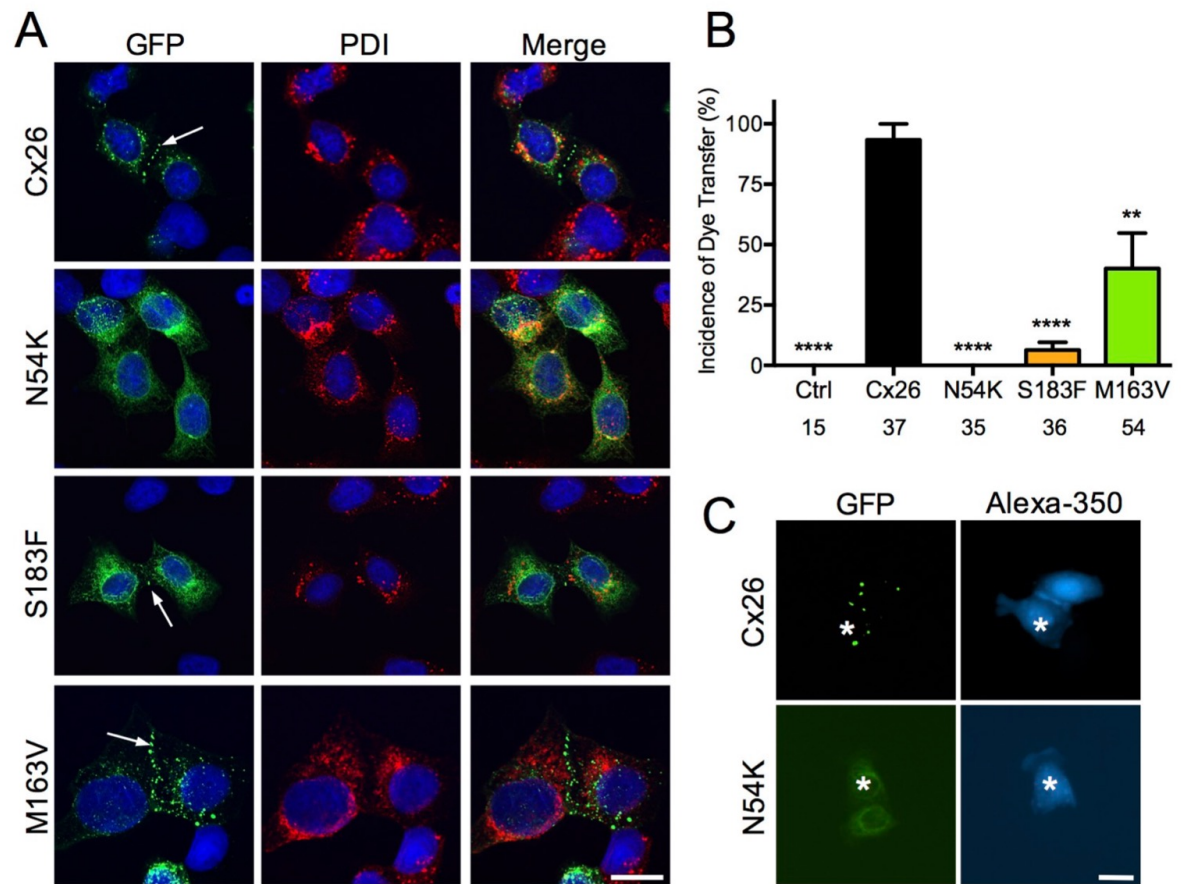


Figure 2.2

Fig. 2.2. Cx26 mutants linked to skin disease are frequently localized to intracellular compartments and have limited dye transfer capability. (A) HeLa cells expressing GFP-tagged Cx26, N54K, M163V, or S183F mutants (green) were immunolabeled for protein disulfide isomerase (PDI, red), a resident protein of the endoplasmic reticulum, and stained with Hoechst (blue) to denote the nuclei. Cx26 and the M163V mutant form numerous gap junction plaques at cell interfaces (arrows). N54K and S183F mutants were mostly located within the cell while the S183F mutant formed a few gap junction plaques. (B) Alexa-Fluor-350 dye transfer in pairs or clusters of HeLa cells expressing N54K and S183F mutants was negligible whereas ~ 40% of the cells expressing the M163V mutant transferred dye (C). Example images of dye-transfer experiments showing successful (Cx26) and unsuccessful dye-transfer (N54K). ** $p < 0.01$, **** $p < 0.0001$, $N = 3$ separate experiments. The number of cells that were microinjected to test for dye transfer in each case is noted in (B). Ctrl represents untransfected HeLa cells. Scale bar in (A, C) = 20 μ m.

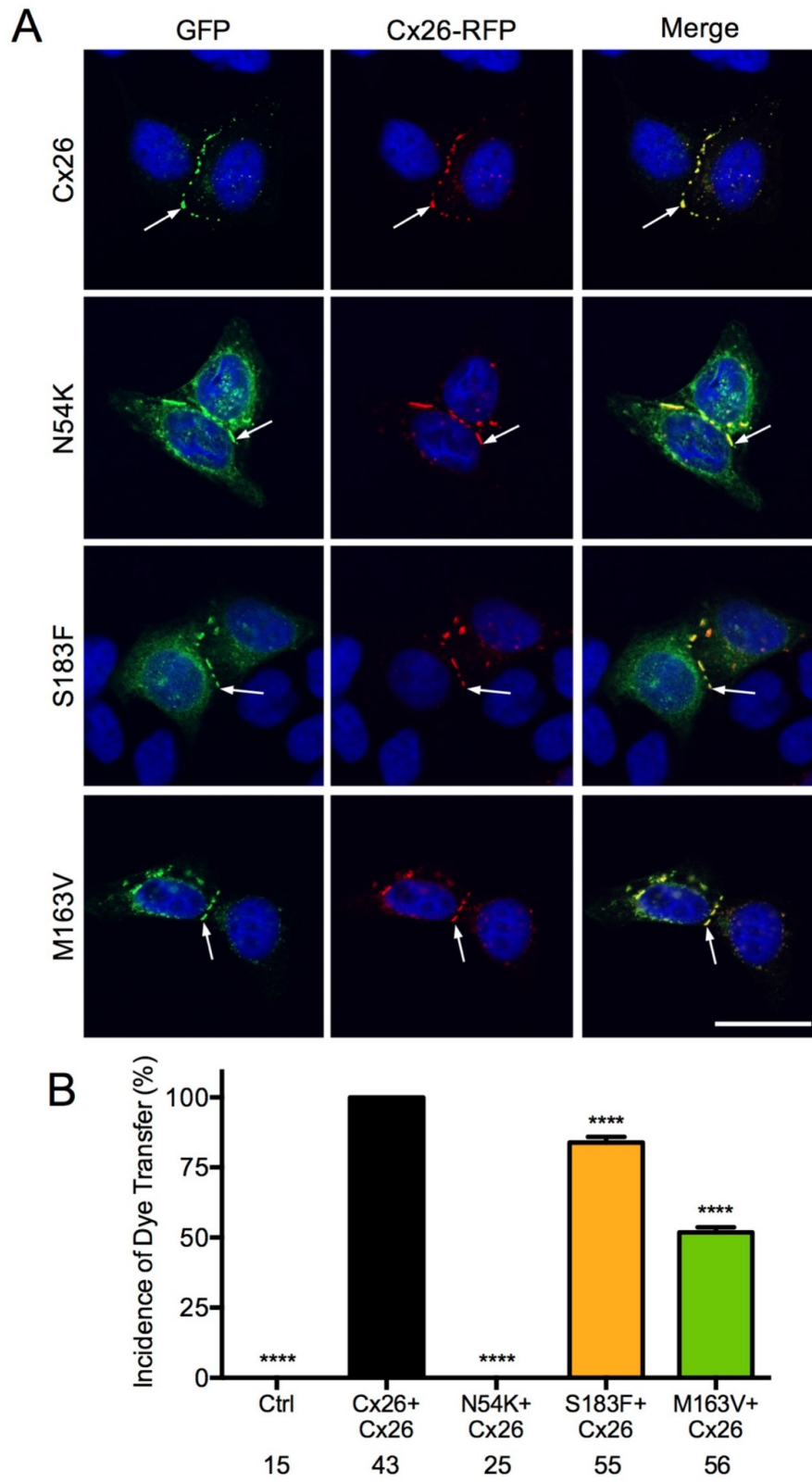


Figure 2.3

Fig. 2.3. Cx26 mutants exhibit dominant-negative properties on Cx26 in HeLa cells. (A) HeLa cells expressing GFP-tagged Cx26 or N54K, M163V, and S183F mutants (green) together with Cx26-RFP (red) were stained with Hoechst (blue). All mutants formed gap junction plaques at cell interfaces (arrows) and colocalized with Cx26-RFP. (B) Untransfected control cells (Ctrl), or cells expressing the N54K mutant together with Cx26 failed to pass microinjected Alexa-350 dye. Cells expressing S183F and M163F mutants together with Cx26-RFP had reduced incidences of dye transfer compared to cells expressing Cx26-GFP. **** $p < 0.0001$, $N = 3$ separate experiments. The number of cells that were microinjected is noted in (B). Scale bar = 20 μ m.

2.3.4 N54K and S183F mutants display trans-dominant effects on Cx30

Since Cx26 and Cx30 are co-expressed in the same keratinocytes as well as several cell types of the inner ear (Jagger and Forge, 2015), we engineered HeLa cells to express RFP-tagged Cx30 and GFP-tagged Cx26 mutants to assess potential trans-dominant interactions. Cx26 as well as the M163V and S183F mutants were able to form gap junction plaques at the cell surface and often colocalized with Cx30 (**Fig. 2.4A**). The N54K mutant formed very few plaques and remained in an ER-like distribution pattern but also appeared to impair the ability of Cx30 to form abundant gap junction plaques indicating a trans-dominant effect on Cx30 trafficking (**Fig. 2.4A**). Next we determined if the Cx26 mutants exhibited a trans-dominant effects on Cx30 channel function using Alexa-Fluor-350 dye-transfer studies (**Fig. 2.4B**). Microinjected HeLa cells expressing Cx30 alone, or co-expressing Cx30 and Cx26 had nearly 100% incidence of dye-transfer. However, cells coexpressing Cx30 and either the N54K or S183F mutants had significantly reduced ability to pass dye indicating that these mutants had a trans-dominant effect on Cx30 channel function. Interestingly, the M163V mutant did not significantly reduce the ability of Cx30 positive cells to pass dye.

2.3.5 N54K displays mild trans-dominant effect on endogenous Cx43

To assess the impact of Cx26 mutants in a more tissue-relevant cell, we engineered REKs to express Cx26 mutants and determined their potential for trans-dominant effects on endogenous Cx43. The N54K mutant formed fewer gap junction plaques than Cx26 and remained mostly intracellular (**Fig. 2.5A, B**). The M163V and S183F mutants formed numerous gap junction plaques although the S183F mutant was found in a typical ER-like distribution pattern (**Fig. 2.5A**). None of the Cx26 mutants appeared to impair Cx43 gap junction plaque formation (**Fig. 2.5B**). REKs engineered to express Cx26 mutants were microinjected with Alex-Fluor-350 which readily passes through both Cx26 and Cx43 gap junction channels. Only cells expressing the N54K mutant exhibited a significant decrease in dye transfer suggesting that the N54K mutant had a modest trans-dominant-negative effect on endogenous Cx43. (**Fig. 2.5C**).

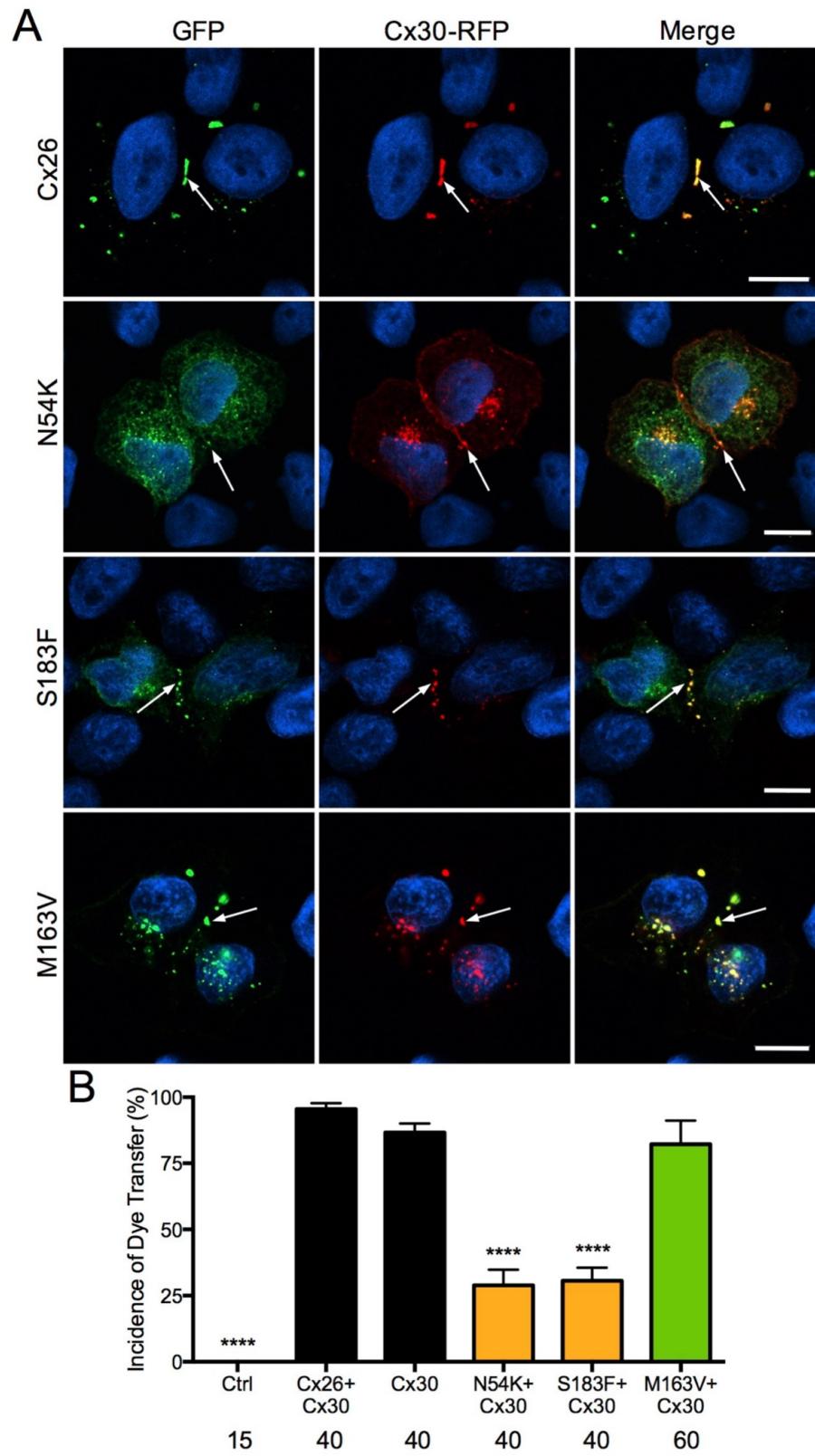


Figure 2.4

Fig. 2.4. Cx26 mutants linked to syndromic disease exhibit trans-dominant properties on Cx30 in HeLa cells. (A) HeLa cells expressing GFP-tagged Cx26, N54K, M163V, and S183F mutants (green) and RFP-tagged Cx30 (red) were stained with Hoechst (blue). S183F and M163V mutants formed abundant gap junction plaques at cell interfaces (arrows) and colocalized with Cx30, while S183F mutants were also located within the cell. N54K mutants remained mostly within the cell although they formed a few gap junction plaques (arrows) and impaired the ability of Cx30 to assemble gap junctions at the cell surface. (B) Cells expressing the M163V mutant together with Cx30 had dye transfer abilities similar to cells expressing Cx26 and Cx30, or Cx30 alone, whereas the incidences of dye transfer in cells expressing the N54K and S183F mutants together with Cx30 was markedly reduced. **** $p < 0.0001$, $N \geq 3$ separate experiments. The number of cells that were microinjected in each situation is noted in (B). Scale bar = 20 μ m.

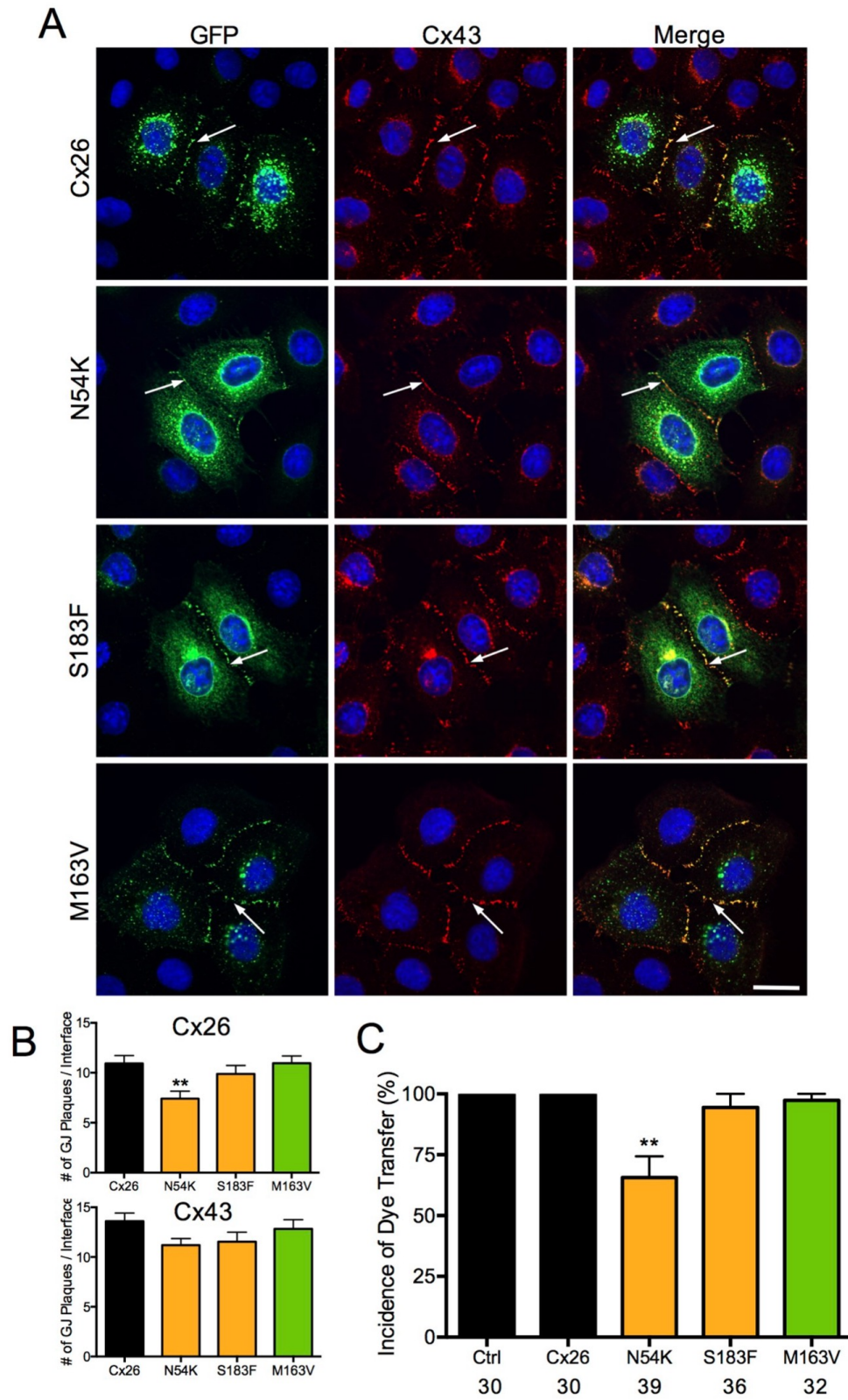


Figure 2.5

Fig. 2.5. The N54K mutant exhibits trans-dominant inhibition of endogenous Cx43 in REKs. (A) REKs expressing GFP-tagged Cx26, N54K, M163V, and S183F mutants (green) with endogenous Cx43 immunolabelled in red were stained with Hoechst (blue). The N54K and S183F mutants were inefficient at forming gap junction plaques and were often found intracellular. The M163V mutant formed abundant GJ plaques similar to Cx26. (B) The N54K mutant formed fewer gap junction plaques compared to Cx26, however endogenous Cx43 gap junction formation was not impaired by any of the mutants. (C) REKs expressing the N54K mutant had reduced dye transfer capabilities compared to untransfected REKs (Ctrl), and REKs expressing Cx26. $**p>0.01$, $n \geq 24$ individual images. The number of cells microinjected is noted in (C). Scale bar = 20 μ m.

2.3.6 N54K and S183F mutants display reduced hemichannel function

Aside from GJIC and trafficking defects, mutant connexins may further disrupt hemichannel properties. We therefore used a propidium iodide (PI) dye uptake assay to assess the function of mutant hemichannels in normal extracellular solution (ECS) and divalent-cation-free ECS (DCF-ECS) which stimulates hemichannels to open (Fasciani et al., 2013). All mutant expressing cells displayed minimal PI uptake in ECS conditions, and similar to Cx26, the M163V mutant exhibited nearly 100% incidence of PI uptake in DCF-ECS, indicating fully functional hemichannel activity (**Fig. 2.6B**). Interestingly, in DCF-ECS, cells expressing the N54K mutant demonstrated approximately 60% incidence of PI uptake suggesting moderately functional hemichannel formation, while cells expressing the S183F mutant displayed no increase in PI uptake, indicating non-functional hemichannel formation (**Fig. 2.6B**).

2.4 Discussion

Due to a high carrier frequency of *GJB2* mutations in the population and greater than 100 disease causing Cx26 mutants now identified in humans (Lee and White, 2009; Martin and van Steensel, 2015; Xu and Nicholson, 2013), understanding how distinct *GJB2* mutations cause disease is critical when considering any prospective therapies. The scope of possible Cx26 dysfunction is vast considering the possibility of gain- or loss-of functions of gap junctions, hemichannels, or additions to the connexin interactome that may present anywhere throughout the Cx26 life-cycle. Furthermore, the complexity of Cx26 dysfunction is compounded by its potential to interact with several co-expressed connexin binding partners in numerous different tissues including the skin and inner ear. The pleiotropic nature of Cx26-linked diseases raises obvious questions as to how specific *GJB2* gene mutations lead to hearing loss, or hearing loss combined with skin disorders of varying severity. Here we studied five autosomal dominant Cx26 mutants: four that cause hearing loss in addition to various skin disorders (N14K, D50N, N54K, S183F), and one that causes hearing loss alone (M163V). We found that the N14K and D50N mutants which cause wide spread and severe skin lesions overtly induced cell death, whereas the N54K and S183F mutants which cause regional and moderate skin lesions, had defects in connexin trafficking, as well as impaired gap junction

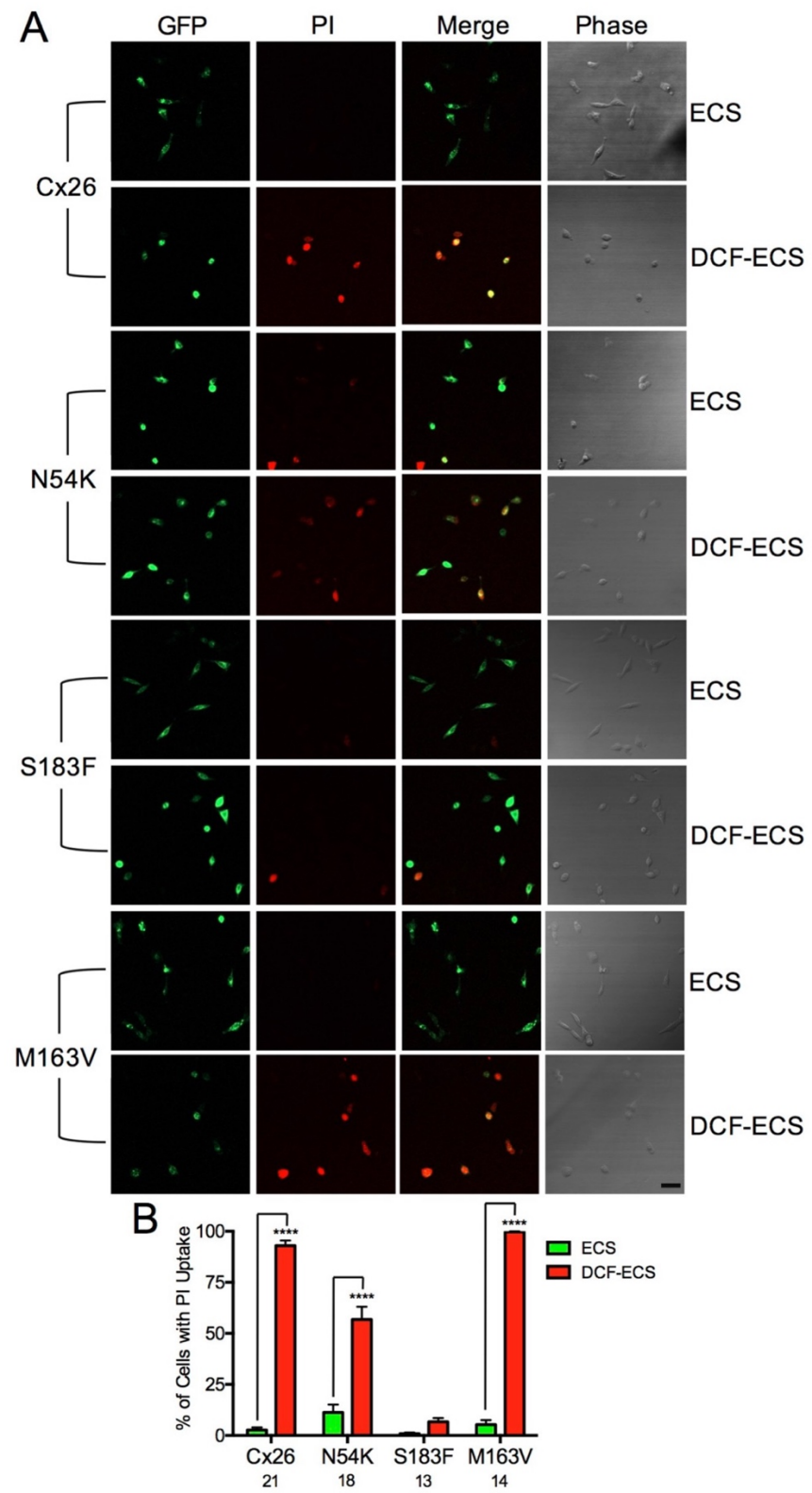


Figure 2.6

Fig. 2.6. Cx26 mutants linked to syndromic disease display reduced hemichannel function in HeLa cells. (A) Isolated HeLa cells that were engineered to express GFP-tagged Cx26, N54K, S183F, or M163V mutants were incubated in PI-containing ECS or DCF-ECS and the incidence of PI-uptake was quantified from random image fields. Image fields captured GFP-tagged connexins (green) and intracellular PI-uptake (red). (B) In DCF-ECS, cells expressing the N54K mutant displayed approximately 60% incidence of PI-uptake and cells expressing the S183F mutant displayed minimal PI-uptake. Cells expressing the M183V mutant, much like Cx26, exhibited nearly 100% incidence of PI-uptake. All mutants, except for S183F, demonstrated increased PI-uptake in DCF-ECS compared to control ECS conditions. **** $p > 0.0001$, N=3 separate experiments. The number of image fields is noted below the histogram in (B). Scale bar = 50 μ m.

and hemichannel function (**Fig. 2.7**). In addition, the M163V mutant which causes moderate hearing loss alone, displayed only impaired gap junction function (**Fig. 2.7**) with no trans-dominant properties on other co-expressed members of the connexin family. We also showed that while all mutants displayed dominant-negative properties on wild type Cx26, the syndromic N54K and S183F mutants trans-dominantly impaired the function of co-expressed Cx30 and/or Cx43 gap junctions (**Fig. 2.7**).

Several extensive reviews have discussed the functional characteristics of over 60 distinct disease-causing Cx26 mutants that were investigated using heterologous expression models (Garcia et al., 2015; Lee et al., 2009; Xu and Nicholson, 2013). These reports have elucidated some major characteristics of disease causing mutants: a reduction or ablation of gap junction formation/function, altered selectivity of signaling molecules, and aberrant hemichannel activity. While syndromic and non-syndromic mutations affect amino acid residues in cytoplasmic, extracellular, and transmembrane domains, the majority of syndromic mutations cluster to the N-terminal and EL1 domains (Garcia et al., 2016b; Lee and White, 2009; Martin and van Steensel, 2015; Xu and Nicholson, 2013). Additionally, it seems that mutants which alter molecular selectivity lead only to non-syndromic hearing loss whereas aberrant hemichannels are almost exclusively associated with severe syndromic disease (Garcia et al., 2016b; Xu and Nicholson, 2013). Recently, the S17F mutant which leads to a relatively severe form of KIDS, has been shown to form essentially non-functional homomeric gap junctions or hemichannels, yet oddly produces hyperactive heteromeric hemichannels with Cx43 (Garcia et al., 2015). This finding further established that aberrant hemichannels are a common characteristic of KIDS mutants, but importantly, it demonstrated the need to carefully examine mutants for trans-dominant effects on co-expressed connexins – including non-traditional binding partners. It is important to note that a trans-dominant interaction with a non-traditional binding partner such as Cx43, can be considered a gain-of-function property. Therefore, we also explored possible trans-dominant effects on Cx30 which is co-expressed with Cx26 in the skin and cochlea, as well as Cx43, which is co-expressed with Cx26 in the skin and also found in the cochlea. Furthermore, at least eight additional mutants have been identified in patients that still require functional analysis (Martin and van Steensel, 2015). This report describes the M163V and S183F mutants which have been limitedly investigated (Bruzzzone et al., 2003; Shuja et al., 2016), and the N54K mutant which was merely reported once in a patient with

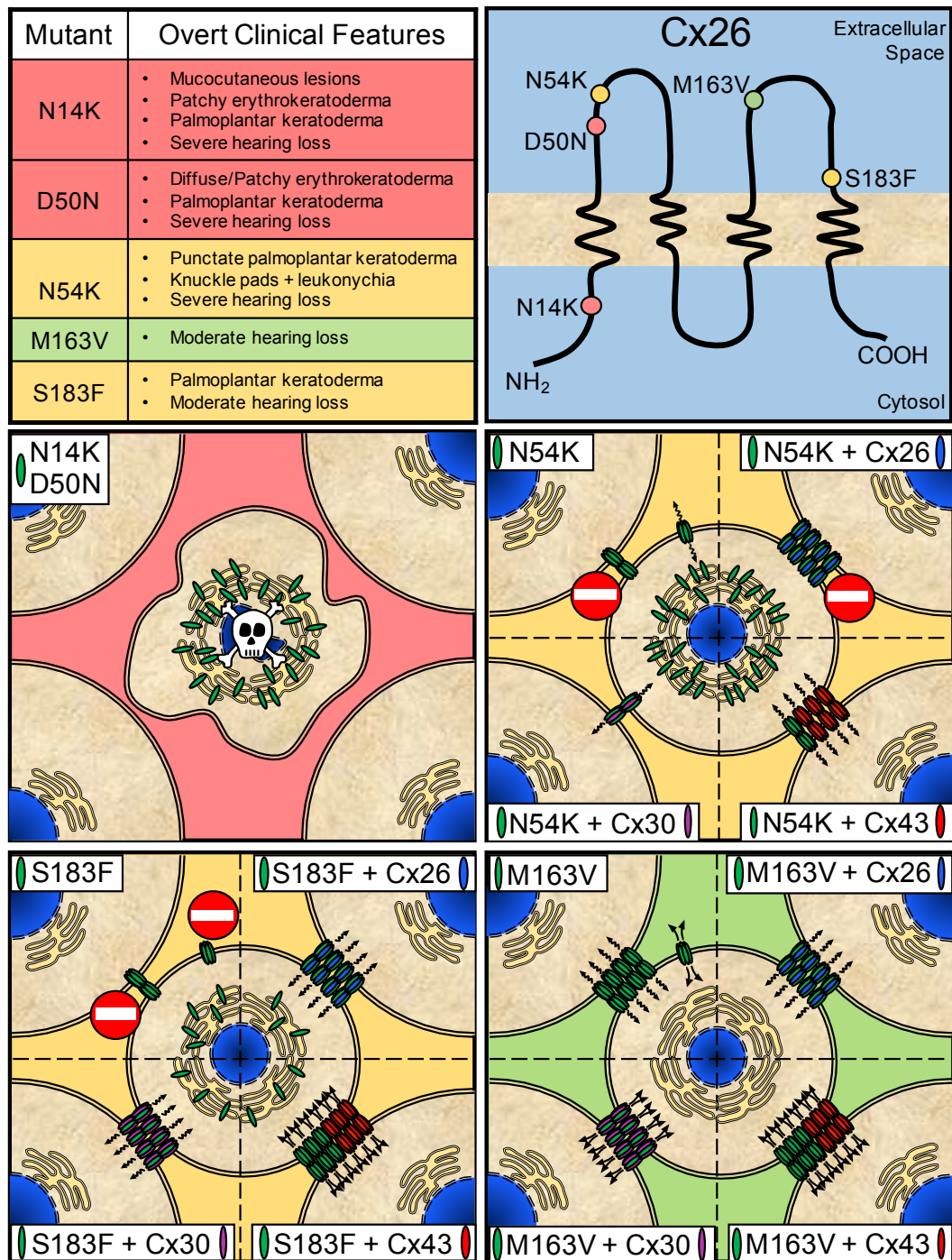


Figure 2.7

Fig. 2.7. Modelling the cellular characteristics of autosomal dominant *GJB2* mutations.

Table of the 5 Cx26 mutants and their associated clinical features (top left). Schematic of the Cx26 polypeptide chain including the approximate location of each mutant included in the study (top right). Every subsequent square displays the localization (intracellular and/or membrane trafficking), channel formation and gap junction and hemichannel function (highly functional = double arrows, reduced function = wavy arrows, non-functional = no entry symbol) of each Cx26 mutant (green), and is separated into quadrants corresponding to the context of cells co-expressing the mutant with Cx26 (blue), Cx30 (purple), or Cx43 (red). Mutants linked to severe syndromic disease are watermarked in red, mutants linked to moderate syndromic disease are watermarked in yellow, and mutants linked to non-syndromic hearing loss are watermarked in green.

Bart-Pumphrey Syndrome (Richard et al., 2004) and remains otherwise unexamined. N14K and D50N mutants are linked to KIDS which is one of the most severe Cx26-linked skin disorders. Patients present with erythrokeratoderma, PPK, and frequent cutaneous infections can lead to fatal septicemia early in life (Cogshall et al., 2013). We found these mutants strongly induced cell death such that meaningful channel function information was unattainable. However, reports suggest they form “leaky” hemichannels when expressed in *Xenopus oocytes* where they induce blebbing and substantially reduce cell viability (Lee et al., 2009; Sanchez et al., 2016; Sanchez et al., 2013). Cx26 hemichannels are sensitive to hyperpolarization by extracellular Ca^{2+} such that they remain closed under physiological conditions (Fasciani et al., 2013). However, reduced Ca^{2+} sensitivity by N14K, D50N, and several other KIDS mutants promotes hemichannel opening that can diminish transmembrane ion gradients and release molecules including ATP that affect cell viability (Sanchez and Verselis, 2014). Excessive ATP release is also known to stimulate purinergic signaling capable of mobilizing intracellular Ca^{2+} , and releasing pro-inflammatory cytokines (Burnstock et al., 2012). In the epidermis, these mutants may also be able to disrupt the normal epidermal Ca^{2+} gradient and lipid processing (Bosen et al., 2015), which can result in barrier defects and a compensatory hyperproliferative response that drives hyperkeratosis in KIDS (Garcia et al., 2016a). Interestingly, N14 and D50 are pore-lining residues (Garcia et al., 2016a) suggesting that changes to the structure of the Cx26 channel pore can produce the aberrant hemichannel properties that stand at the forefront of KIDS skin pathogenesis.

The N54K is linked to moderately severe Bart-Pumphrey Syndrome featuring PPK, knuckle-pads, leukonychia, and deafness, meanwhile the S183F mutant is linked to PPK with deafness. Although no well-defined pathogenic mechanisms for PPK have been established, our findings suggest that the high intracellular retention of N54K and S183F mutants is a common characteristic of Cx26 mutants linked to PPK. Indeed, this trafficking defect has been indicated in previous reports (de Zwart-Storm et al., 2008a; Martin and van Steensel, 2015; Marziano et al., 2003; Thomas et al., 2005). The patient with Bart-Pumphrey Syndrome harbouring the N54K Cx26 mutant in (Richard et al., 2004) was reported to have a compensatory increase in epidermal Cx30 expression. N54 is an invariably conserved residue in the connexin family among numerous species (Richard et al., 2004) and forms hydrogen bonds with L56 from the opposing hemichannel (Maeda et al., 2009). Interestingly, we found that the N54K mutant

impaired Cx30 trafficking and dye transfer, suggesting that Cx30 compensation may act to overcome a trans-dominant hindrance of Cx26:Cx30 heteromeric gap junction formation between keratinocytes. This study, and only a handful of others (Common et al., 2003; Di et al., 2005; Donnelly et al., 2012; Man et al., 2007; Mhaske et al., 2013) investigated Cx26 mutants in a relevant keratinocyte model rather than connexin-deficient reference cells. We found that only REKs expressing the N54K mutant had reduced dye transfer. This suggests that N54K Cx26 may also exert trans-dominant effects on endogenous Cx43 which may be an important etiological factor in Bart-Pumphrey Syndrome skin. Recently, Shuja and colleagues demonstrated that S183F Cx26 does not form gap junctions or hemichannels in *Xenopus oocytes* and junctional conductance was reduced in cells co-expressing Cx43 (Shuja et al., 2016). We also found that the S183F mutant inhibited dye transfer in cells co-expressing Cx30, pointing towards trans-dominant interactions of co-expressed connexins as a mechanism of disease. Since S183 is a highly conserved residue in the connexin family among many species (de Zwart-Storm et al., 2008b), we suggest that the S183 residue may have an indirect role in inter-protomer binding. Additionally, moderately leaky heteromeric hemichannels formed by S183F Cx26 and Cx43 (Shuja et al., 2016), similar to those composed of S17F Cx26 and Cx43, may also contribute to PPK. Nevertheless, our findings provide additional evidence for the impact of trans-dominant interactions between connexins in skin disease where disease severity may be linked to the extent of trans-dominant influence – particularly in skin regions exposed to greater mechanical stress.

In this study, only the M163V mutant is linked to hearing loss without added skin disease. Since Cx26 is proposed to play an important role in potassium recycling in the inner ear (Jagger and Forge, 2015) and dozens of hearing loss Cx26 mutants display reduced or no gap junction function (Xu and Nicholson, 2013), it is not surprising that we found the M163V mutant had a dominant negative effect on Cx26. However, Cx30 is also highly expressed with Cx26 in the inner ear (Jagger and Forge, 2015) such that compensation might be able to rescue hearing. However, several studies have shown that Cx30 cannot functionally compensate for Cx26 in the inner ear (Cohen-Salmon et al., 2002; Qu et al., 2012; Teubner et al., 2003). This may explain why the M163V mutant leads to hearing loss despite that HeLa cells co-expressing the M163V mutant and Cx30 passed dye at levels not unlike HeLa cells expressing Cx30 or Cx30 co-expressed with Cx26. Including our findings from syndromic mutants, we

suggest that mutants with trafficking defects, trans-dominant properties, and that induce cell death lead to skin phenotypes, whereas mutants with reduced gap junction function, but do not interfere with other co-expressed connexins produce non-syndromic hearing loss.

Human epidermis expresses 7 different connexins in overlapping populations of keratinocytes (Di et al., 2001; Martin et al., 2014) making the epidermis a more robust system compared to the cochlea. Fortunately, this high degree of redundant intercellular communication affords the epidermis with resiliency in response to *GJB2* mutations that have minor effects on protein function. Because fewer connexin types are expressed within the cochlea and compensation may be limited, small perturbations in connexin function are capable of disrupting normal hearing. This may speak to the reason why *GJB2* mutations almost never produce skin disease alone yet Cx26-linked syndromic and non-syndromic deafness is ordinary. While the majority of autosomal dominant *GJB2* mutations produce hearing loss in addition to skin disease, we posit that strongest predictors of syndromic disease severity actually stem from the trans-dominant status and gain-of-function properties of Cx26 mutant gap junctions and hemichannels. Finally, this study provides evidence in support of genetic screening when faced with complex syndromic diseases.

2.5 Acknowledgements and Funding

We would like to thank Dr. Christian C. G. Naus for the Cx26 cDNA construct and Dr. Vincent C. Hascall for the REKs. This research was supported by a Canadian Institutes of Health Research grant 123228 to DWL.

2.6 References

- Alexander, D.B., and G.S. Goldberg. 2003. Transfer of biologically important molecules between cells through gap junction channels. *Curr Med Chem.* 10:2045-2058.
- Avshalumova, L., J. Fabrikant, and A. Koriakos. 2014. Overview of skin diseases linked to connexin gene mutations. *Int J Dermatol.* 53:192-205.
- Baden, H.P., and J. Kubilus. 1983. The growth and differentiation of cultured newborn rat keratinocytes. *J Invest Dermatol.* 80:124-130.
- Berger, A.C., J.J. Kelly, P. Lajoie, Q. Shao, and D.W. Laird. 2014. Mutations in Cx30 that are linked to skin disease and non-syndromic hearing loss exhibit several distinct cellular pathologies. *J Cell Sci.* 127:1751-1764.
- Bosen, F., A. Celli, D. Crumrine, K. vom Dorp, P. Ebel, H. Jastrow, P. Dormann, E. Winterhager, T. Mauro, and K. Willecke. 2015. Altered epidermal lipid processing and calcium distribution in the KID syndrome mouse model Cx26S17F. *FEBS Lett.* 589:1904-1910.
- Bruzzone, R., V. Veronesi, D. Gomes, M. Bicego, N. Duval, S. Marlin, C. Petit, P. D'Andrea, and T.W. White. 2003. Loss-of-function and residual channel activity of connexin26 mutations associated with non-syndromic deafness. *FEBS Lett.* 533:79-88.
- Burnstock, G., G.E. Knight, and A.V. Greig. 2012. Purinergic signaling in healthy and diseased skin. *J Invest Dermatol.* 132:526-546.
- Chan, D.K., and K.W. Chang. 2014. GJB2-Associated Hearing Loss: Systematic Review of Worldwide Prevalence, Genotype, and Auditory Phenotype. *Laryngoscope.* 124:E34-E53.
- Coggsall, K., T. Farsani, B. Ruben, T.H. McCalmont, T.G. Berger, L.P. Fox, and K. Shinkai. 2013. Keratitis, ichthyosis, and deafness (KID) syndrome: A review of infectious and neoplastic complications. *Journal of the American Academy of Dermatology.* 69:127-134.
- Cohen-Salmon, M., T. Ott, V. Michel, J.P. Hardelin, I. Perfettini, M. Eybalin, T. Wu, D.C. Marcus, P. Wangemann, K. Willecke, and C. Petit. 2002. Targeted ablation of connexin26 in the inner ear epithelial gap junction network causes hearing impairment and cell death. *Curr Biol.* 12:1106-1111.
- Common, J.E., W.L. Di, D. Davies, H. Galvin, I.M. Leigh, E.A. O'Toole, and D.P. Kelsell. 2003. Cellular mechanisms of mutant connexins in skin disease and hearing loss. *Cell Commun Adhes.* 10:347-351.

- D'Adamo, P., V.I. Guerci, A. Fabretto, F. Faletra, D.L. Grasso, L. Ronfani, M. Montico, M. Morgutti, P. Guastalla, and P. Gasparini. 2009. Does epidermal thickening explain GJB2 high carrier frequency and heterozygote advantage? *Eur J Hum Genet.* 17:284-286.
- de Zwart-Storm, E.A., H. Hamm, J. Stoevesandt, P.M. Steijlen, P.E. Martin, M. van Geel, and M.A. van Steensel. 2008a. A novel missense mutation in GJB2 disturbs gap junction protein transport and causes focal palmoplantar keratoderma with deafness. *J Med Genet.* 45:161-166.
- de Zwart-Storm, E.A., M. van Geel, P.A. van Neer, P.M. Steijlen, P.E. Martin, and M.A. van Steensel. 2008b. A novel missense mutation in the second extracellular domain of GJB2, p.Ser183Phe, causes a syndrome of focal palmoplantar keratoderma with deafness. *Am J Pathol.* 173:1113-1119.
- Di, W.L., Y. Gu, J.E. Common, T. Aasen, E.A. O'Toole, D.P. Kelsell, and D. Zicha. 2005. Connexin interaction patterns in keratinocytes revealed morphologically and by FRET analysis. *J Cell Sci.* 118:1505-1514.
- Di, W.L., E.L. Rugg, I.M. Leigh, and D.P. Kelsell. 2001. Multiple epidermal connexins are expressed in different keratinocyte subpopulations including connexin 31. *J Invest Dermatol.* 117:958-964.
- Djalilian, A.R., D. McGaughey, S. Patel, E.Y. Seo, C. Yang, J. Cheng, M. Tomic, S. Sinha, A. Ishida-Yamamoto, and J.A. Segre. 2006. Connexin 26 regulates epidermal barrier and wound remodeling and promotes psoriasiform response. *J Clin Invest.* 116:1243-1253.
- Donnelly, S., G. English, E.A. de Zwart-Storm, S. Lang, M.A. van Steensel, and P.E. Martin. 2012. Differential susceptibility of Cx26 mutations associated with epidermal dysplasias to peptidoglycan derived from *Staphylococcus aureus* and *Staphylococcus epidermidis*. *Exp Dermatol.* 21:592-598.
- Elfgang, C., R. Eckert, H. Lichtenberg-Fraté, A. Butterweck, O. Traub, R.A. Klein, D.F. Hülser, and K. Willecke. 1995. Specific permeability and selective formation of gap junction channels in connexin-transfected HeLa cells. *J Cell Biol.* 129:805-817.
- Fasciani, I., A. Temperan, L.F. Perez-Atencio, A. Escudero, P. Martinez-Montero, J. Molano, J.M. Gomez-Hernandez, C.L. Paino, D. Gonzalez-Nieto, and L.C. Barrio. 2013. Regulation of connexin hemichannel activity by membrane potential and the extracellular calcium in health and disease. *Neuropharmacology.* 75:479-490.
- Garcia, I.E., F. Bosen, P. Mujica, A. Pupo, C. Flores-Munoz, O. Jara, C. Gonzalez, K. Willecke, and A.D. Martinez. 2016a. From Hyperactive Connexin26 Hemichannels to Impairments in Epidermal Calcium Gradient and Permeability Barrier in the Keratitis-Ichthyosis-Deafness Syndrome. *J Invest Dermatol.* 136:574-583.

- Garcia, I.E., J. Maripillan, O. Jara, R. Ceriani, A. Palacios-Munoz, J. Ramachandran, P. Olivero, T. Perez-Acle, C. Gonzalez, J.C. Saez, J.E. Contreras, and A.D. Martinez. 2015. Keratitis-ichthyosis-deafness syndrome-associated Cx26 mutants produce nonfunctional gap junctions but hyperactive hemichannels when co-expressed with wild type Cx43. *J Invest Dermatol.* 135:1338-1347.
- Garcia, I.E., P. Prado, A. Pupo, O. Jara, D. Rojas-Gomez, P. Mujica, C. Flores-Munoz, J. Gonzalez-Casanova, C. Soto-Riveros, B.I. Pinto, M.A. Retamal, C. Gonzalez, and A.D. Martinez. 2016b. Connexinopathies: a structural and functional glimpse. *BMC Cell Biol.* 17 Suppl 1:17.
- Huang, T., Q. Shao, A. MacDonald, L. Xin, R. Lorentz, D. Bai, and D.W. Laird. 2013. Autosomal recessive GJA1 (Cx43) gene mutations cause oculodentodigital dysplasia by distinct mechanisms. *J Cell Sci.* 126:2857-2866.
- Jagger, D.J., and A. Forge. 2015. Connexins and gap junctions in the inner ear--it's not just about K(+) recycling. *Cell Tissue Res.* 360:633-644.
- Laird, D.W. 2006. Life cycle of connexins in health and disease. *Biochem J.* 394:527-543.
- Lazic, T., K.A. Horii, G. Richard, D.I. Wasserman, and R.J. Antaya. 2008. A report of GJB2 (N14K) Connexin 26 mutation in two patients--a new subtype of KID syndrome? *Pediatr Dermatol.* 25:535-540.
- Lee, J.R., A.M. Derosa, and T.W. White. 2009. Connexin mutations causing skin disease and deafness increase hemichannel activity and cell death when expressed in *Xenopus* oocytes. *J Invest Dermatol.* 129:870-878.
- Lee, J.R., and T.W. White. 2009. Connexin-26 mutations in deafness and skin disease. *Expert Rev Mol Med.* 11:e35.
- Maeda, S., S. Nakagawa, M. Suga, E. Yamashita, A. Oshima, Y. Fujiyoshi, and T. Tsukihara. 2009. Structure of the connexin 26 gap junction channel at 3.5 Å resolution. *Nature.* 458:597-602.
- Man, Y.K.S., C. Trollove, D. Tattersall, A.C. Thomas, A. Papakonstantinou, D. Patel, C. Scott, J. Chong, D.J. Jagger, E.A. O'Toole, H. Navsaria, M.A. Curtis, and D.P. Kelsell. 2007. A deafness-associated mutant human connexin 26 improves the epithelial barrier In vitro. *J Membrane Biol.* 218:29-37.
- Marlin, S., E.N. Garabedian, G. Roger, L. Moatti, N. Matha, P. Lewin, C. Petit, and F. Denoyelle. 2001. Connexin 26 gene mutations in congenitally deaf children: pitfalls for genetic counseling. *Arch Otolaryngol Head Neck Surg.* 127:927-933.
- Martin, P.E., J.A. Easton, M.B. Hodgins, and C.S. Wright. 2014. Connexins: sensors of epidermal integrity that are therapeutic targets. *FEBS Lett.* 588:1304-1314.

- Martin, P.E., and M. van Steensel. 2015. Connexins and skin disease: insights into the role of beta connexins in skin homeostasis. *Cell Tissue Res.* 360:645-658.
- Marziano, N.K., S.O. Casalotti, A.E. Portelli, D.L. Becker, and A. Forge. 2003. Mutations in the gene for connexin 26 (GJB2) that cause hearing loss have a dominant negative effect on connexin 30. *Human Molecular Genetics.* 12:805-812.
- Mazereeuw-Hautier, J., E. Bitoun, J. Chevrant-Breton, S.Y. Man, C. Bodemer, C. Prins, C. Antille, J.H. Saurat, D. Atherton, J.I. Harper, D.P. Kelsell, and A. Hovnanian. 2007. Keratitis-ichthyosis-deafness syndrome: disease expression and spectrum of connexin 26 (GJB2) mutations in 14 patients. *Br J Dermatol.* 156:1015-1019.
- Mhaske, P.V., N.A. Levit, L.P. Li, H.Z. Wang, J.R. Lee, Z. Shuja, P.R. Brink, and T.W. White. 2013. The human Cx26-D50A and Cx26-A88V mutations causing keratitis-ichthyosis-deafness syndrome display increased hemichannel activity. *Am J Physiol-Cell Ph.* 304:C1150-C1158.
- Penuela, S., R. Bhalla, X.Q. Gong, K.N. Cowan, S.J. Celetti, B.J. Cowan, D. Bai, Q. Shao, and D.W. Laird. 2007. Pannexin 1 and pannexin 3 are glycoproteins that exhibit many distinct characteristics from the connexin family of gap junction proteins. *J Cell Sci.* 120:3772-3783.
- Qu, Y., W. Tang, B. Zhou, S. Ahmad, Q. Chang, X. Li, and X. Lin. 2012. Early developmental expression of connexin26 in the cochlea contributes to its dominate functional role in the cochlear gap junctions. *Biochem Biophys Res Commun.* 417:245-250.
- Richard, G., N. Brown, A. Ishida-Yamamoto, and A. Krol. 2004. Expanding the phenotypic spectrum of Cx26 disorders: Bart-Pumphrey syndrome is caused by a novel missense mutation in GJB2. *J Invest Dermatol.* 123:856-863.
- Sanchez, H.A., N. Slavi, M. Srinivas, and V.K. Verselis. 2016. Syndromic deafness mutations at Asn 14 differentially alter the open stability of Cx26 hemichannels. *J Gen Physiol.* 148:25-42.
- Sanchez, H.A., and V.K. Verselis. 2014. Aberrant Cx26 hemichannels and keratitis-ichthyosis-deafness syndrome: insights into syndromic hearing loss. *Front Cell Neurosci.* 8:354.
- Sanchez, H.A., K. Villone, M. Srinivas, and V.K. Verselis. 2013. The D50N mutation and syndromic deafness: altered Cx26 hemichannel properties caused by effects on the pore and intersubunit interactions. *J Gen Physiol.* 142:3-22.
- Scott, C.A., D. Tattersall, E.A. O'Toole, and D.P. Kelsell. 2012. Connexins in epidermal homeostasis and skin disease. *Biochim Biophys Acta.* 1818:1952-1961.

- Shuja, Z., L. Li, S. Gupta, G. Mese, and T.W. White. 2016. Connexin26 Mutations Causing Palmoplantar Keratoderma and Deafness Interact with Connexin43, Modifying Gap Junction and Hemichannel Properties. *J Invest Dermatol.* 136:225-235.
- Teubner, B., V. Michel, J. Pesch, J. Lautermann, M. Cohen-Salmon, G. Sohl, K. Jahnke, E. Winterhager, C. Herberhold, J.P. Hardelin, C. Petit, and K. Willecke. 2003. Connexin30 (Gjb6)-deficiency causes severe hearing impairment and lack of endocochlear potential. *Hum Mol Genet.* 12:13-21.
- Thomas, T., K. Jordan, J. Simek, Q. Shao, C. Jedszko, P. Walton, and D.W. Laird. 2005. Mechanisms of Cx43 and Cx26 transport to the plasma membrane and gap junction regeneration. *J Cell Sci.* 118:4451-4462.
- Xu, J., and B.J. Nicholson. 2013. The role of connexins in ear and skin physiology - functional insights from disease-associated mutations. *Biochim Biophys Acta.* 1828:167-178.

Chapter 3

Mice harboring disease-linked Cx26 and Cx30 mutants display volar skin abnormalities but retain most wound healing properties.

Here we generated a novel, viable, and fertile mouse (Cx26^{K14-S17F/+}) which expresses the keratitis-ichthyosis-deafness syndrome (KIDS) mutant (S17F Cx26) driven from the keratin 14 promoter. This mutant mouse mirrors several Cx26-linked human skin pathologies suggesting that the etiology of Cx26-linked skin disease indeed stems from epidermal expression of the Cx26 mutant. Cx26^{K14-S17F/+} foot pad epidermis formed severe palmoplantar keratoderma which expressed elevated levels of Cx26 and filaggrin. Primary keratinocytes isolated from Cx26^{K14-S17F/+} neonates had reduced GJIC and migration. Furthermore, Cx26^{K14-S17F/+} mouse skin healed normally after wounding but exhibited abnormal epidermal remodeling. Mice harbouring the Clouston Syndrome A88V Cx30 mutant (Cx30^{A88V/+}, Cx30^{A88V/A88V}) showed no skin abnormalities or wound healing defects suggesting that compared to humans, Cx30 may have a less critical role in mouse epidermis. Taken together, we suggest that Cx26 helps regulate keratinocyte differentiation, especially in palmoplantar skin, but mice harbouring Cx26 and Cx30 mutants retain most skin wound healing properties.

A version of this chapter will be submitted for publication before the end of the year.

Authors: Eric R. Press, Katanya C. Alaga, Kevin Barr, Qing Shao, Felicitas Bosen, Klaus Willecke and Dale W. Laird

3.1 Introduction

Gap junction channels allow for direct intercellular communication by facilitating the passage of small molecular messengers between the cytosol of adjacent cells (Alexander and Goldberg, 2003). Individual cells may also exchange signaling molecules with the extracellular environment through hemichannels at the cell membrane (Saez et al., 2005). Gap junction channels are composed of docked hemichannels from adjacent cells, each of which contains six oligomerized connexin (Cx) subunits. Connexins comprise a family of transmembrane proteins that have large clinical significance due to the discovery of abundant disease-causing mutations in connexin genes. Notably, mutations in the genes encoding Cx26 and Cx30 cause syndromic diseases where patients suffer from hearing loss and a broad range of skin abnormalities that vary in localization and severity (Avshalumova et al., 2014; Martin and van Steensel, 2015; Scott et al., 2012). Interestingly, Cx26 and Cx30 mutants can give rise to diseases affecting one or multiple tissues and mutants with similar functional characteristics often lead to similar phenotypes, suggesting specific functional anomalies are closely tied to disease outcomes (Martin and van Steensel, 2015; Xu and Nicholson, 2013). Not surprisingly however, Cx26 and Cx30 are both expressed in the cochlea and epidermis, and they share a similar localization pattern within the epidermal strata (Yum et al., 2007), and likely form heteromeric channels between keratinocytes.

The human epidermis expresses up to 7 distinct connexin proteins in overlapping populations of keratinocytes highlighting the complexity of gap junctional intercellular communication (GJIC) in this tissue (Di et al., 2001). Two distinct mouse models demonstrated that persistent epidermal Cx26 expression promoted a hyperproliferative, inflammatory response suggesting a delicate balance of individual connexins may be required for epidermal health (Djalilian et al., 2006). A key factor likely involved in regulating keratinocyte differentiation is an increasing intracellular Ca^{2+} gradient between keratinocytes of the stratum basale and stratum granulosum (Adams et al., 2012; Bikle et al., 2012). Gap junction channels are known to pass signaling molecules such as IP_3 that regulate intracellular Ca^{2+} handling, which may have a profound influence on the synthesis and assembly of skin barrier components such as filaggrin and ceramides (Bosen et al., 2015; Sandilands et al., 2009). Furthermore, it is well known that following cutaneous wounding, multiple connexins including Cx26, Cx30, and Cx43, are

dynamically regulated within the epidermis suggesting they play a major role in coordinating wound healing events such as keratinocyte proliferation, migration, and differentiation (Brandner et al., 2004; Churko and Laird, 2013). In fact, numerous studies employing Cx43 knock-down strategies have demonstrated beneficial wound healing outcomes (Churko et al., 2012; Coutinho et al., 2003; Ghatnekar et al., 2015; Mori et al., 2006; Qiu et al., 2003) which strongly promotes Cx43 as a therapeutic target for chronic wounds. Despite the evidence supporting the influence of connexins on epidermal health, the roles of Cx26 and Cx30 in the skin are still incompletely understood, particularly in the context of healing wounds.

Several Cx26 mutants, including the S17F mutant, are linked to keratitis-ichthyosis-deafness syndrome (KIDS); a rare and severe autosomal dominant disease featuring generalized dry/scaly skin, patchy erythematous keratoderma and palmoplantar keratoderma (Coggshall et al., 2013). In some cases, frequent cutaneous infections lead to fatal septicemia early in life (Coggshall et al., 2013). *In vitro* ectopic expression studies have revealed hyperactive or “leaky” hemichannels as a likely pathogenic characteristic of KIDS mutants (Garcia et al., 2015; Lee et al., 2009). Interestingly, the S17F mutant does not form functional gap junction channels or hemichannels on its own (Garcia et al., 2015; Richard et al., 2002), but rather forms heteromeric hyperactive hemichannels when co-expressed with wild type Cx26 or Cx43 (Garcia et al., 2015). A transgenic mouse that globally expresses the S17F mutant replicates several KIDS phenotypes in addition to features typically associated with separate Cx26-linked diseases (Schutz et al., 2011). However, because these mice have low viability and it is still unknown how the mutant specifically affects the epidermis, we generated a tissue-specific mouse that harbours the S17F mutant in the epidermis (Cx26^{K14-S17F/+}). The A88V Cx30 mutant is known to cause the highly variable Clouston Syndrome (Common et al., 2003); a rare autosomal dominant disease that presents with PPK, regional hyperpigmentation, alopecia, nail dystrophy, clubbed fingers, and in some cases hearing loss (Kibar et al., 2000; Sugiura et al., 2013). The A88V mutant forms a small number of partially functional gap junctions (Berger et al., 2014) in addition to hyperactive hemichannels that release excessive ATP into the extracellular space and induce cell death (Essenfelder et al., 2004). A transgenic mouse that globally expresses the A88V Cx30 mutant (Cx30^{A88V/A88V}) exhibits hyperproliferative sebaceous glands leading to a greasy coat as well as mild hyperkeratosis of foot pad skin (Bosen et al., 2014). While numerous abnormal cellular characteristics of Cx26

and Cx30 mutants have been identified, and several transgenic mice have been generated to model human connexin-linked skin disorders, the etiology of these diseases as well and their impact on cutaneous wound healing remains poorly understood.

Therefore, by using our novel Cx26^{K14-S17F/+} mouse and the Cx30^{A88V/A88V} mouse described in Bosen *et al.* (2014), we aimed to assess how Cx26 and Cx30 mutants produce skin disease to ultimately gain further insight into the role of these proteins in healthy skin. We found that S17F Cx26, but not A88V Cx30 produced severe PPK, wherein expression of Cx26 as well as filaggrin was elevated in foot pad skin indicating deregulated differentiation. Moreover, primary keratinocytes from Cx26^{K14-S17F/+} mice had reduced gap junctional coupling and changes in migration. Lastly, both Cx26 and Cx30 mutant mice retain most of the properties associated with active wound healing.

3.2 Materials and Methods

3.2.1 Genetically-Modified Mice

All animal experiments were approved by the Animal Use Committee at Western University in accordance with guidelines from the Canadian Council for Animal Care. Cx26^{K14-S17F/+} mice (hereafter referred to as S17F/+) were generated in-house, on a mixed C57BL/6 and 129Sv background. Heterozygous floxed mice (Cx26^{flloxS17F/+} - generated in Schütz *et al.*, (2011) and obtained from Dr. K. Willecke) were crossed with homozygous keratin 14 Cre mice (*Gjb2*^{tm2.2Kwi/Cnrm}, Jackson Labs) which were obtained from Dr. L. Dagnino. S17F/+ mice express S17F Cx26 heterozygously in basal cells of the epidermis, as well as the oral and vaginal epithelium (Dassule et al., 2000). Cx30^{A88V/+} and Cx30^{A88V/A88V} mice, (hereafter referred to as A88V/+ and A88V/A88V, respectively) were generated by Bosen and colleagues (Bosen et al., 2014) and obtained from Dr. K. Willecke. Due to the differences in genetic background between mouse strains, all animal experiments used wild-type littermates as controls (hereafter referred to as Control). Roughly equal proportions of male and female mice were used for all experiments.

3.2.2 Mouse Genotyping

Ear notches at the time of weaning were incubated overnight at 58°C in a proteinase K solution composed of 0.6 mg of proteinase K (Cat# 25530-049; Invitrogen) dissolved in buffer containing 20 mM Tris Cl pH 8.3, 50 mM KCl, 2.5 mM MgCl₂, and 0.5% Tween 20. The digested tissue solution was incubated for 10 minutes at 95°C and DNA amplification was carried out by polymerase chain reaction (PCR). PCR mixtures included 10x PCR buffer (Cat# 1360566; Invitrogen), 50 mM MgCl (Cat# 11392196; Invitrogen), 10 µM dNTPs (Cat# 10297-018; Invitrogen), and Platinum Taq polymerase (Cat# 10966-018; Invitrogen). Samples were run for 40 cycles with the annealing temperature set to 57°C for S17F/+ samples, and 65°C for the A88V/+ and A88V/A88V samples. PCR products were run on a 2% agarose gel including 200 µg of ethidium bromide, and gels were visualized under ultra-violet light.

3.2.3 Skeletal Staining

Seven day old mice were euthanized, neatly eviscerated to reveal the skeleton, and the skeleton was stained according to a modified protocol from (McLeod, 1980). Skeletons were dehydrated in 95% overnight and fixed in acetone for 24 hours. Skeletons were stained for 4 days using a solution containing 0.015% alcian blue, 0.05% alizarin red, and 5% acetic acid in 70% ethanol as described in (Wang et al., 2007b). Finally, skeletons were cleared using 1% KOH in ddH₂O until the stained vertebrae and intervertebral disks were clearly visible. Two animals per genotype were used for skeletal staining.

3.2.4 Micro-Computed Tomography

Micro-computed tomography (µCT) scans of euthanized 3-month-old S17F/+ and control whole mouse bodies were obtained using the eXplore speCZT µCT scanner (GE Healthcare) at Robarts Research Institute (London, ON, Canada) to assess the bone structure underlying the S17F/+ truncated tail or skeletal abnormalities in the digits. Further technical specifications and image processing techniques are outlined in (Caskenette et al., 2016). Briefly, scans were acquired with a voxel size of 100 µm³ and 3D composite images were reconstructed and manipulated using MicroView software (GE Healthcare Biosciences). One S17F/+ and one control mouse were used to create isosurface images.

3.2.5 Tissue Lysates and Immunoblotting

Foot pad skin was dissected, frozen with liquid nitrogen, and pulverized with a cold mortar and pestle over dry ice. Lysates were generated by dissolving the pulverized tissue in 2x immunoprecipitation buffer (containing 1% Triton X-100, 150 mM NaCl, 10 mM Tris, 1 mM EDTA, 1 mM EGTA, 0.5% NP-40, 1.0 mg of NaF, 1.0 mg of Na₃VO₄, and a Complete Mini protease inhibitor tablet (Roche Cat# 10570500)). Lysates were stored at -80°C until electrophoresis. Protein concentration was determined with standard bicinchoninic acid assay. Lysates were run on a 12% polyacrylamide gel using SDS-PAGE and protein was transferred to nitrocellulose membranes with the iBlot dry transfer system (7 minute transfer). Membranes were blocked in 2% BSA in PBST and probed with 1:1000 mouse anti-Cx26 (Invitrogen Cat# 138100), 1:1000 rabbit anti-Cx30 (Invitrogen Cat# 71-2200), 1:5000 rabbit anti-Cx43 (Sigma Cat# 112M4824), 1:5000 mouse anti-GAPDH (Millipore Cat# 2145925), 1:1000 mouse anti-keratin 14 (ThermoFisher Cat# MA5-11599), 1:1000 rabbit anti-filaggrin (Covance Cat# PRB-417P), and 1:400 rabbit anti-proliferating cell nuclear antigen (PCNA) (Santa Cruz Cat# FL-261:sc-7907) antibodies. Secondary antibodies included AlexaFluor680 (Cat# A21076; Life Technologies) and IRDye800 (Cat# 24058; Rockland) and membranes were visualized using the Odyssey infrared imaging system. An unpaired t-test (for S17F/+) or one-way ANOVA (for A88V/+ and A88V/A88V) was performed on the mean intensity (K counts) of biological replicates.

3.2.6 Immunohistochemistry and Immunofluorescence Imaging

Foot pad skin was fixed with 10% neutral buffered formalin overnight at 4°C, paraffin embedded, sectioned, and stained with hematoxylin and eosin for histological analysis according to (Stewart et al., 2013). Separate tissue samples were also fixed, cryopreserved in 30% sucrose in PBS, embedded in 1% low melting point agarose containing 18% sucrose and 0.01% NaN₃, flash frozen with liquid nitrogen, and cryosectioned for immunofluorescent imaging. Frozen sections were blocked in 3% BSA + 0.2% Triton X-100 and labeled with 1:400 rabbit anti-Cx26 (Invitrogen Cat# 512800), 1:400 rabbit anti-Cx30, 1:500 rabbit anti-Cx43, 1:200 mouse anti-keratin 14, 1:200 rabbit anti-filaggrin, and 1:400 rabbit anti-Ki67 (Abcam Cat# ab66155). The secondary antibodies used were 1:500 anti-rabbit Alexa488 (Life Technologies Cat# A11008), 1:500 anti-rabbit Alexa555 (Life Technologies Cat# A21429),

and 1:500 anti-mouse Alexa488 (Life Technologies Cat# A11017). Sections were counter-stained with Hoechst, mounted using Airvol, and imaged with a Zeiss LSM 800 confocal microscope equipped with ZenWorks software. Images were captured with a 40x water immersion objective.

3.2.7 Wound Healing Assays

Three month old mice were anesthetized with isoflurane, administered analgesics subcutaneously, then a small section of dorsal hair was shaved and depilated with Nair, and the skin was sterilized using the standard 3-stage preparation. Wounds were performed using a 5mm human punch biopsy to remove the full thickness of the skin as described in (Churko et al., 2011b). Briefly, dorsal skin was held taut and a punch biopsy tool was twisted on the skin with light pressure until a full-thickness circle of skin was removed. Skin tension was released and allowed to retract for approximately 30 seconds before imaging. Wound inspection and imaging was performed the day of surgery, and every second day until fully healed. Wound sizes were measured using ImageJ in a blinded fashion. A two-way ANOVA was performed on the mean wound area of at least 6 mice per genotype.

3.2.8 Cell Lines

Connexin-rich rat epidermal keratinocytes (REKs) were originally described in (Baden and Kubilus, 1983) were provided by Dr. V. Hascall. Cells were grown in DMEM (Life Technologies Cat# 11965-092) supplemented with fetal bovine serum (Gibco Cat# 12484-028), 2 mM L-glutamine (Life Technologies Cat# 25030-081), penicillin and streptomycin according to (Penuela et al., 2007).

3.2.9 Primary Murine Keratinocyte Culture

Keratinocytes were isolated from neonatal mice (P2-P3) according to (Churko et al., 2012) with minor procedural adjustments. Briefly, complete body skin was carefully dissected from neonates was rinsed in Ca^{2+} and Mg^{2+} free PBS (Invitrogen Cat# 14190-144) containing 5 $\mu\text{g/mL}$ gentamycin (Invitrogen Cat# 15750-060). Skins were floated dermis side down over 1.5 mL of 50 cU/mL dispase (Corning Cat#354235) at 4°C overnight with gentle rocking. The epidermis was gently separated from the dermis, minced with sterile scissors, and incubated in 0.25% trypsin-EDTA (Invitrogen Cat# 25200-056) for ~10 minutes at 37°C. The cell

suspension was removed and placed into 1.5 mL of Keratinocyte Serum-Free Medium (K-SFM) (Invitrogen Cat# 37010-022) supplemented with 1.4 mM CaCl_2 and 1.5 mL of stock trypsin neutralizer solution (Invitrogen Cat# R-002-100), and centrifuged. The pellet was resuspended in K-SFM supplemented with 0.05 mM CaCl_2 , poured through a 70 μm cell strainer (Falcon Cat# 21008-952), and plated in dishes pre-coated with 50 $\mu\text{g/mL}$ collagen I (BD Biosciences Cat# 354236). The next day, cells were washed 2 times with Ca^{2+} and Mg^{2+} free PBS then incubated in K-SFM containing 1.4 mM CaCl_2 . Cells were used for experiments between 48-72 hours following initial plating.

3.2.10 Calcein-AM Dye Recovery

Primary mouse keratinocytes and REKs were grown on 35mm glass bottom dishes and pre-loaded for 10 minutes at 37°C in a 0.3 mM isotonic glucose solution containing 2 $\mu\text{L/mL}$ calcein-AM dissolved in DMSO. Cells were washed in PBS and photobleached to 20% of original fluorescence intensity with a 488 nm argon laser at 50% strength. Images were subsequently captured every 10 seconds for approximately 10 minutes with a LSM 800 Zeiss confocal microscope and a 40x water-immersion lens. Image series were exported to ImageJ and fluorescence recovery of photobleached cells were measured using the Time Series Analyzer V3 plugin. Fluorescence recovery curves displayed summarized data and a one-way ANOVA was performed on the area under the curve (AUC) of biological replicates.

3.2.11 Scratch-Wound Assay

Primary mouse keratinocytes were seeded at 1×10^6 cells per 35 mm gridded dish (Sarstedt Cat# 83.1800.001). Culture dishes were pre-coated with collagen as previously described and following 48 hours of incubation in K-SFM containing 1.4 mM CaCl_2 , cells were rinsed with Ca^{2+} and Mg^{2+} free PBS and scraped with a P1000 pipette tip. Cells were then replenished with K-SFM containing no supplements or CaCl_2 and images of 10 identical sections per dish (0.5 mm^2), were captured at 24 and 48 hours following the scrape. For each image, the gap between keratinocyte fronts was measured in 5 similar regions and an unpaired t-test (S17F/+ cultures) or a one-way ANOVA (A88V/+ and A88V/A88V cultures) was performed on the calculated migration distances of replicates.

3.2.12 Scrape-Load Assay

Primary mouse keratinocytes were seeded at 1×10^6 cells per 35 mm dish and incubated in K-SFM containing 1.4 mM CaCl_2 for 48 hours. Cells were washed twice with warm HBSS and then incubated in HBSS containing 2.5% Lucifer Yellow and 1% DiI. Cells were scraped with a sharp surgical blade and incubated at 37°C for 5 minutes. Cells were then washed 3 times with warm HBSS and images with a Leica inverted epifluorescent microscope using a 20x objective. Five similar fields were imaged for each experimental replicate. For each image, Lucifer Yellow transfer distance minus DiI transfer distance was calculated, and a one-way ANOVA was performed on the calculated means of biological replicates.

3.2.13 Statistical Analysis

Graph Pad Prism version 6 was used for all statistical analysis and statistical significance was noted when $p < 0.05$. All student's t-tests were two tailed. All histogram values represent the mean + SEM.

3.3 Results

3.3.1 Epidermal expression of S17F Cx26, but not A88V Cx30, results in severe skin features plus comorbidities

S17F/+ mice harbouring the mutated *Gjb2* gene only in cells expressing keratin 14 (basal keratinocytes) resulted in a tissue-defined transgenic mouse that expressed the S17F mutant under the control of the endogenous Cx26 promoter. This primarily epidermis expression profile was capable of reproducing KIDS skin features in a novel mutant mouse in addition to several intriguing phenotypes (**Fig. 3.1**). S17F/+ pups were visibly smaller and had red, dry, scaly skin (**Fig. 3.1A**). PCR analysis of skin tissue confirmed the heterozygous expression of S17F Cx26 (**Fig. 3.1B**). Contrary to global Cx26^{S17F/+} mice (Schutz et al., 2011), our tissue-defined S17F/+ mice had no loss of viability and were born in equal proportion to wild type littermates (**Fig. 3.1C**). Interestingly, S17F/+ mice were approximately 15% smaller by 3 months of age (**Fig. 3.1E**), and had a shortened tail (**Fig. 3.1D**) which coincided with the formation of a cutaneous bulb at the distal tail by post-natal day 7 (**Fig. 3.1F, G**). This appeared to impair proper vertebral formation within the bulb preventing normal tail growth (**Fig. 3.1H**).

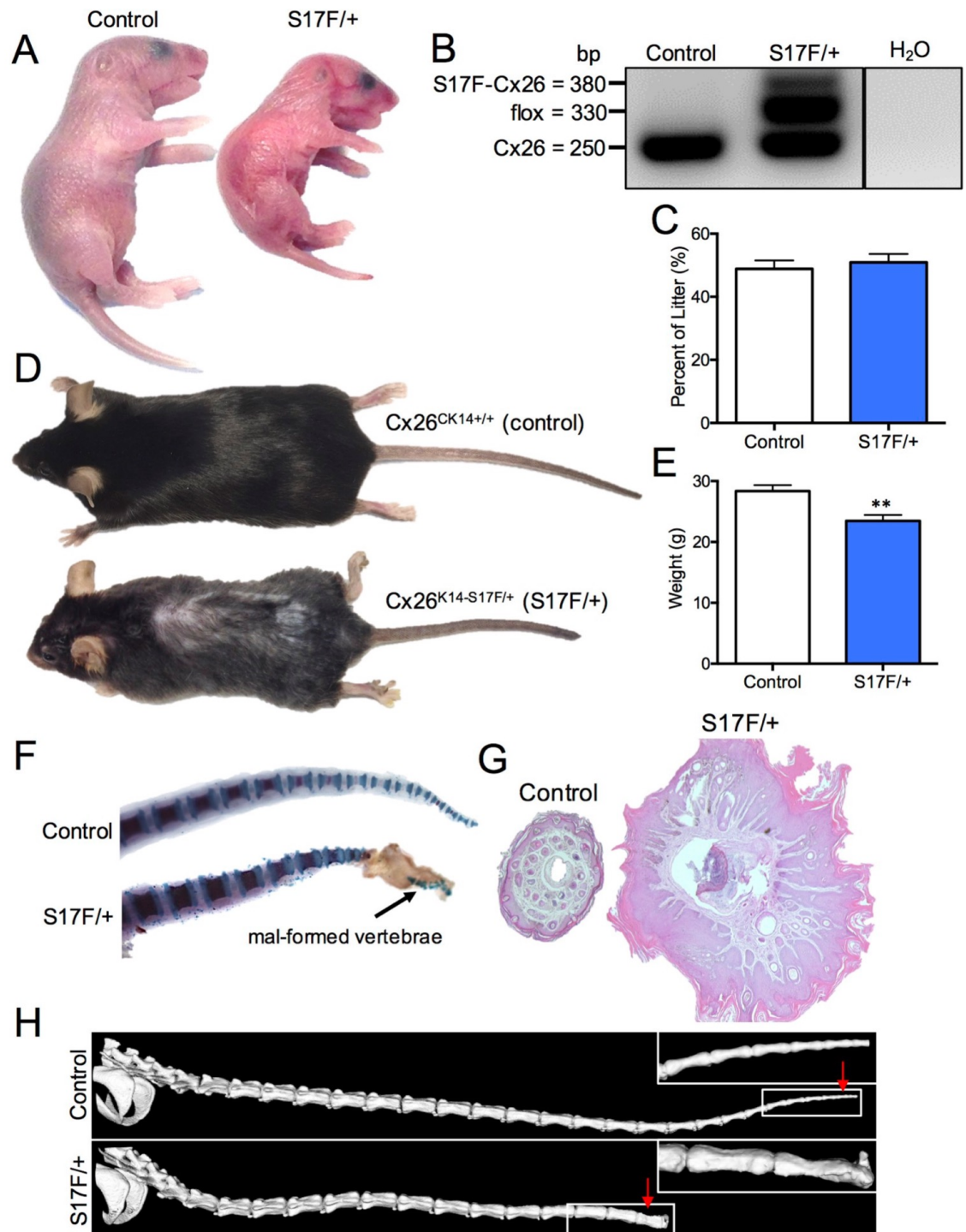


Figure 3.1

Fig. 3.1. S17F/+ mice mimic KIDS skin characteristics and have several additional phenotypes. (A) S17F/+ neonates were smaller and visually distinguishable from control littermates. (B) Skin sample PCR amplification confirms the heterozygous expression of S17F Cx26 in S17F/+ mice. (C) Litters contained equal portions of S17F/+ and control pups with no loss of mouse viability ($n \geq 148$). (D) Representative photos of 3-month-old S17F/+ and control mice reveal moderate differences in size but a pronounced tail phenotype. (E) Whole mouse weights at 3 months of age showed S17F/+ mice are ~15% smaller (** $p < 0.01$, $N \geq 17$). (F) Skeletal stains of P7 tails revealed vertebral malformations underlying the tail phenotype in S17F/+ mice. (G) Cross-section of a distal tail paraffin section stained with hematoxylin and eosin revealed grossly thickened epidermis. (H) μ CT scans of 3-month-old mouse tails revealed vertebral abnormalities in S17F/+ mice. Red arrows in (H) denote the relative locations of cross sections in (G).

Severe PPK was clearly visible in adult S17F/+ mice in which foot pad epidermis displayed protruding hyperpigmented calluses (**Fig. 3.2A**). Histological examination confirmed a gross thickening of vital epidermal layers (stratum basale, spinosum, and granulosum) (**Fig. 3.2B**). In addition to the bulbous region at the distal tail, middle regions of tail epidermis also displayed moderate thickening of these vital layers (**Fig. 3.2B**).

The Cx30 mutant mice (homozygotes indicated as A88V/A88V and heterozygotes as A88V/+) were previously described in (Bosen et al., 2014) and reported to have hyperproliferative sebaceous glands and mild hyperkeratosis of foot pad skin. Besides a greasy matted coat, we found no cutaneous phenotypes, nor a measureable thickening of foot pad epidermis (**Fig. 3.3A**).

3.3.2 S17F Cx26, but not A88V Cx30, disrupts keratinocyte differentiation in foot pad epidermis

Tissue lysates of hind foot pad skin from 3-month-old S17F/+ mice showed elevated levels of Cx26 (**Fig. 3.2C**). While no differences in Cx30 or Cx43 levels were detected in mutant epidermis, all three connexins had large overlapping distribution profiles that were clearly distinguishable from control epidermis (**Fig. 3.2D**). Each connexin formed abundant gap junction plaques indicating that the S17F Cx26 mutant does not impair connexin trafficking *in vivo*. S17F/+ epidermis also had normal levels of keratin 14 (expressed in basal keratinocytes) but a greater amount of filaggrin (expressed in the stratum granulosum and corneum) which was found in numerous suprabasal keratinocyte layers (**Fig. 3.4A, B**). Epidermal proliferation was not affected based on Ki67 (**Fig. 3.4C**) and proliferating cell nuclear antigen (PCNA) assessment (**Fig. 3.4D**). Foot pad epidermis from A88V/+ and A88V/A88V mice had no changes in epidermal connexin expression level (**Fig. 3.3B**) or distribution pattern (**Fig. 3.3C**). Additionally, A88V/+ and A88V/A88V epidermis were similar to control epidermis for keratin and filaggrin expression, as well as proliferation (**Fig. 3.5**). Together these findings suggest epidermal S17F Cx26 but not A88V Cx30 disrupts keratinocyte proliferation-differentiation balance and promotes the formation of PPK in mice.

3.3.3 Primary keratinocytes harvested from S17F/+ mice exhibit reduced GJIC and collective cell migration

Keratinocytes were harvested from newborn connexin mutant mice and WT littermates to assess the influence of physiological levels of S17F Cx26 and A88V Cx30 on keratinocyte

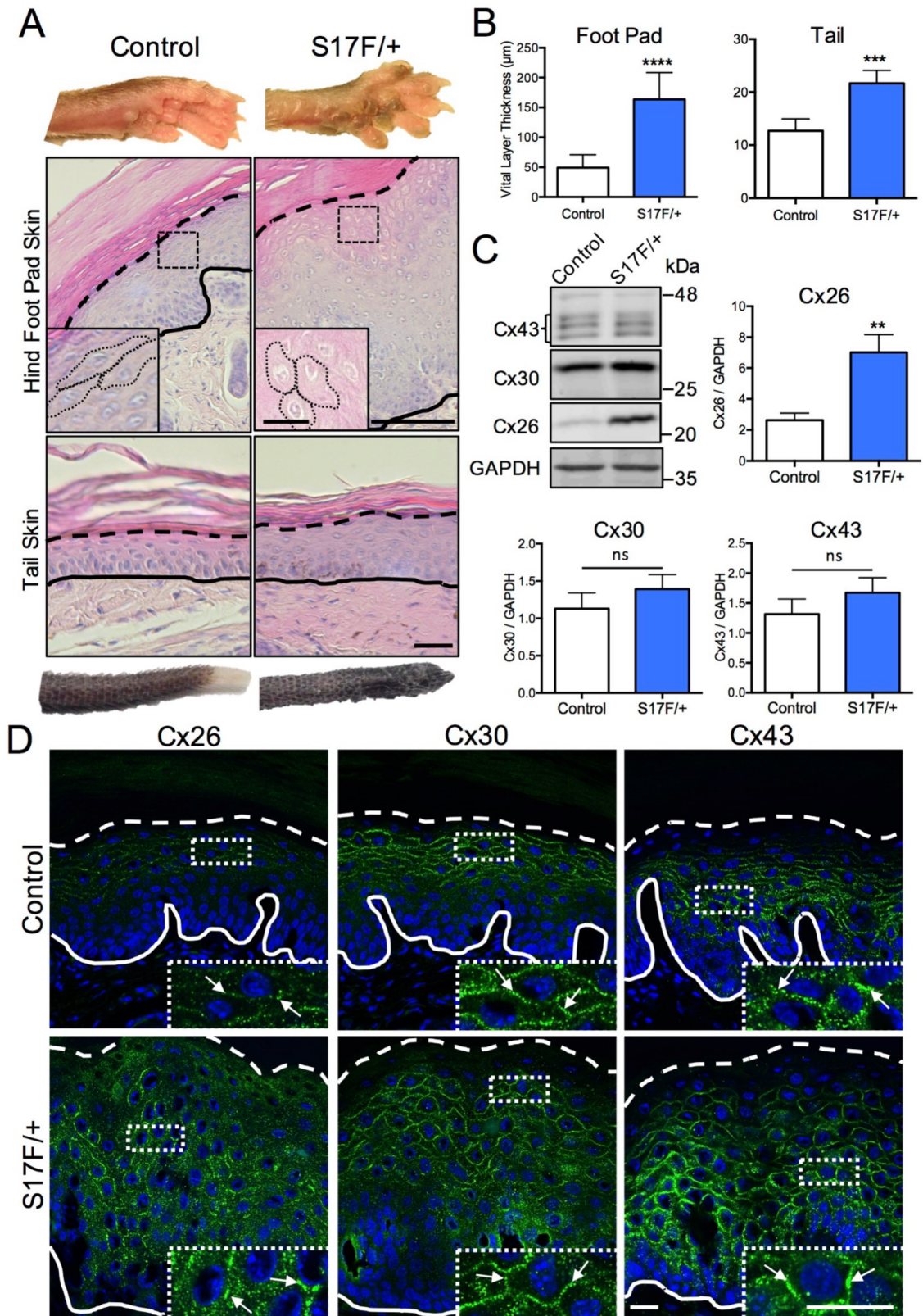


Figure 3.2

Fig. 3.2. S17F/+ mice display thicker foot pad and tail epidermis, and deregulated epidermal connexin expression. (A) 3-month-old S17F/+ mice exhibit severe foot pad epidermal thickening including abnormal non-squamous keratinocytes in suprabasal layers as well as thicker tail epidermis compared to controls (B) (unpaired t-test, *** $p < 0.001$, **** $p < 0.0001$, $N \geq 7$). (C) Foot pad skin lysates from 3-month-old S17F/+ mice exhibited elevated levels of Cx26 expression compared to controls (unpaired t-test, ** $p < 0.01$, ns = $p > 0.05$, $N \geq 10$). (D) Cryosections of 3-month-old S17F/+ foot pad epidermis revealed that Cx26, Cx30, and Cx43 formed abundant gap junctions in a broad range of keratinocyte layers. Complete and dashed lines denote the dermis-epidermis boundary and stratum granulosum-corneum boundary, respectively. Scale bar in (A-upper) = 50 μ m (inset = 10 μ m), (A-lower) = 10 μ m, (D) = 20 μ m (inset = 20 μ m).

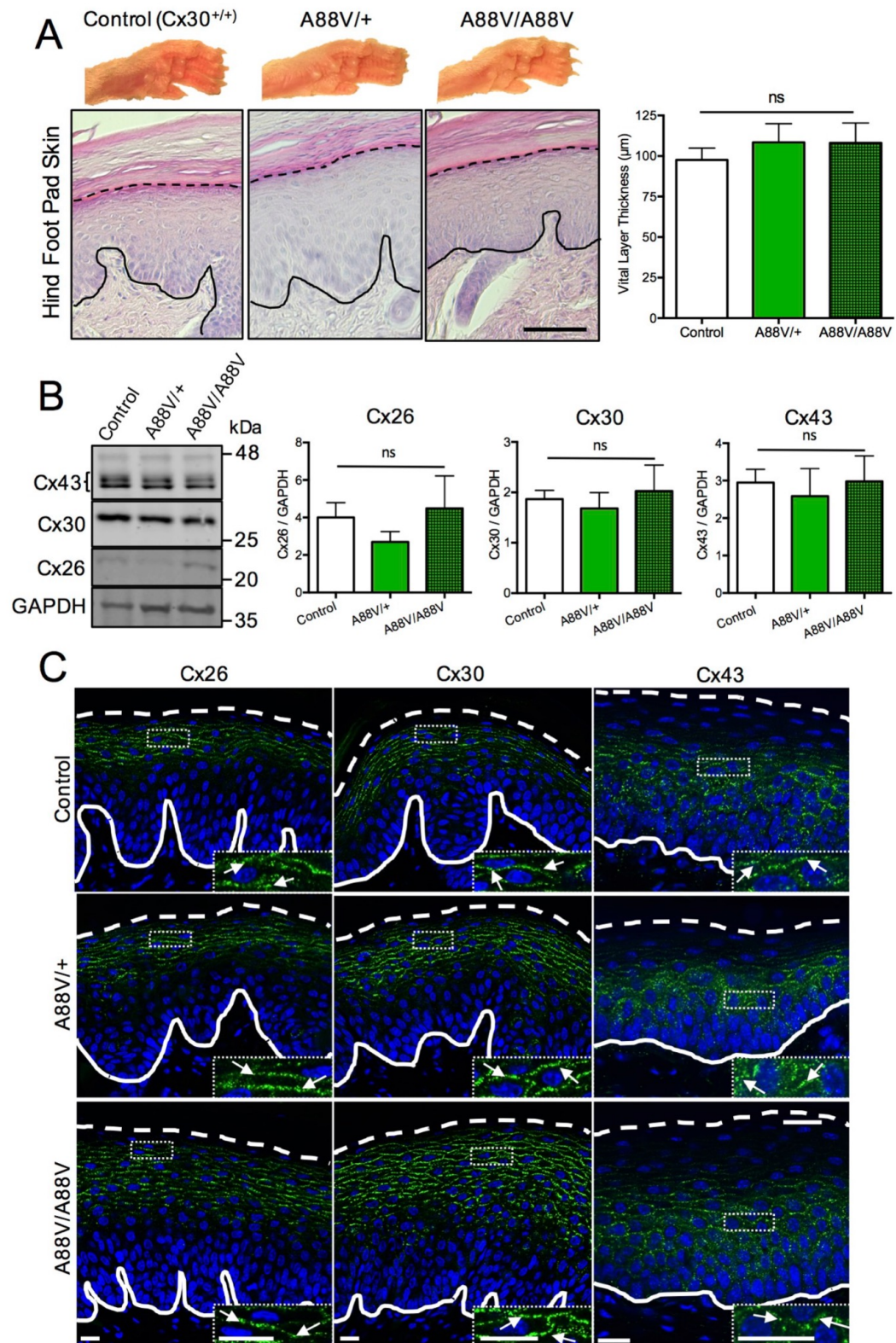


Figure 3.3

Fig. 3.3. A88V/+ and A88V/A88V mice display normal foot pad epidermis and connexin expression. (A) Foot pad skin from 3-month-old mutant mice displayed normal epidermal appearance and thickness (ns = $p > 0.05$, $N \geq 5$) and no differences in Cx26, Cx30, and Cx43 expression (B) (ns = $p > 0.05$, $N = 7$). (C) Foot pad skin cryosections from 3-month-old mutant mice also displayed Cx26, Cx30, and Cx43 formed abundant gap junction plaques (arrows in insets) and were expression in discrete keratinocyte layers. Complete and dashed lines denote the dermis-epidermis boundary, and the stratum granulosum-corneum boundaries, respectively. Scale bar in (A) = $50\mu\text{m}$ (C) = $20\mu\text{m}$, (inset = $20\mu\text{m}$).

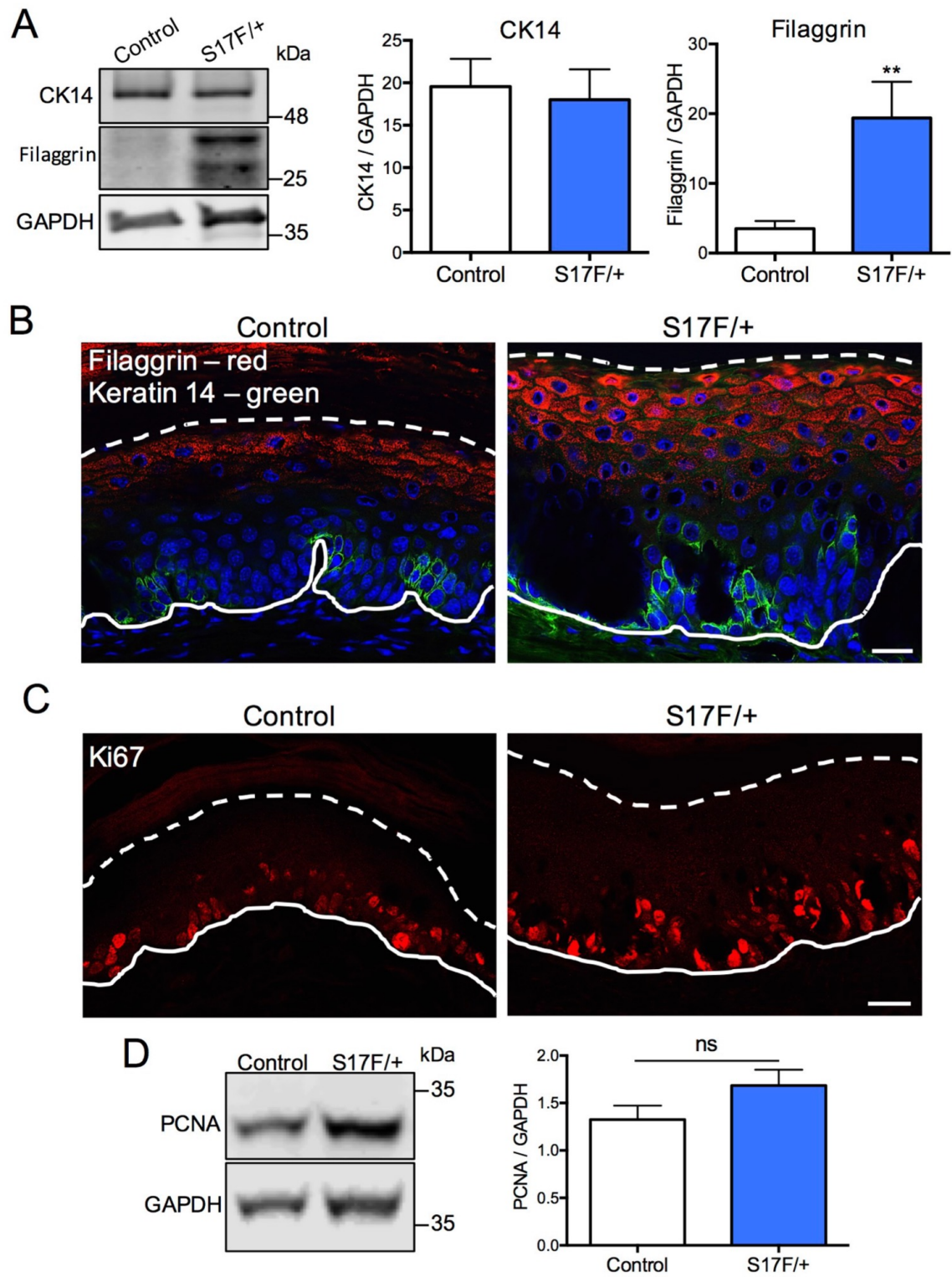


Figure 3.4

Fig. 3.4. S17F/+ mice display abnormal keratinocyte differentiation in foot pad epidermis. (A) Foot pad skin lysates from 3-month-old S17F/+ mice have elevated filaggrin, but normal keratin 14 levels compared to controls (** $p < 0.01$, $N \geq 10$). (B) 3-month-old foot pad epidermis labeled for filaggrin (red) and keratin 14 (green) revealed elevated filaggrin labelling of suprabasal keratinocytes in S17F/+ epidermis. (C) 3-month-old foot pad epidermis labeled for Ki67 (red) and lysates immunoblotted for PCNA (D) demonstrated unaltered levels of cell proliferation in S17F/+ epidermis (ns = $p > 0.05$, $N \geq 10$). Complete and dashed lines denote the dermis-epidermis boundary and stratum granulosum-corneum boundary, respectively. Scale bar in (B) and (C) = 20 μ m.

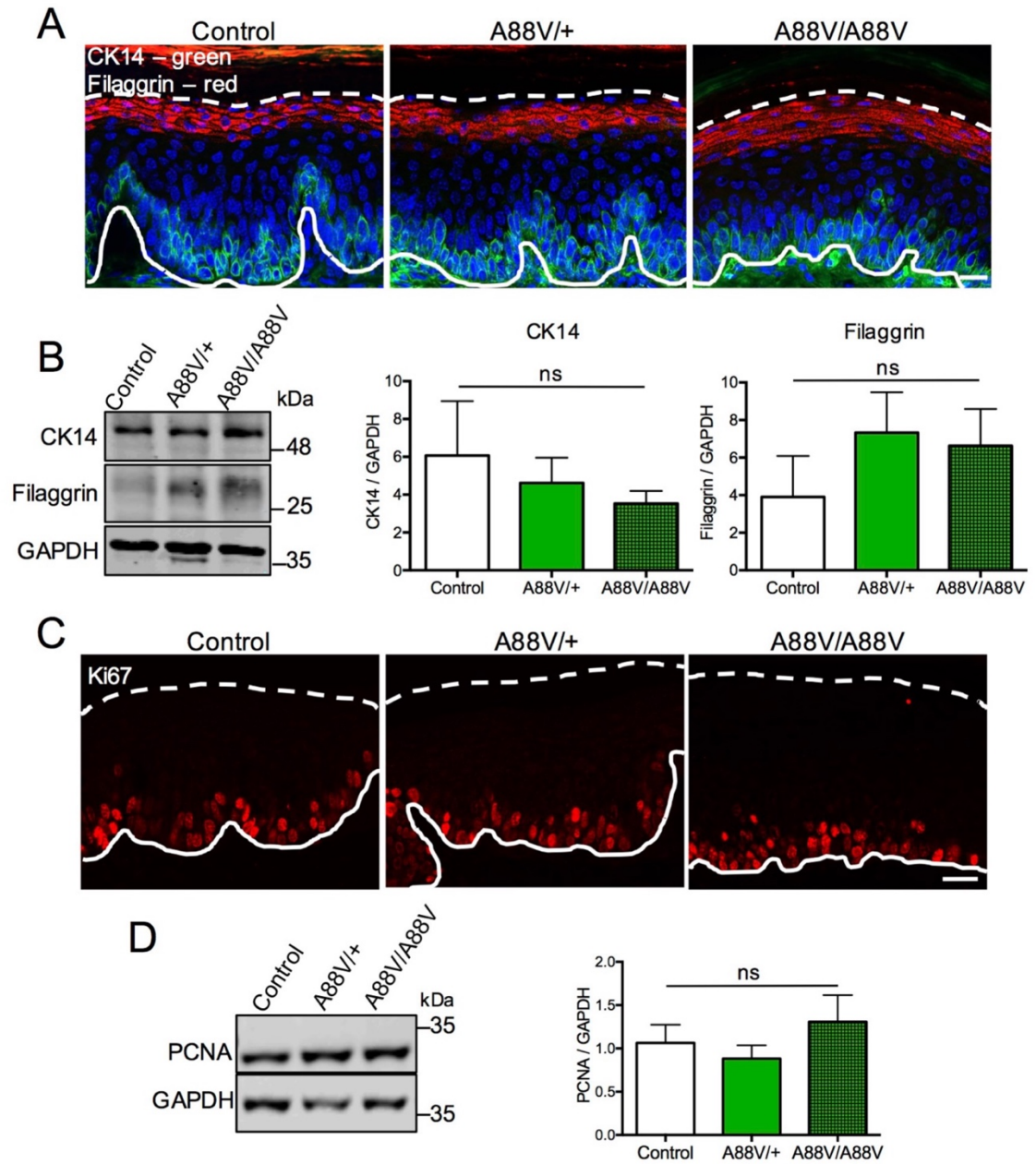


Figure 3.5

Fig. 3.5. A88V/+ and A88V/A88V mice display normal keratinocyte differentiation and proliferation in foot pad epidermis. (A) 3-month-old A88V/+ and A88V/A88V foot pad skin cryosections revealed similar localization of immunolabelled filaggrin (red) and keratin 14 (green) which were also expressed at normal levels in foot pad skin lysates (B) (ns = $p > 0.05$, N = 7). Foot pad epidermis immunolabelled for Ki67 (C) and lysates immunoblotted for PCNA (D) displayed unaltered levels of cell proliferation in A88V/+ and A88V/A88V epidermis (ns = $p > 0.05$, N=7). Scale bar in (A, C) = 20 μ m.

and migration. Similar to a well characterized rat epidermal keratinocyte (REK) cell line (**Fig. 3.6A**), nearly all primary cells labeled thoroughly with keratin 14 and intermediate filaments were clearly visible under high magnification (**Fig. 3.6B**), indicating a highly pure keratinocyte population. In dense clustered regions, cells stratified and increased filaggrin expression, mimicking the behavior of stratified keratinocytes in live epidermis (**Fig. 3.6B**). Keratinocyte cultures were incubated in media containing 1.4mM CaCl_2 for 24 hours to stimulate differentiation and the subsequent expression of Cx26 and Cx30. Compared to controls, S17F/+ cultures appeared to form fewer and smaller Cx26 gap junction plaques between cells, and demonstrated reduced fluorescence recovery following photobleaching (**Fig. 3.7A, B**). Furthermore, S17F/+ cultures displayed reduced collective migration in response to scratch wounds (**Fig. 3.7C**). Keratinocytes from A88V/A88V mice also appeared to form far fewer Cx26 and Cx30 gap junction plaques compared to A88V/+ and control cultures (**Fig. 3.8A**). Interestingly, A88V/A88V keratinocytes displayed no differences in GJIC yet demonstrated increased collective migration in response to scratch wounds (**Fig. 3.8C**). Together these findings suggest Cx26 intercellular communication may influence keratinocyte migration whereas Cx30 may influence migration in a GJIC independent mechanism.

3.3.4 S17F/+ mice display irregular dorsal skin remodeling and tail skin wound healing

Since dynamic regulation of Cx26 and Cx30 coincides with different stages of wound healing, we tested whether mutant Cx26 or Cx30 mutant mice had any overt wound healing defects. Between 3 and 4 months of age, a punch biopsy of depilated dorsal skin created a wound in which healing was monitored. S17F/+ mice displayed no differences in wound size at any stage of recovery (**Fig. 3.9A**) however, repaired epidermis was measurably thicker in S17F/+ mice suggesting possible aberrant epidermal remodeling in response to the wound (**Fig. 3.9B**). No differences in wound healing or abnormalities in repaired epidermis were found in Cx30 mutant mouse dorsal wounds (**Fig. 3.9 C, D**).

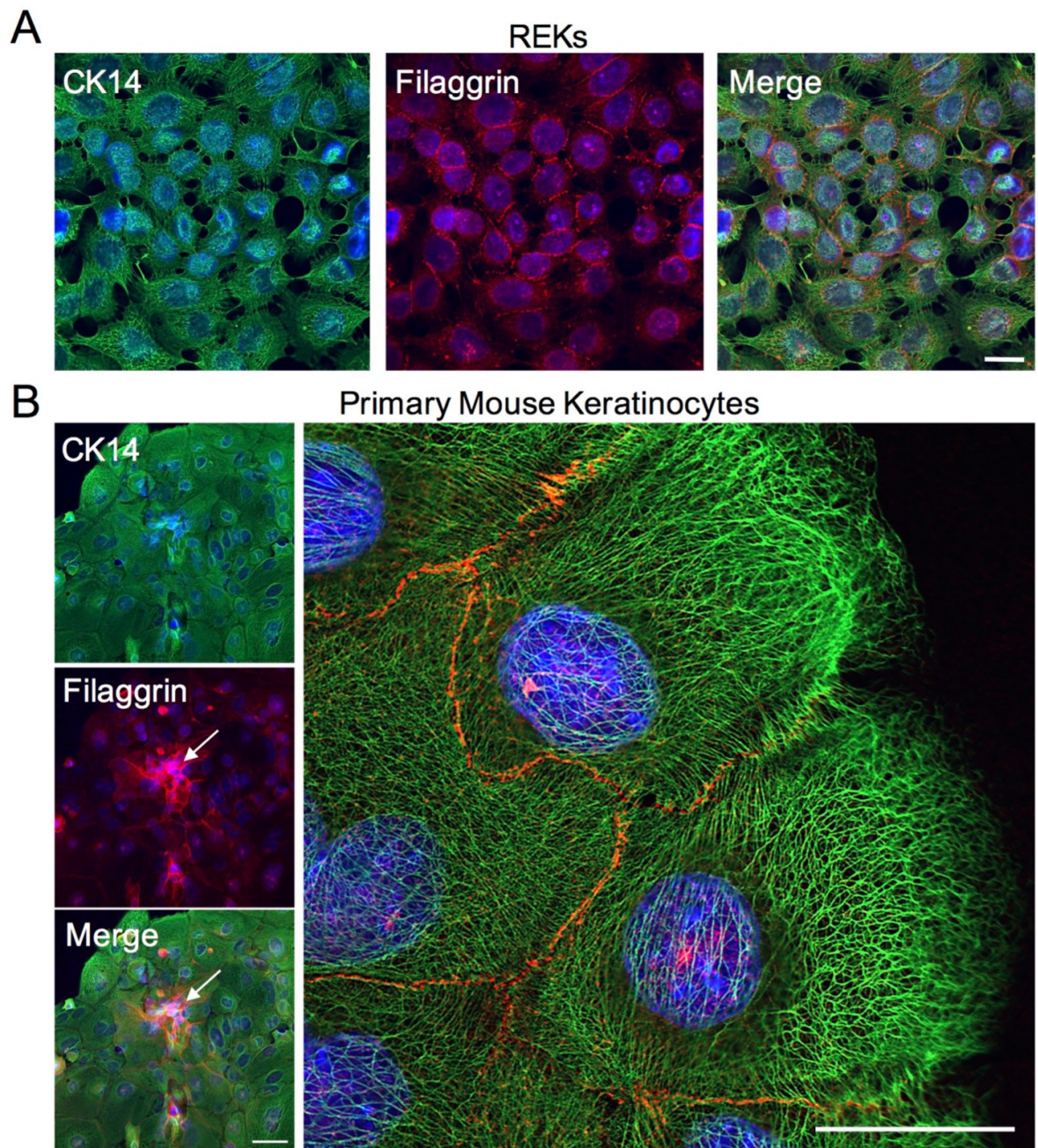


Figure 3.6

Fig. 3.6. Isolated keratinocyte cultures are highly pure. Similar to well-characterized REKs (A), highly pure primary keratinocyte cultures (B) immunolabelled extensively with keratin 14 (green) and demonstrated elevated filaggrin expression in regions where cells began to stratify (left). Individual keratin filaments were visible under high magnification (right). Scale bar in (A) = 10 μ m, (B-left) = 20 μ m, (B-right) = 10 μ m.

wherein patients express connexin mutants with defects in cellular communication (van Steensel, 2004). The epidermis relies on complex GJIC to coordinate a balance of cell proliferation and differentiation for the maintenance of rapid physiological turnover and

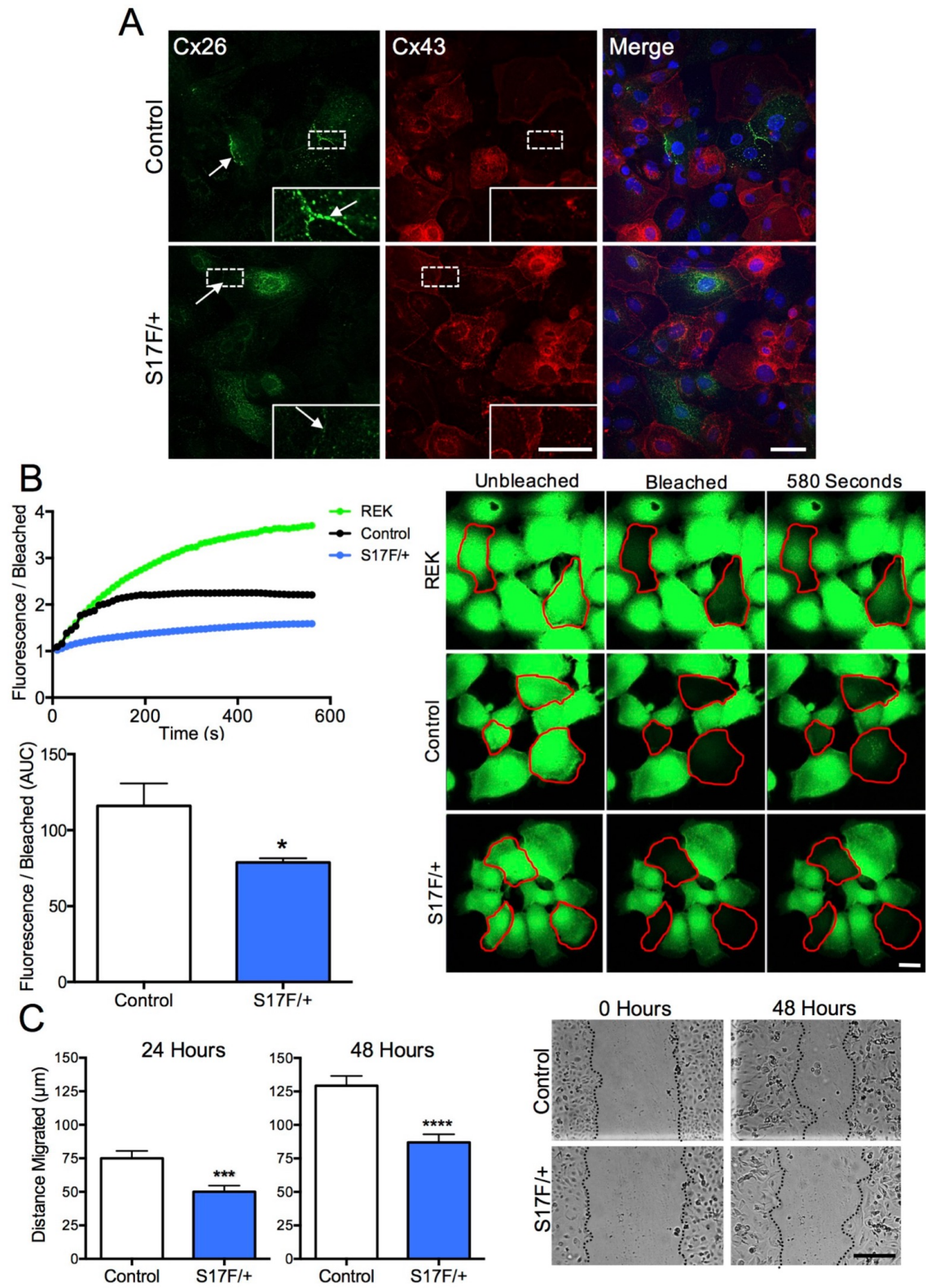


Figure 3.7

Fig. 3.7. Keratinocytes isolated from S17F/+ neonates have reduced GJIC and collective cell migration. (A) S17F/+ keratinocyte cultures appeared to form fewer and smaller Cx26 gap junctions between cells. (B) S17F/+ keratinocytes have reduced calcein-AM fluorescence recovery after photobleaching compared to controls indicative of reduced GJIC (* $p < 0.05$, $N = 8$). (C) Collective keratinocyte migration in response to scratch-wounds was reduced in S17F/+ cultures compared to controls (*** $p < 0.001$, **** $p < 0.0001$, $N = 4$ separate experiments). Scale bar in (A) = 20 μm (inset = 10 μm), (B) = 10 μm , (C) = 100 μm .

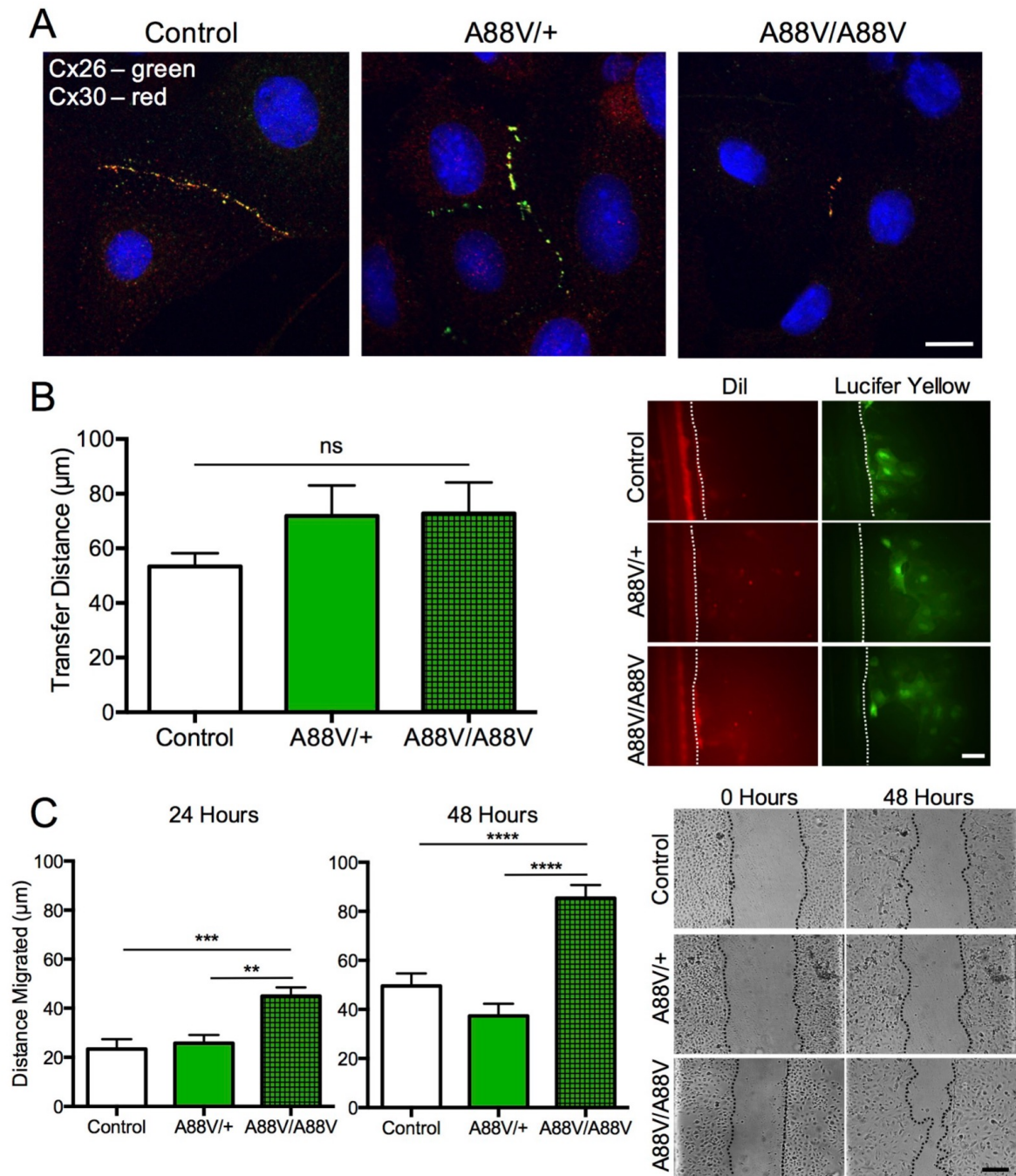


Figure 3.8

Fig. 3.8. Keratinocytes from A88V/A88V mice display normal GJIC but increased collective cell migration. (A) Keratinocytes from A88V/A88V mice appeared to form fewer gap junction plaques compared to control and A88V/+ keratinocytes. (B) Following scrape-loading, mutant keratinocytes displayed similar Lucifer yellow dye transfer to controls (ns = $p > 0.05$, N = 4). DiI is a gap junction impermeable tracer to denote keratinocytes at the scrape edge denoted by the dashed line. (C) A88V/A88V keratinocytes exhibited increased collective cell migration compared to A88V/+ and control keratinocytes (** $p < 0.01$, *** $p < 0.001$, **** $p < 0.0001$, N = 4). Scale bar in (A) = 10 μ m, (B) = 20 μ m, (C) = 50 μ m.

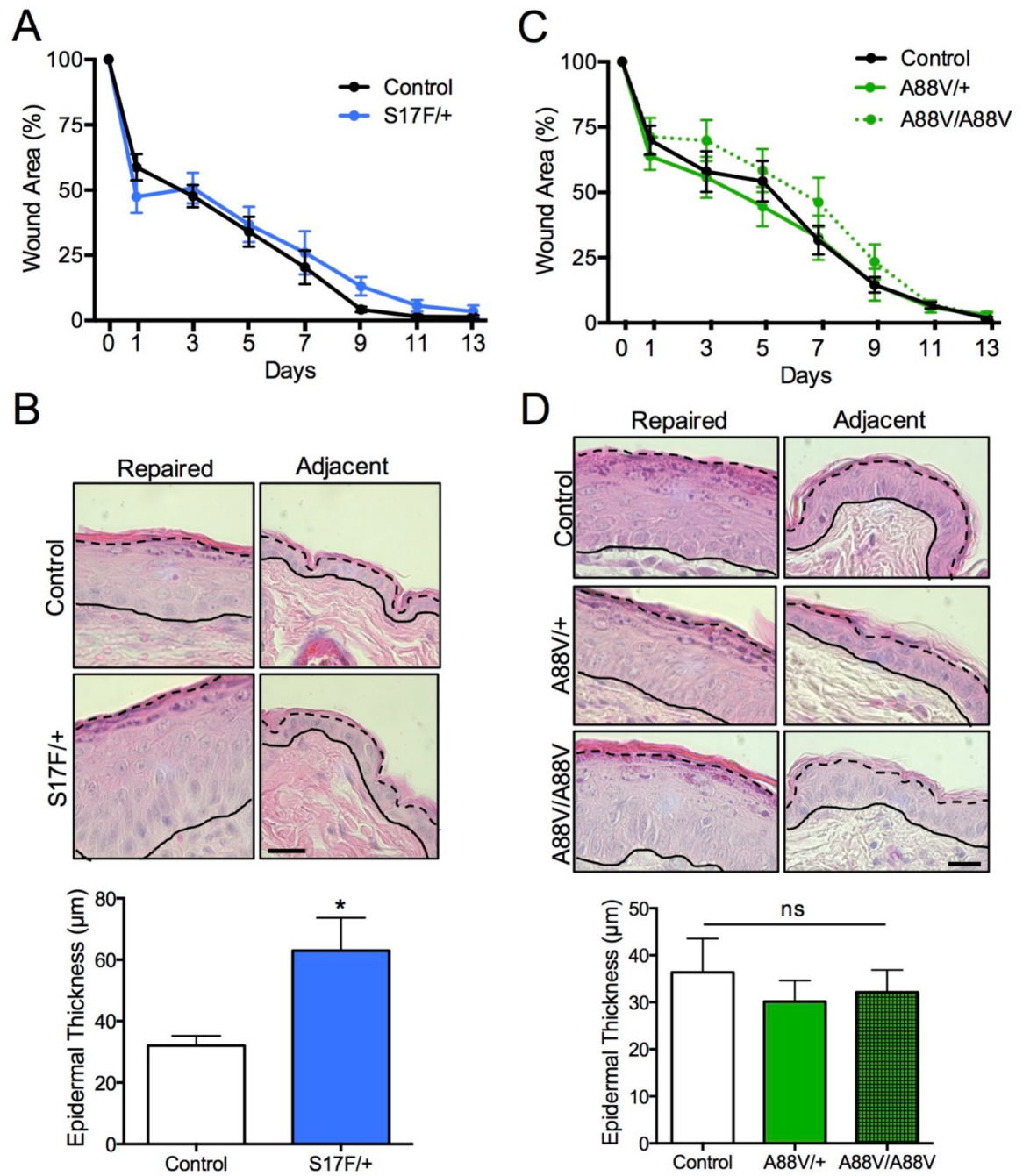


Figure 3.9

Fig. 3.9. Mutant mice display normal wound closure, but S17F/+ mice exhibit abnormal epidermis remodeling. (A) Dorsal skin wound closure was found to be normal in S17F/+ as well as A88V/+ and A88V/A88V mice (C), however, epidermis remodeling following wound closure generated thicker epidermis in S17F/+ mice compared to controls (B) (* $p < 0.05$, $N \geq 4$). (D) A88V/+ and A88V/A88V mice displayed normal epidermis remodeling following wound closure. Scale bar in (B, D) = 10 μ m.

3.4 Discussion

Connexin-linked skin diseases encompass a diverse array of congenital skin abnormalities resiliency to injury. Of particular interest are Cx26 and Cx30 linked skin diseases due to the large number of distinct gene mutations that lead to syndromic diseases featuring variable skin disorders (Martin and van Steensel, 2015). Patients dominantly expressing the S17F Cx26 or A88V Cx30 mutants are diagnosed with KIDS and Clouston Syndrome, respectively, and display some dissimilar phenotypes, but share the common characteristic of PPK (Lamartine et al., 2000; Richard et al., 2002). Although mutant connexins undoubtedly underpin these diseases, specific pathogenic mechanisms are poorly understood and the question of whether these patients have wound healing defects has not been explored. In this study, we generated a novel tissue-specific S17F Cx26 mouse and used the previously described A88V Cx30 mouse (Bosen et al., 2014) to address these questions. We found that our novel Cx26^{K14-S17F/+} mice displayed severe PPK and importantly, no decrease in viability. Foot pad epidermis of S17F/+ mice displayed increased Cx26 expression and irregular localization profiles of epidermal connexins. Furthermore, S17F/+ foot pad epidermis exhibited elevated filaggrin expression, but normal expression of keratin 14 and displayed normal proliferation. Primary keratinocytes isolated from connexin mutant neonates displayed altered GJIC and migration abilities in culture. S17F/+ skin exhibited aberrant epidermal remodeling during wound healing but wounds healed at a similar rate to littermate control mice. Lastly, A88V/+ and A88V/A88V mice displayed no epidermal phenotypes or differences in wound healing compared to controls.

S17F Cx26 was first linked to KIDS in 2002 (Richard et al., 2002) and is now understood to form non-functional gap junction channels or hemichannels but does form hyperactive heteromeric hemichannels with wild type Cx26 and Cx43 in culture (Garcia et al., 2015). Many syndromic Cx26 mutants fail to form functional channels (Xu and Nicholson, 2013), however studies investigating separate KIDS linked mutants reveal that hyperactive hemichannels may be a strong etiological factor in KIDS (Garcia et al., 2015; Gerido et al., 2007; Lee et al., 2009). A mutant mouse globally expressing S17F Cx26 was found to replicate KIDS skin and hearing phenotypes making it a suitable model for KIDS (Schutz et al., 2011). However, one drawback with this model was a sharp loss of mouse viability. To

alleviate this concern and to directly assess the role of the S17F Cx26 mutant in the epidermis, we generated a conditional mutant mouse which expresses the mutant in cells expressing keratin 14. We showed here that indeed epidermal expression of S17F Cx26 produced the severe PPK seen in KIDS, as well as a short, blunted tail reminiscent of autoamputated digits in patients with the Cx26-linked Vohwinkel Syndrome (Maestrini et al., 1999). Furthermore, tissue-specific S17F Cx26 mice were generally healthy suggesting that expression of S17F Cx26 in other tissues such as liver, kidney, brain, and gut may reduce mouse viability.

The nearly universal feature of PPK in connexin-linked skin diseases suggests that proper GJIC is crucial to maintain highly stratified volar epidermis (Avshalumova et al., 2014). We found an imbalance of keratinocyte proliferation and differentiation in foot pad epidermis of S17F/+ mice indicated by increased filaggrin expression yet normal expression of Ki67 and PCNA. Since filaggrin condenses the keratin cytoskeleton in differentiated keratinocytes, we surprisingly observed that suprabasal keratinocytes from S17F/+ foot pad skin did not appear to adopt a squamous morphology like those in control epidermis. We also showed that Cx26, Cx30, and Cx43 were not confined to specific keratinocyte layers but rather were expressed in most keratinocytes, further suggesting deregulated differentiation. Calcium homeostasis in the epidermis is thought to have a large impact on keratinocyte differentiation (Adams et al., 2012), and since Ca^{2+} mobilizing molecules such as IP_3 and ATP are permissible by gap junctions and hemichannels, the calcium profile in lesioned epidermis is an attractive, albeit difficult element to assess. Interestingly, Bosen and colleagues showed that unlike control littermates, global S17F Cx26 mice exhibited large amounts of Ca^{2+} in the stratum corneum, suggesting that S17F Cx26 may disrupt the calcium profile in the epidermis (Bosen et al., 2015). As some connexin hemichannels are known to release ATP in response to mechanical stimulation (Bao et al., 2004; Baroja-Mazo et al., 2013; Saez et al., 2005), it is plausible that mutant connexins in the mechanical environment of volar skin could stimulate aberrant purinergic signaling that disrupts calcium homeostasis and finally differentiation (Baroja-Mazo et al., 2013; Martin et al., 2014). Furthermore, lesions of flexural skin regions are also commonly observed in KIDS and Vohwinkel Syndrome patients (Avshalumova et al., 2014; Cogshall et al., 2013) further supporting mechanically stimulated Cx26 mutants in skin pathogenesis. Nevertheless, investigations into the mechanical sensitivity of Cx26 mutants is warranted to shed light on this notion.

Keratinocytes isolated from our mice demonstrated that physiological levels of S17F Cx26 led to reduced gap junctional coupling and a similar reduction in collective cell migration. Following wounding, undamaged keratinocytes at the wound edge initiate re-epithelialization by migrating under the coagulum (Martin, 1997). During this process, a transient reduction of cell surface Cx43 favours cell migration by reducing cell-cell adhesion through its binding partner zona occludens-1, a protein linked to junctional complexes (Mendoza-Naranjo et al., 2012). Our results suggest that Cx26, which is thought to only bind an ubiquitin-ligase protein (Henzl et al., 2004), can also influence cell migration through direct intercellular communication. It is well documented, yet poorly understood why Cx26 and Cx30 are transiently upregulated in wound edge keratinocytes (Coutinho et al., 2003; Davis et al., 2013; Goliger and Paul, 1995; Kretz et al., 2003), however our results suggest this may generate a highly coupled keratinocyte network to optimize collective cell migration. To our surprise, S17F/+ cultures also appeared to form fewer and smaller gap junction plaques in light of extensive Cx26 gap junction formation in intact S17F/+ epidermis. Reduced gap junction formation by S17F Cx26 has however, been reported in HeLa cells (Garcia et al., 2015), therefore the disparagement of connexin expression between native epidermis and *in vitro* models highlights the importance of using mutant mouse models in understanding connexin-linked pathologies.

Because Cx26 is dynamically regulated during wound healing (Brandner et al., 2004) and KIDS patients develop inflammatory skin lesions (Coggshall et al., 2013), it raises questions as to whether KIDS patients have abnormal wound healing. There are currently no reports of KIDS patients exhibiting wound healing defects, however, the protective care these patients require (Coggshall et al., 2013) and the rare nature of this disease argues that a wound healing defect may be under reported. In one study linking Cx26 levels to wound healing, two mouse models with persistent epidermal Cx26 expression developed inflammatory lesions and wounds which displayed improper remodeling (Djalilian et al., 2006) suggesting that Cx26 may contribute to the inflammatory and remodeling phases of wound healing. However, the S17F/+ mice used in our study displayed no overt wound healing defects, and if this finding can be extrapolated to humans, this would suggest that KIDS patients may actually heal wounds well. That being said, our findings also suggest that the abnormal keratinocyte differentiation required for epidermal remodeling may result in thicker epidermis in the healed

skin from KIDS patients. We also demonstrated that hyperkeratotic foot pad epidermis in S17F/+ mice had elevated levels of Cx26, suggesting that while unchallenged skin was relatively normal, challenged skin by weight bearing or wound healing may provide the conditions for S17F Cx26 to disrupt epidermal physiology. Although the exact nature of these conditions remains uncertain, our findings support the notion that S17F Cx26 disrupts epidermal homeostasis by deregulating keratinocyte differentiation.

Contrary to our S17F/+ mice, mice globally expressing A88V Cx30 showed almost no evidence of skin disease, as the only differential elements were found between A88V/A88V and control primary keratinocytes. Since differences arose only once mutant keratinocytes were isolated *in vitro*, this suggests the influence of A88V Cx30 was easily overcome in native epidermis where other regulatory are likely at play. Despite differences in genetic background, the striking dissimilarity of disease presentation between our mouse models, which express functionally similar connexin mutants, suggests that Cx30 may play a minimal role in murine epidermis. This notion is supported by the observation that adult Cx30 null mice displayed no obvious cutaneous phenotypes (Dere et al., 2003).

Lastly, Clouston Syndrome is a highly variable disease in humans which suggests that other genetic predispositions likely play a large part in disease presentation. For example, Clouston Syndrome patients do not generally have hearing loss, however one patient expressing A88V Cx30 in addition to a benign Cx26 mutant exhibited mild deafness (Sugiura et al., 2013). Despite subtle differences between murine and human epidermis, our findings strongly support the generation and assessment of animal models that mirror connexin-linked diseases.

3.5 Acknowledgements and Funding

We would like to thank Dr. Katherine Willmore, Joseph Umoh, and Dr. David Holdsworth for helping generate the μ CT images as well as Dawn Marie Bryce for assistance with the skeletal staining technique. We would also like to thank Charles Walewski, Layo Alaga, and Ruichen Shang for assisting with image quantitation. This research was funded by a Canadian Institutes of Health Research grant (123228) to DWL.

3.6 References

- Adams, M.P., D.G. Mallet, and G.J. Pettet. 2012. Active regulation of the epidermal calcium profile. *J Theor Biol.* 301:112-12.
- Alexander, D.B., and G.S. Goldberg. 2003. Transfer of biologically important molecules between cells through gap junction channels. *Curr Med Chem.* 10:2045-2058.
- Avshalumova, L., J. Fabrikant, and A. Koriakos. 2014. Overview of skin diseases linked to connexin gene mutations. *Int J Dermatol.* 53:192-205.
- Baden, H.P., and J. Kubilus. 1983. The growth and differentiation of cultured newborn rat keratinocytes. *J Invest Dermatol.* 80:124-130.
- Bao, L., F. Sachs, and G. Dahl. 2004. Connexins are mechanosensitive. *Am J Physiol Cell Physiol.* 287:C1389-1395.
- Baroja-Mazo, A., M. Barbera-Cremades, and P. Pelegrin. 2013. The participation of plasma membrane hemichannels to purinergic signaling. *Biochim Biophys Acta.* 1828:79-93.
- Berger, A.C., J.J. Kelly, P. Lajoie, Q. Shao, and D.W. Laird. 2014. Mutations in Cx30 that are linked to skin disease and non-syndromic hearing loss exhibit several distinct cellular pathologies. *J Cell Sci.* 127:1751-1764.
- Bikle, D.D., Z. Xie, and C.L. Tu. 2012. Calcium regulation of keratinocyte differentiation. *Expert Rev Endocrinol Metab.* 7:461-472.
- Bosen, F., A. Celli, D. Crumrine, K. vom Dorp, P. Ebel, H. Jastrow, P. Dormann, E. Winterhager, T. Mauro, and K. Willecke. 2015. Altered epidermal lipid processing and calcium distribution in the KID syndrome mouse model Cx26S17F. *FEBS Lett.* 589:1904-1910.
- Bosen, F., M. Schutz, A. Beinhauer, N. Strenzke, T. Franz, and K. Willecke. 2014. The Clouston syndrome mutation connexin30 A88V leads to hyperproliferation of sebaceous glands and hearing impairments in mice. *FEBS Lett.* 588:1795-1801.
- Brandner, J.M., P. Houdek, B. Husing, C. Kaiser, and I. Moll. 2004. Connexins 26, 30, and 43: differences among spontaneous, chronic, and accelerated human wound healing. *J Invest Dermatol.* 122:1310-1320.
- Caskenette, D., S. Penuela, V. Lee, K. Barr, F. Beier, D.W. Laird, and K.E. Willmore. 2016. Global deletion of Pax3 produces multiple phenotypic effects in mouse humeri and femora. *J Anat.* 228:746-756.

- Churko, J.M., J.J. Kelly, A. Macdonald, J. Lee, J. Sampson, D. Bai, and D.W. Laird. 2012. The G60S Cx43 mutant enhances keratinocyte proliferation and differentiation. *Exp Dermatol*. 21:612-618.
- Churko, J.M., and D.W. Laird. 2013. Gap junction remodeling in skin repair following wounding and disease. *Physiology (Bethesda)*. 28:190-198.
- Churko, J.M., Q. Shao, X.Q. Gong, K.J. Swoboda, D. Bai, J. Sampson, and D.W. Laird. 2011. Human dermal fibroblasts derived from oculodentodigital dysplasia patients suggest that patients may have wound-healing defects. *Hum Mutat*. 32:456-466.
- Coggshall, K., T. Farsani, B. Ruben, T.H. McCalmont, T.G. Berger, L.P. Fox, and K. Shinkai. 2013. Keratitis, ichthyosis, and deafness (KID) syndrome: A review of infectious and neoplastic complications. *Journal of the American Academy of Dermatology*. 69:127-134.
- Common, J.E., W.L. Di, D. Davies, H. Galvin, I.M. Leigh, E.A. O'Toole, and D.P. Kelsell. 2003. Cellular mechanisms of mutant connexins in skin disease and hearing loss. *Cell Commun Adhes*. 10:347-351.
- Coutinho, P., C. Qiu, S. Frank, K. Tamber, and D. Becker. 2003. Dynamic changes in connexin expression correlate with key events in the wound healing process. *Cell Biol Int*. 27:525-541.
- Dassule, H.R., P. Lewis, M. Bei, R. Maas, and A.P. McMahon. 2000. Sonic hedgehog regulates growth and morphogenesis of the tooth. *Development*. 127:4775-4785.
- Davis, N.G., A. Phillips, and D.L. Becker. 2013. Connexin dynamics in the privileged wound healing of the buccal mucosa. *Wound Repair Regen*. 21:571-578.
- Dere, E., M.A. De Souza-Silva, C. Frisch, B. Teubner, G. Sohl, K. Willecke, and J.P. Huston. 2003. Connexin30-deficient mice show increased emotionality and decreased rearing activity in the open-field along with neurochemical changes. *Eur J Neurosci*. 18:629-638.
- Di, W.L., E.L. Rugg, I.M. Leigh, and D.P. Kelsell. 2001. Multiple epidermal connexins are expressed in different keratinocyte subpopulations including connexin 31. *J Invest Dermatol*. 117:958-964.
- Djalilian, A.R., D. McGaughey, S. Patel, E.Y. Seo, C. Yang, J. Cheng, M. Tomic, S. Sinha, A. Ishida-Yamamoto, and J.A. Segre. 2006. Connexin 26 regulates epidermal barrier and wound remodeling and promotes psoriasiform response. *J Clin Invest*. 116:1243-1253.
- Essenfelder, G.M., R. Bruzzone, J. Lamartine, A. Charollais, C. Blanchet-Bardon, M.T. Barbe, P. Meda, and G. Waksman. 2004. Connexin30 mutations responsible for

- hidrotic ectodermal dysplasia cause abnormal hemichannel activity. *Hum Mol Genet.* 13:1703-1714.
- Garcia, I.E., J. Maripillan, O. Jara, R. Ceriani, A. Palacios-Munoz, J. Ramachandran, P. Olivero, T. Perez-Acle, C. Gonzalez, J.C. Saez, J.E. Contreras, and A.D. Martinez. 2015. Keratitis-ichthyosis-deafness syndrome-associated Cx26 mutants produce nonfunctional gap junctions but hyperactive hemichannels when co-expressed with wild type Cx43. *J Invest Dermatol.* 135:1338-1347.
- Gerido, D.A., A.M. DeRosa, G. Richard, and T.W. White. 2007. Aberrant hemichannel properties of Cx26 mutations causing skin disease and deafness. *Am J Physiol Cell Physiol.* 293:C337-345.
- Ghatnekar, G.S., C.L. Grek, D.G. Armstrong, S.C. Desai, and R.G. Gourdie. 2015. The effect of a connexin43-based Peptide on the healing of chronic venous leg ulcers: a multicenter, randomized trial. *J Invest Dermatol.* 135:289-298.
- Goliger, J.A., and D.L. Paul. 1995. Wounding alters epidermal connexin expression and gap junction-mediated intercellular communication. *Mol Biol Cell.* 6:1491-1501.
- Henzl, M.T., I. Thalmann, J.D. Larson, E.G. Ignatova, and R. Thalmann. 2004. The cochlear F-box protein OCP1 associates with OCP2 and connexin 26. *Hear Res.* 191:101-109.
- Kibar, Z., M.P. Dube, J. Powell, C. McCuaig, S.J. Hayflick, J. Zonana, A. Hovnanian, U. Radhakrishna, S.E. Antonarakis, A. Benohanian, A.D. Sheeran, M.L. Stephan, R. Gosselin, D.P. Kelsell, A.L. Christianson, F.C. Fraser, V.M. Der Kaloustian, and G.A. Rouleau. 2000. Clouston hidrotic ectodermal dysplasia (HED): genetic homogeneity, presence of a founder effect in the French Canadian population and fine genetic mapping. *Eur J Hum Genet.* 8:372-380.
- Kretz, M., C. Euwens, S. Hombach, D. Eckardt, B. Teubner, O. Traub, K. Willecke, and T. Ott. 2003. Altered connexin expression and wound healing in the epidermis of connexin-deficient mice. *J Cell Sci.* 116:3443-3452.
- Lamartine, J., G. Munhoz Essenfelder, Z. Kibar, I. Lanneluc, E. Callouet, D. Laoudj, G. Lemaitre, C. Hand, S.J. Hayflick, J. Zonana, S. Antonarakis, U. Radhakrishna, D.P. Kelsell, A.L. Christianson, A. Pitaval, V. Der Kaloustian, C. Fraser, C. Blanchet-Bardon, G.A. Rouleau, and G. Waksman. 2000. Mutations in GJB6 cause hidrotic ectodermal dysplasia. *Nat Genet.* 26:142-144.
- Lee, J.R., A.M. Derosa, and T.W. White. 2009. Connexin mutations causing skin disease and deafness increase hemichannel activity and cell death when expressed in *Xenopus* oocytes. *J Invest Dermatol.* 129:870-878.
- Maestrini, E., B.P. Korge, J. Ocana-Sierra, E. Calzolari, S. Cambiaghi, P.M. Scudder, A. Hovnanian, A.P. Monaco, and C.S. Munro. 1999. A missense mutation in connexin26,

- D66H, causes mutilating keratoderma with sensorineural deafness (Vohwinkel's syndrome) in three unrelated families. *Hum Mol Genet.* 8:1237-1243.
- Martin, P. 1997. Wound healing--aiming for perfect skin regeneration. *Science.* 276:75-81.
- Martin, P.E., J.A. Easton, M.B. Hodgins, and C.S. Wright. 2014. Connexins: sensors of epidermal integrity that are therapeutic targets. *FEBS Lett.* 588:1304-1314.
- Martin, P.E., and M. van Steensel. 2015. Connexins and skin disease: insights into the role of beta connexins in skin homeostasis. *Cell Tissue Res.* 360:645-658.
- McLeod, M.J. 1980. Differential staining of cartilage and bone in whole mouse fetuses by alcian blue and alizarin red S. *Teratology.* 22:299-301.
- Mendoza-Naranjo, A., P. Cormie, A.E. Serrano, R. Hu, S. O'Neill, C.M. Wang, C. Thrasivoulou, K.T. Power, A. White, T. Serena, A.R. Phillips, and D.L. Becker. 2012. Targeting Cx43 and N-cadherin, which are abnormally upregulated in venous leg ulcers, influences migration, adhesion and activation of Rho GTPases. *PLoS One.* 7:e37374.
- Mori, R., K.T. Power, C.M. Wang, P. Martin, and D.L. Becker. 2006. Acute downregulation of connexin43 at wound sites leads to a reduced inflammatory response, enhanced keratinocyte proliferation and wound fibroblast migration. *J Cell Sci.* 119:5193-5203.
- Penuela, S., R. Bhalla, X.Q. Gong, K.N. Cowan, S.J. Celetti, B.J. Cowan, D. Bai, Q. Shao, and D.W. Laird. 2007. Pannexin 1 and pannexin 3 are glycoproteins that exhibit many distinct characteristics from the connexin family of gap junction proteins. *J Cell Sci.* 120:3772-3783.
- Qiu, C., P. Coutinho, S. Frank, S. Franke, L.Y. Law, P. Martin, C.R. Green, and D.L. Becker. 2003. Targeting connexin43 expression accelerates the rate of wound repair. *Current Biology.* 13:1697-1703.
- Richard, G., F. Rouan, C.E. Willoughby, N. Brown, P. Chung, M. Ryyanen, E.W. Jabs, S.J. Bale, J.J. DiGiovanna, J. Uitto, and L. Russell. 2002. Missense mutations in GJB2 encoding connexin-26 cause the ectodermal dysplasia keratitis-ichthyosis-deafness syndrome. *American Journal of Human Genetics.* 70:1341-1348.
- Saez, J.C., M.A. Retamal, D. Basilio, F.F. Bukauskas, and M.V.L. Bennett. 2005. Connexin-based gap junction hemichannels: Gating mechanisms. *Bba-Biomembranes.* 1711:215-224.
- Sandilands, A., C. Sutherland, A.D. Irvine, and W.H. McLean. 2009. Filaggrin in the frontline: role in skin barrier function and disease. *J Cell Sci.* 122:1285-1294.

- Schutz, M., T. Auth, A. Gehrt, F. Bosen, I. Korber, N. Strenzke, T. Moser, and K. Willecke. 2011. The connexin26 S17F mouse mutant represents a model for the human hereditary keratitis-ichthyosis-deafness syndrome. *Hum Mol Genet.* 20:28-39.
- Scott, C.A., D. Tattersall, E.A. O'Toole, and D.P. Kelsell. 2012. Connexins in epidermal homeostasis and skin disease. *Biochim Biophys Acta.* 1818:1952-1961.
- Stewart, M.K.G., X.Q. Gong, K.J. Barr, D.L. Bai, G.I. Fishman, and D.W. Laird. 2013. The severity of mammary gland developmental defects is linked to the overall functional status of Cx43 as revealed by genetically modified mice. *Biochemical Journal.* 449:401-413.
- Sugiura, K., M. Teranishi, Y. Matsumoto, and M. Akiyama. 2013. Clouston syndrome with heterozygous GJB6 mutation p.Ala88Val and GJB2 variant p.Val27Ile revealing mild sensorineural hearing loss and photophobia. *JAMA Dermatol.* 149:1350-1351.
- van Steensel, M.A. 2004. Gap junction diseases of the skin. *Am J Med Genet C Semin Med Genet.* 131C:12-19.
- Wang, G.Y., A. Woods, H. Agoston, V. Ulici, M. Glogauer, and F. Beier. 2007. Genetic ablation of Rac1 in cartilage results in chondrodysplasia. *Developmental Biology.* 306:612-623.
- Xu, J., and B.J. Nicholson. 2013. The role of connexins in ear and skin physiology - functional insights from disease-associated mutations. *Biochim Biophys Acta.* 1828:167-178.
- Yum, S.W., J.X. Zhang, V. Valiunas, G. Kanaporis, P.R. Brink, T.W. White, and S.S. Scherer. 2007. Human connexin26 and connexin30 form functional heteromeric and heterotypic channels. *Am J Physiol-Cell Ph.* 293:C1032-C1048.

4 General Discussion

A high degree of GJIC is a hallmark of stratified epidermis (Scott et al., 2012). This communication is, in part, facilitated by Cx26 and Cx30 gap junctions and it is well known that their proper assembly and function is critical for overall skin health (Martin and van Steensel, 2015). This thesis compiles the analyses of several connexin-linked skin diseases at the level of cells and the intact epidermis. Using transgenic mice, primary keratinocytes, and reference cell lines, we examined the cellular characteristics of Cx26 and Cx30 mutants and their link to disease. The goal of this work is to elucidate genotype/phenotype relationships of distinct connexin mutants as they relate to skin disease and to further understand the contribution of these critical molecules in epidermal physiology. Here, I will establish a narrative to integrate our findings within the current literature, discuss their clinical implications, and present questions for continued investigation.

4.1 Learning outcomes from transgenic mice

Limitations to the clinical translatability of cell-based experiments have forced researchers to develop animal models to better understand, not only the disease-causing features of connexin mutants, but also the role of connexins in normal skin development, healing, and homeostasis. Excluding the novel Cx26^{K14-S17F/+} mouse used in the current study, at least 10 different mouse models have been generated as tools to investigate disease-linked connexins (i.e. Cx26, Cx30, Cx30.3, Cx31, and Cx43) in skin physiology (Bakirtzis et al., 2003; Bosen et al., 2014; Churko et al., 2012; Cogliati et al., 2015; Djalilian et al., 2006; Maass et al., 2004; Mese et al., 2011; Schnichels et al., 2007; Schutz et al., 2011). Five of these models feature *GJB2* modifications that have helped reveal the pathogenesis of KIDS and Vohwinkel Syndrome (Bakirtzis et al., 2003; Mese et al., 2011; Schutz et al., 2011), whereby a role was proposed for Cx26 in epidermal barrier establishment and cutaneous wound healing (Djalilian et al., 2006). In addition, Cx30 (Dere et al., 2003) and Cx31 (Plum et al., 2001) null mice displayed no cutaneous phenotypes despite their expression in normal healthy skin. While it may therefore be compelling to suggest that Cx30 and Cx31 are unlikely candidates for human skin disease, in fact, mutations in their genes are linked to Clouston Syndrome, KIDS, and erythrokeratoderma variabilis (Lamartine et al., 2000; Lilly et al., 2016; Richard et al., 1998).

These findings strongly suggest that the presence of a connexin mutant can lead to more pathology than the entire absence of the same connexin. Also, the redundancy of GJIC within the epidermis likely protects the skin from disease when one connexin is ablated. In our current study, we took the approach of using partially characterized connexin mutants to assess their impact on the keratinocytes and the epidermis, and further modeled two connexin mutants in mouse models of human skin diseases.

Within the steadily-solidifying paradigm that the scope of disease manifestation is governed by the gain- or loss-of function status of Cx26 mutants, we chose to model KIDS using the S17F mutant. First pass analyses demonstrated that this mutant conformed to the loss-of-function grouping as no functional homomeric gap junction channels or hemichannels could be observed (Garcia et al., 2015; Lee et al., 2009), however, a careful consideration of gain-of-function properties neatly investigated by Isaac Garcia and colleagues first demonstrated the extended influence of S17F Cx26 on Cx43. Since Cx26 and Cx43 do not normally intermix in connexons (Gemel et al., 2004), the curious ability of a non-functional Cx26 mutant to trans-dominantly bind Cx43 and form hyperactive complexes is indeed an odd concept in connexin biology. Nevertheless, this surprising finding added substantial value to, not only our understanding of KIDS, but also the study of connexinopathies, since it demonstrated the legitimacy of considering all possible connexin interactions within each disease context. Schütz and colleagues took the next step by first introducing the S17F mutant into a mouse model (Schutz et al., 2011). This mouse exhibited a dysfunctional epidermal barrier, annular tail restrictions, foot pad hyperplasia, and moderate hearing loss, making it a suitable model for KIDS (Schutz et al., 2011). However, the global expression of this mutant significantly reduced mouse viability, suggesting that tissue-specific knock-in of the mutant Cx26 would be beneficial. Thus, using the Cx26^{+/-floxS17F} mouse provided by Dr. Willecke, we crossed it with a mouse expressing Cre-recombinase driven from the keratin 14 promoter. Herein, we demonstrated that epidermis specific expression of S17F Cx26 does not reduce mouse viability. We further showed that our mice had an intact epidermal barrier as evaluated by using the exact protocol from (Schutz et al., 2011) (refer to Appendix 1). This observation was surprising and suggested that perhaps S17F Cx26 expression in embryonic tissues may interfere with the establishment of the epidermal barrier *in utero* and contribute to their poor prognosis. Cx26 is indeed expressed in the labyrinth layer of the fetal mouse placenta and

interestingly, Cx26 null embryos die by 11 days post coitum due to a placental defect (Gabriel et al., 1998). Direct empirical comparison of the development of global mutant and tissue specific versions of this mouse may shed light on the nature of the barrier defect and loss of viability in global mutant mice, and could further point to developmental complications in patients who harbour KIDS mutations. Nevertheless, our novel mutant mouse model allowed us to evaluate the influence of the S17F Cx26 on the epidermis alone, and whether this expression profile can disrupt wound healing which involves numerous unaffected cell types such as fibroblasts, leukocytes, and endothelial cells.

Primary keratinocytes isolated from S17F/+ mice demonstrated reduced migratory capabilities and brought into question whether the mice may exhibit wound healing defects. We therefore assessed wound healing using a standard dorsal skin punch biopsy and measured wound closure over a period of 13 days. While we found no differences in wound closure between S17F/+ mice and controls, we must acknowledge that wound-edge keratinocytes migrate beneath the coagulum (Martin, 1997) and were therefore not visible within our assay. Furthermore, it is understood that murine wound closure is accomplished primarily by dermal fibroblast contraction to bring wound edges in close proximity, and differs from human healing which favours keratinocyte re-epithelialization (Reid et al., 2004; Wong et al., 2011). The Cx30 A88V mutant mouse used in our study also did not display any wound repair defects. Together, one might conclude that patients harboring either of these connexin mutations would heal normally from an acute skin wound. To that end, there is no documented clinical reports that this cohort of patients have acute skin wounding defects but these events are not routinely reported in clinically studies. Since wound closure is somewhat different between mice and humans, caution needs to be exercised in translating our mouse findings to the human populous.

In Chapter 2, we demonstrated that the cellular characteristics of Cx26 mutants could predict disease outcomes. Our findings suggested that mutations at highly conserved amino acid residues (N54K and S183F) can affect connexin binding and trafficking and are linked to moderate skin diseases. In addition, mutations that interfere with properties of the channel pore (N14K and D50N) led to cell death in culture and are linked to inflammatory skin diseases. While we could not determine that cell death was driven by mutant hyperactive

hemichannels, there is a body of literature that supports their contribution to cell death as well as inflammation (Essenfelder et al., 2004; Garcia et al., 2015; Gerido et al., 2007; Lee et al., 2009; Levit and White, 2015). This alludes to the question of how hyperactive hemichannels may promote inflammation in live epidermis. Conceptually, it can be surmised that since hemichannels are conduits for molecular exchange between the cytosol and extracellular milieu, their aberrant activity can radically disrupt the extracellular concentration of permissible molecular messengers, including inflammatory mediators. Mechanistically, a study demonstrated that Cx26-expressing human keratinocytes, generated a strong ATP release response following acute exposure to peptidoglycan (PGN) harvested from the opportunistic pathogen, *S. aureus* (Donnelly et al., 2012). Furthermore, they showed that PGN challenged keratinocytes expressing KIDS mutants generated even stronger ATP responses and led to exaggerated interleukin-6 release, demonstrating the interaction between KIDS mutant hemichannels, purinergic signaling, and inflammation. Finally, these responses were abolished by the connexin channel blocker, carbenoxolone (Donnelly et al., 2012). In addition to forming non-functional gap junctions, S17F Cx26 was shown to potently inhibit intercellular dye transfer in cells co-expressing Cx43 (Garcia et al., 2015). This supports our finding that S17F/+ primary keratinocytes demonstrated reduced gap junctional coupling. While hyperactive hemichannels have been strongly linked to the inflammatory nature of KIDS, we wondered if reduced GJIC also contributed to the skin phenotype observed in our mice. Fortunately, we can begin to address this question by examining the findings from a mouse that was generated to model human Vohwinkel Syndrome by expressing D66H Cx26 in suprabasal keratinocytes (Bakirtzis et al., 2003). This mutant is not associated with hyperactive hemichannels, however, similar to S17F Cx26, it inhibits Cx26 and Cx43 mediated GJIC (Rouan et al., 2001). The D66H Cx26 mouse is the only Cx26 mutant mouse to model a non-inflammatory skin disease and displays scaling skin with a dense, thick corneal layer (Bakirtzis et al., 2003). In addition, Cx26 and Cx30 were highly intracellular in suprabasal keratinocytes of mutant epidermis and resulted in increased DNA fragmentation suggesting that reduced keratinocyte GJIC may deregulate terminal differentiation (cornification) (Bakirtzis et al., 2003). Empirical comparison of hyperkeratotic lesions from the D66H Cx26 mouse and KIDS mice (S17F and G45E Cx26) may shed light on the influence of loss-of-function versus gain-of-function mutants *in vivo*.

Taken together, our findings and the literature involving Cx26 mutants and Cx26 mutant mice, suggest that reduced GJIC via intracellular connexin retention or reduced gap junction function may result in deregulated keratinocyte differentiation and abnormal skin phenotypes.

4.2 Therapeutic strategies for connexin linked skin diseases and wound healing

Over a decade of applied research towards connexin-based therapies has generated potential improvements for the treatment of several chronic health complications such as neuroinflammatory disorders, vasculopathies, ocular disorders, and notably, chronic skin wounds (Becker et al., 2016). Using *in vitro* and animal models of wound healing, some researchers have developed successful connexin-based strategies to improve wound healing and as a result, have spurred spinoff companies to commercialize novel connexin therapeutics (Becker et al., 2016; Ghatnekar and Elstrom, 2013). Of note, Cx43-targeted therapeutic compounds developed by CoDa Therapeutics and FirstString Research have delivered promising improvements for the healing of chronic venous and diabetic leg ulcers (Ghatnekar and Elstrom, 2013) (clinical results update from [CoDa](#)). The vast majority of connexin-based therapeutics focus on Cx43 largely due to the wealth of prior research demonstrating its involvement in many chronic and acute disease states (Nakase et al., 2004; Ormonde et al., 2012; Sutcliffe et al., 2015; Wang et al., 2007a). CoDa Therapeutics is developing strategies to target both Cx43 protein translation using antisense oligodeoxynucleotides, and Cx43 channel function using targeted mimetic peptides or non-specific small molecules such as HCB1019 (Becker et al., 2016). FirstString Research is another company highly focused on targeting the C-terminal tail of Cx43 to modulate its function with the intent of improving chronic wound healing (Becker et al., 2016; Ghatnekar and Elstrom, 2013).

To date, there are no targeted therapies for Cx26 or Cx30-linked skin disease and the current clinical treatments rely mainly on early diagnosis and management; especially for severe diseases such as KIDS (Coggshall et al., 2013). Maintenance of the skin barrier is of upmost importance for such patients since infectious and inflammatory complications are common and can be life-threatening (Coggshall et al., 2013). Therefore, patients must treat hyperkeratotic plaques with keratolytic and retinoid compounds, frequently moisturize the skin, and generously apply antibiotic and antifungal agents (Coggshall et al., 2013; Levit and

White, 2015). However, some studies have demonstrated that certain clinically approved small molecules such as mefloquin, carbenoxolone, and benzopyran have the ability to block Cx26 channels demonstrating their potential for therapeutic impact (Cao and Zheng, 2014; Donnelly et al., 2012; Levit et al., 2015; Levit and White, 2015). Indeed, the greatest therapeutic value may come from attenuating hemichannel activity since their link to diseased states is well outlined (Levit and White, 2015), yet their contribution to normal skin physiology is largely undetermined. There are, however, no clinical trials for any such therapies due to the inadequate number of recruitable patients (Levit and White, 2015). Fortunately for S17F Cx26 KIDS patients, the Cx43-targeted therapies from CoDa and FirstString may in fact provide clinical relief due to the specific involvement of Cx43 in their pathophysiology. In addition, the connexin mimetic peptide, Gap19, which targets the intracellular loop of Cx43, inhibits Cx43 hemichannels without affecting GJIC as shown in astrocytes (Abudara et al., 2014). It would certainly be interesting to assess its effectiveness in S17F Cx26 expressing keratinocytes, as perhaps aberrant heteromeric hemichannels may be neutralized without disrupting normal Cx43 function.

As evidence builds for the impact of Cx26 on wound healing, we may begin to see Cx26-targeted therapeutics emerge in applied clinical research. Since abnormal expression of both Cx26 and Cx43 has been established in non-healing diabetic wounds (Becker et al., 2012; Wang et al., 2007a), there may be considerable therapeutic value in pursuing Cx26-targeted wound therapies, which would undoubtedly provide sufficient patient numbers to organize clinical trials. In addition, such therapies may provide relief for patients with congenital Cx26-linked diseases.

4.3 References

- Abudara, V., J. Bechberger, M. Freitas-Andrade, M. De Bock, N. Wang, G. Bultynck, C.C. Naus, L. Leybaert, and C. Giaume. 2014. The connexin43 mimetic peptide Gap19 inhibits hemichannels without altering gap junctional communication in astrocytes. *Front Cell Neurosci.* 8:306.
- Bakirtzis, G., R. Choudhry, T. Aasen, L. Shore, K. Brown, S. Bryson, S. Forrow, L. Tetley, M. Finbow, D. Greenhalgh, and M. Hodgins. 2003. Targeted epidermal expression of mutant Connexin 26(D66H) mimics true Vohwinkel syndrome and provides a model for the pathogenesis of dominant connexin disorders. *Hum Mol Genet.* 12:1737-1744.
- Becker, D.L., A.R. Phillips, B.J. Duft, Y. Kim, and C.R. Green. 2016. Translating connexin biology into therapeutics. *Semin Cell Dev Biol.* 50:49-58.
- Becker, D.L., C. Thrasyvoulou, and A.R. Phillips. 2012. Connexins in wound healing; perspectives in diabetic patients. *Biochim Biophys Acta.* 1818:2068-2075.
- Bosen, F., M. Schutz, A. Beinhauer, N. Strenzke, T. Franz, and K. Willecke. 2014. The Clouston syndrome mutation connexin30 A88V leads to hyperproliferation of sebaceous glands and hearing impairments in mice. *FEBS Lett.* 588:1795-1801.
- Cao, Y., and O.J. Zheng. 2014. Tonabersat for migraine prophylaxis: a systematic review. *Pain Physician.* 17:1-8.
- Churko, J.M., J.J. Kelly, A. Macdonald, J. Lee, J. Sampson, D. Bai, and D.W. Laird. 2012. The G60S Cx43 mutant enhances keratinocyte proliferation and differentiation. *Exp Dermatol.* 21:612-618.
- Cogshall, K., T. Farsani, B. Ruben, T.H. McCalmont, T.G. Berger, L.P. Fox, and K. Shinkai. 2013. Keratitis, ichthyosis, and deafness (KID) syndrome: A review of infectious and neoplastic complications. *Journal of the American Academy of Dermatology.* 69:127-134.
- Cogliati, B., M. Vinken, T.C. Silva, C.M. Araujo, T.P. Aloia, L.M. Chaible, C.M. Mori, and M.L. Dagli. 2015. Connexin 43 deficiency accelerates skin wound healing and extracellular matrix remodeling in mice. *J Dermatol Sci.* 79:50-56.
- Dere, E., M.A. De Souza-Silva, C. Frisch, B. Teubner, G. Sohl, K. Willecke, and J.P. Huston. 2003. Connexin30-deficient mice show increased emotionality and decreased rearing activity in the open-field along with neurochemical changes. *Eur J Neurosci.* 18:629-638.
- Djalilian, A.R., D. McGaughey, S. Patel, E.Y. Seo, C. Yang, J. Cheng, M. Tomic, S. Sinha, A. Ishida-Yamamoto, and J.A. Segre. 2006. Connexin 26 regulates epidermal barrier

- and wound remodeling and promotes psoriasiform response. *J Clin Invest.* 116:1243-1253.
- Donnelly, S., G. English, E.A. de Zwart-Storm, S. Lang, M.A. van Steensel, and P.E. Martin. 2012. Differential susceptibility of Cx26 mutations associated with epidermal dysplasias to peptidoglycan derived from *Staphylococcus aureus* and *Staphylococcus epidermidis*. *Exp Dermatol.* 21:592-598.
- Essenfelder, G.M., R. Bruzzone, J. Lamartine, A. Charollais, C. Blanchet-Bardon, M.T. Barbe, P. Meda, and G. Waksman. 2004. Connexin30 mutations responsible for hidrotic ectodermal dysplasia cause abnormal hemichannel activity. *Hum Mol Genet.* 13:1703-1714.
- Gabriel, H.D., D. Jung, C. Butzler, A. Temme, O. Traub, E. Winterhager, and K. Willecke. 1998. Transplacental uptake of glucose is decreased in embryonic lethal connexin26-deficient mice. *J Cell Biol.* 140:1453-1461.
- Garcia, I.E., J. Maripillan, O. Jara, R. Ceriani, A. Palacios-Munoz, J. Ramachandran, P. Olivero, T. Perez-Acle, C. Gonzalez, J.C. Saez, J.E. Contreras, and A.D. Martinez. 2015. Keratitis-ichthyosis-deafness syndrome-associated Cx26 mutants produce nonfunctional gap junctions but hyperactive hemichannels when co-expressed with wild type Cx43. *J Invest Dermatol.* 135:1338-1347.
- Gemel, J., V. Valiunas, P.R. Brink, and E.C. Beyer. 2004. Connexin43 and connexin26 form gap junctions, but not heteromeric channels in co-expressing cells. *Journal of Cell Science.* 117:2469-2480.
- Gerido, D.A., A.M. DeRosa, G. Richard, and T.W. White. 2007. Aberrant hemichannel properties of Cx26 mutations causing skin disease and deafness. *Am J Physiol Cell Physiol.* 293:C337-345.
- Ghatnekar, G.S., and T.A. Elstrom. 2013. Translational strategies for the development of a wound healing technology (idea) from bench to bedside. *Methods Mol Biol.* 1037:567-581.
- Lamartine, J., G. Munhoz Essenfelder, Z. Kibar, I. Lanneluc, E. Callouet, D. Laoudj, G. Lemaitre, C. Hand, S.J. Hayflick, J. Zonana, S. Antonarakis, U. Radhakrishna, D.P. Kelsell, A.L. Christianson, A. Pitaval, V. Der Kaloustian, C. Fraser, C. Blanchet-Bardon, G.A. Rouleau, and G. Waksman. 2000. Mutations in GJB6 cause hidrotic ectodermal dysplasia. *Nat Genet.* 26:142-144.
- Lee, J.R., A.M. Derosa, and T.W. White. 2009. Connexin mutations causing skin disease and deafness increase hemichannel activity and cell death when expressed in *Xenopus* oocytes. *J Invest Dermatol.* 129:870-878.

- Levit, N.A., C. Sellitto, H.Z. Wang, L. Li, M. Srinivas, P.R. Brink, and T.W. White. 2015. Aberrant connexin26 hemichannels underlying keratitis-ichthyosis-deafness syndrome are potently inhibited by mefloquine. *J Invest Dermatol.* 135:1033-1042.
- Levit, N.A., and T.W. White. 2015. Connexin hemichannels influence genetically determined inflammatory and hyperproliferative skin diseases. *Pharmacol Res.* 99:337-343.
- Lilly, E., C. Sellitto, L.M. Milstone, and T.W. White. 2016. Connexin channels in congenital skin disorders. *Semin Cell Dev Biol.* 50:4-12.
- Maass, K., A. Ghanem, J.S. Kim, M. Saathoff, S. Urschel, G. Kirfel, R. Grummer, M. Kretz, T. Lewalter, K. Tiemann, E. Winterhager, V. Herzog, and K. Willecke. 2004. Defective epidermal barrier in neonatal mice lacking the C-terminal region of connexin43. *Mol Biol Cell.* 15:4597-4608.
- Martin, P. 1997. Wound healing--aiming for perfect skin regeneration. *Science.* 276:75-81.
- Martin, P.E., and M. van Steensel. 2015. Connexins and skin disease: insights into the role of beta connexins in skin homeostasis. *Cell Tissue Res.* 360:645-658.
- Mese, G., C. Sellitto, L. Li, H.Z. Wang, V. Valiunas, G. Richard, P.R. Brink, and T.W. White. 2011. The Cx26-G45E mutation displays increased hemichannel activity in a mouse model of the lethal form of keratitis-ichthyosis-deafness syndrome. *Mol Biol Cell.* 22:4776-4786.
- Nakase, T., G. Sohl, M. Theis, K. Willecke, and C.C. Naus. 2004. Increased apoptosis and inflammation after focal brain ischemia in mice lacking connexin43 in astrocytes. *Am J Pathol.* 164:2067-2075.
- Ormonde, S., C.Y. Chou, L. Goold, C. Petsoglou, R. Al-Taie, T. Sherwin, C.N. McGhee, and C.R. Green. 2012. Regulation of connexin43 gap junction protein triggers vascular recovery and healing in human ocular persistent epithelial defect wounds. *J Membr Biol.* 245:381-388.
- Plum, A., E. Winterhager, J. Pesch, J. Lautermann, G. Hallas, B. Rosentreter, O. Traub, C. Herberhold, and K. Willecke. 2001. Connexin31-deficiency in mice causes transient placental dysmorphogenesis but does not impair hearing and skin differentiation. *Dev Biol.* 231:334-347.
- Reid, R.R., H.K. Said, J.E. Mogford, and T.A. Mustoe. 2004. The future of wound healing: pursuing surgical models in transgenic and knockout mice. *J Am Coll Surg.* 199:578-585.
- Richard, G., L.E. Smith, R.A. Bailey, P. Itin, D. Hohl, E.H. Epstein, Jr., J.J. DiGiovanna, J.G. Compton, and S.J. Bale. 1998. Mutations in the human connexin gene GJB3 cause erythrokeratoderma variabilis. *Nat Genet.* 20:366-369.

- Rouan, F., T.W. White, N. Brown, A.M. Taylor, T.W. Lucke, D.L. Paul, C.S. Munro, J. Uitto, M.B. Hodgins, and G. Richard. 2001. trans-dominant inhibition of connexin-43 by mutant connexin-26: implications for dominant connexin disorders affecting epidermal differentiation. *J Cell Sci.* 114:2105-2113.
- Schnichels, M., P. Worsdorfer, R. Dobrowolski, C. Markopoulos, M. Kretz, G. Schwarz, E. Winterhager, and K. Willecke. 2007. The connexin31 F137L mutant mouse as a model for the human skin disease erythrokeratoderma variabilis (EKV). *Hum Mol Genet.* 16:1216-1224.
- Schutz, M., T. Auth, A. Gehrt, F. Bosen, I. Korber, N. Strenzke, T. Moser, and K. Willecke. 2011. The connexin26 S17F mouse mutant represents a model for the human hereditary keratitis-ichthyosis-deafness syndrome. *Hum Mol Genet.* 20:28-39.
- Scott, C.A., D. Tattersall, E.A. O'Toole, and D.P. Kelsell. 2012. Connexins in epidermal homeostasis and skin disease. *Biochim Biophys Acta.* 1818:1952-1961.
- Sutcliffe, J.E., K.Y. Chin, C. Thrasivoulou, T.E. Serena, S. O'Neil, R. Hu, A.M. White, L. Madden, T. Richards, A.R. Phillips, and D.L. Becker. 2015. Abnormal connexin expression in human chronic wounds. *Br J Dermatol.* 173:1205-1215.
- Wang, C.M., J. Lincoln, J.E. Cook, and D.L. Becker. 2007. Abnormal connexin expression underlies delayed wound healing in diabetic skin. *Diabetes.* 56:2809-2817.
- Wong, V.W., M. Sorkin, J.P. Glotzbach, M.T. Longaker, and G.C. Gurtner. 2011. Surgical approaches to create murine models of human wound healing. *J Biomed Biotechnol.* 2011:969618.

Appendix 1

Cx26^{K14-S17F/+} mice have an intact epidermal barrier

One of the principle functions of the skin is to provide a protective barrier from environment insults including UV radiation and opportunistic pathogens, and to limit water loss. As a first pass assessment for water barrier function, a toluidine blue barrier penetration assay was performed. Katanya C. Alaga and I contributed equally to this work.

Methods

The barrier assay was performed exactly as described in (Schutz et al., 2011). Briefly, P1 pups were CO₂ euthanized and put through a series of increasing concentration methanol washes, followed by decreasing concentration methanol washes. Pups were then stained for 15 minutes in an aqueous 0.2% toluidine blue solution. Following staining, the pups were washed several times in 90% ethanol, dried, and imaged with an iPhone5. Areas of dark blue/purple staining indicated toluidine blue dye penetration and therefore a non-functional water barrier. A positive control was performed by making a small laceration to the skin.

Results

We found that similar to littermate controls, S17F/+ epidermis did not stain blue indication little to no epidermal penetration of the water soluble dye. However, epidermal staining was evident in areas of the skin that had been cut, or treated with acetone which disrupts lipids in the epidermal barrier (Tsai et al., 2001). This suggests that neonatal S17F/+ epidermis indeed forms an effective water barrier.

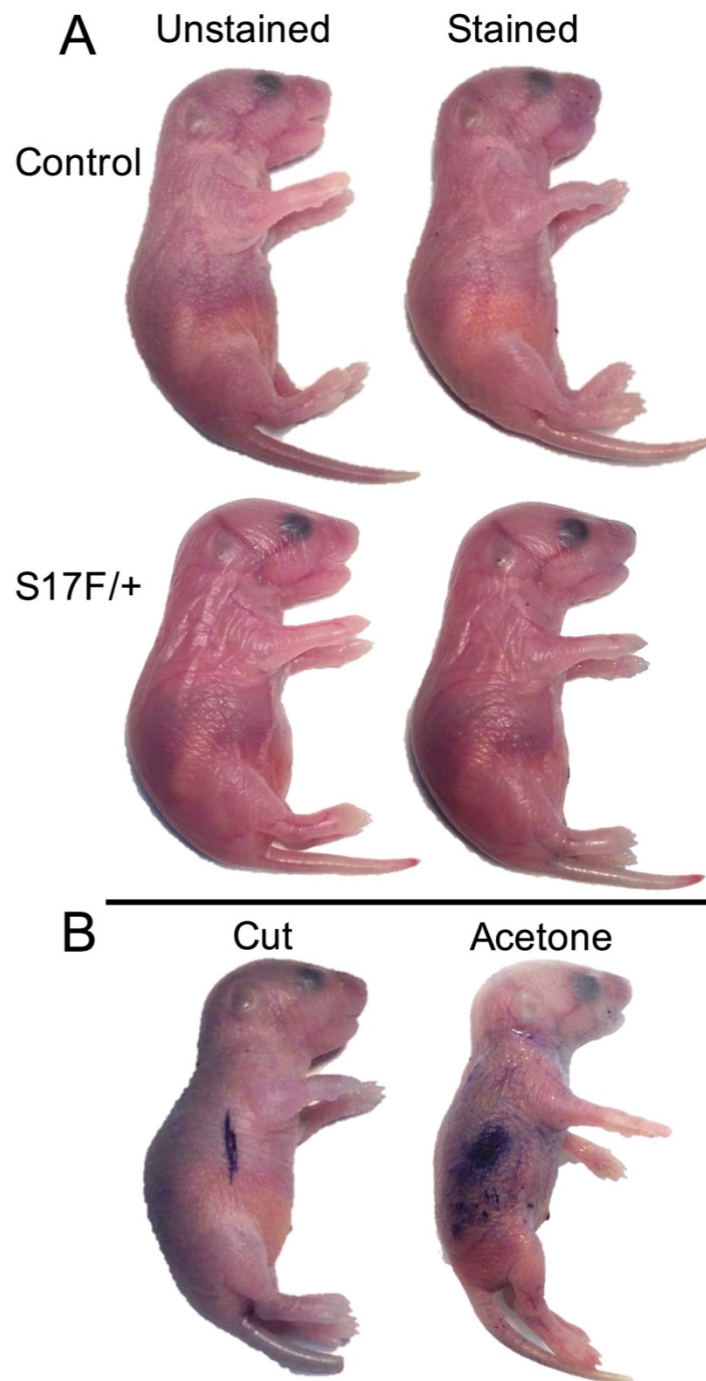


Figure A1. P1 neonates were euthanized and submerged in an aqueous 0.2% toluidine blue solution for 15 minutes. The absence of epidermal staining of both S17F/+ and controls indicates a functional epidermal barrier. A small incision and treatment with acetone were used as a positive control.

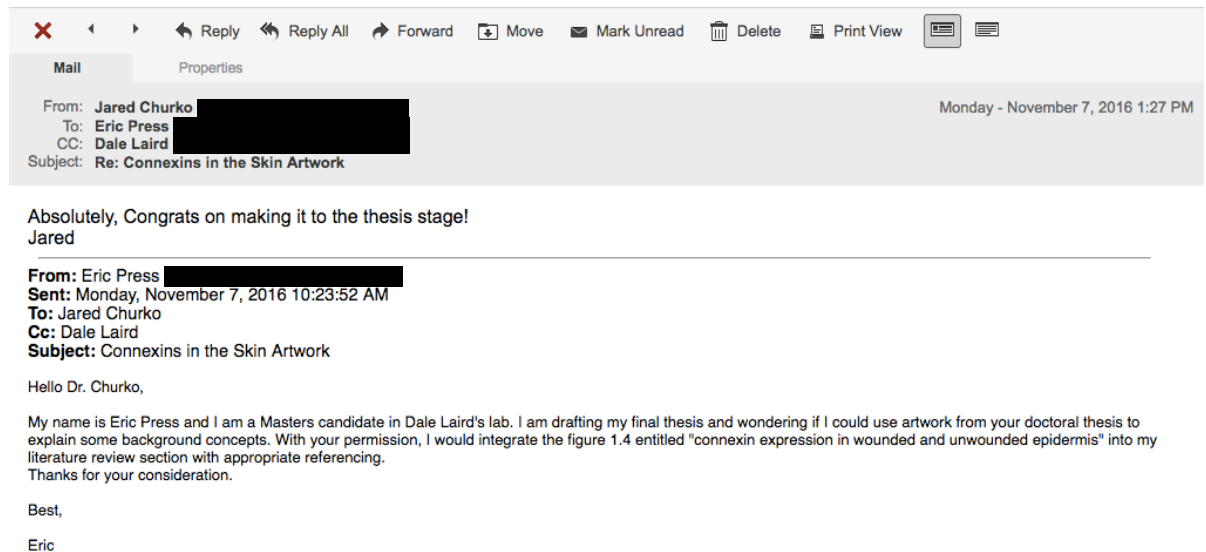
References

- Schutz, M., T. Auth, A. Gehrt, F. Bosen, I. Korber, N. Strenzke, T. Moser, and K. Willecke. 2011. The connexin26 S17F mouse mutant represents a model for the human hereditary keratitis-ichthyosis-deafness syndrome. *Hum Mol Genet.* 20:28-39.
- Tsai, J.C., Sheu, H.M., Hung, P.L., and C.L. Cheng. 2001. Affect of Barrier Disruption by Acetone Treatment on the Permeability of Compounds with Various Lipophilicities: Implications for the Permeability of Compromised Skin. *Journal of Pharmaceutical Sciences.* 90:1242-1254.

Appendix 2

Permissions for Artwork Reproduction

Dr. Jared Churko, a former PhD student in Dr. Dale Laird's lab, generated a graphic to depict the expression of several connexins in adult mouse epidermis. Since I used this graphic in Chapter 1 of this thesis, I have included here his written permission from our email conversation.



Appendix 3

Animal Use Protocol Approval



AUP Number: 2015-030
PI Name: Laird, Dale W
AUP Title: The Role Of Gap Junction In Diseases

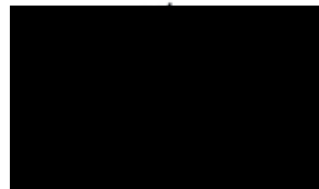
Approval Date: 05/19/2015
Official Notice of Animal Use Subcommittee (AUS) Approval: Your new Animal Use Protocol (AUP) entitled "The Role Of Gap Junction In Diseases

" has been APPROVED by the Animal Use Subcommittee of the University Council on Animal Care. This approval, although valid for four years, and is subject to annual Protocol Renewal.2015-030::1

1. This AUP number must be indicated when ordering animals for this project.
2. Animals for other projects may not be ordered under this AUP number.
3. Purchases of animals other than through this system must be cleared through the ACVS office. Health certificates will be required.

The holder of this Animal Use Protocol is responsible to ensure that all associated safety components (biosafety, radiation safety, general laboratory safety) comply with institutional safety standards and have received all necessary approvals. Please consult directly with your institutional safety officers.

Submitted by: Copeman, Laura
 on behalf of the Animal Use Subcommittee
 University Council on Animal Care



The University of Western Ontario
 Animal Use Subcommittee / University Council on Animal Care
 Health Sciences Centre, • London, Ontario • CANADA – N6A 5C1
 PH: 519-661-2111 ext. 86768 • FL 519-661-2028
 Email: auspc@uwo.ca • <http://www.uwo.ca/animal/website/>

Curriculum Vitae

Name:	Eric Richard Press
Post-secondary Education and Degrees:	<p>University of Western Ontario London, Ontario, Canada 2010 – 2014, BMSc Honours Specialization in Physiology</p> <p>The University of Western Ontario London, Ontario, Canada 2014 – Present, MSc Physiology and Pharmacology</p>
Honours and Awards:	<p>Western Graduate Research Scholarship 2014 – 2016</p> <p>Western Scholarship of Excellence 2010</p> <p>Top Poster in Cell Biology – Annual Physiology and Pharmacology Research Day 2015, 2016</p>
Related Work Experience	<p>Teaching Assistant The University of Western Ontario Physiology 3130Y; Course Coordinator: Tom Stavrakys 2014 – 2016</p>

Publications:

Eric R. Press, John J. Kelly, Katrina Chin, Anton Alaga, Cindy Shao, and Dale W. Laird. Induction of cell death, trans-dominant properties, and reduced channel function of Cx26 mutants predict the severity of diseases linked to *GJB2* mutations. (in final preparation for submission this month).

Eric R. Press, Katanya C. Alaga, Kevin Barr, Cindy Shao, Felicitas Bosen, Klaus Willecke, and Dale W. Laird. Disease-linked connexin26 and connexin30 mutants promote volar skin abnormalities and mild wound healing defects in mice. (in final preparation for submission this month).

Katanya C. Alaga, Eric R. Press, Kevin Barr, Melissa Crawford, Lina Dagnino, and Dale W. Laird. The differential roles of connexin26 and Connexin43 in modulating the epidermal response to UV injury (in final preparation).

Poster Presentations:

Eric Press, Kevin Barr, Qing Shao, Dale W. Laird (November, 2016). Disease-Linked Connexin26 and Connexin30 Mutants Promote Volar Skin Abnormalities and Mild Wound Healing Defects in Mice. Department of Physiology and Pharmacology Research Day. Western University, London, Ontario. **Top Prize**

Eric Press, Kevin Barr, Qing Shao, Dale W. Laird (October, 2016). Disease-Linked Connexin26 and Connexin30 Mutants Promote Volar Skin Abnormalities and Mild Wound Healing Defects in Mice. Department of Anatomy and Cell biology Research Day. Western University, London, Ontario.

Eric Press, Kevin Barr, Wing Shao, Dale W. Laird (March, 2016). A Cx26 mutant alters epidermal homeostasis in a novel Cx26^{CK14-S17F/+} mutant mouse. London Health Research Day. Western University, London, Ontario.

Eric Press, Kevin Barr, Qing Shao, Dale W. Laird (December 2015). A Cx26 mutant alters epidermal homeostasis in a novel Cx26^{CK14-S17F/+} mutant mouse. American Society of Cell Biology 2015 Meeting. San Diego Convention Center, San Diego, California.

Eric Press, Kevin Barr, Wing Shao, Dale W. Laird (November, 2015). A Cx26 mutant alters epidermal homeostasis in a novel Cx26^{CK14-S17F/+} mutant mouse. Department of Physiology and Pharmacology Research Day. Western University, London, Ontario. **Top Prize**

Eric Press, Kevin Barr, Wing Shao, Dale W. Laird (October 2015). A Cx26 mutant alters epidermal homeostasis in a novel Cx26^{CK14-S17F/+} mutant mouse. Department of Anatomy and Cell Biology Research Day. Western University, London, Ontario.